Development of a Modular Steel Structure for Multi-Storey Buildings
by

Akram Mohammed Zain

A thesis submitted in partial fulfillment of the requirements for the degree of

Master of Science

in
STRUCTURAL ENGINEERING

Department of Civil and Environmental Engineering
University of Alberta

Abstract

Modularization of buildings comes in several types, from prefabricated members to full volumetric models. Recently, the introduction of modular construction methods brought numerous benefits to the construction industry. Reducing construction time and costs together with improving quality and safety helped in growing the interest of designers and contractors toward modularization. Although there is wide agreement on modularization benefits to the construction industry, the transition to these new building techniques requires research and understanding of the structural behaviour of modular structures. Furthermore, despite a relatively vast body of research proposing innovative modular steel systems and connections, their application is still limited and they lack a sufficient design requirements in particular in seismic regions. Finally, it is felt that there is a need to develop a new and innovative modular steel lateral load resisting system (LLRS) that can be integrated with the modular system to help in improving construction efficiency, while offering a safe and satisfactory structural performance.

A new modular steel system for multi-storey buildings is proposed in this research project. Two types of modules, gravity and braced, were introduced to carry gravity and lateral loads, respectively. The members and connections were selected based on availability in the market, structural performance, transportation constraints, and fabrication and erection benefits. The proposed braced module consists of steel concentrically braced frames (CBFs) and can be used to carry lateral seismic or wind loads. A six-storey prototype building was then selected to evaluate the construction efficiency and structural response of the proposed modular system under gravity and seismic loads. The building was designed as per the Canadian loading code (NBCC) and steel

design standard (CSA S16). A braced frame sub-assembly consisting of the first- and second-storey modules was simulated using Abaqus program. A nonlinear static (pushover) analysis was then performed to examine the lateral response of the sub-assembly focusing on the member forces and storey drift. The resulting member forces were compared to those predicted by CSA S16. The results confirmed the potential benefits in improving construction efficiency without increasing the construction cost. Furthermore, the results of the evolution of the structural response of the braced module showed satisfactory lateral behaviour without instability or connection failure when braces experience nonlinear response. Finally, the CSA S16 seismic provisions implicit for steel braced concentrically braced frames can be used to design the proposed braced module.

Preface

This thesis is an original work by Akram M. Zain. Parts of Chapters 3, 4 and 5 were part of a paper that was accepted for the Canadian Society for Civil Engineering (CSCE) annual conference 2020. The paper was co-authored by Dr. Ali Imanpour and Prof. Robert Driver.

Dedication

To My lovely Family: My dad, My mom, my wife, my siblings, and my lovely kids (Adam & Ayad). Thank you for all the love and support you surrounded me with. My success is a reflection of your support.

Acknowledgements

I would like to express my deep gratitude to Dr. Ali Imanpour and Dr. Robert Driver, my research supervisors, for their patient guidance, enthusiastic encouragement, and useful critiques of this research work. This project would not have been possible without them. I would like to thank my colleagues from the CISC centre for steel structures education and research (Steel Centre) for their advice throughout this project. Special thanks to Pablo Cano for his help in the model calibration in Abaqus.

I would like to thank Steel Centre partner WF Steel and Crane for sharing their knowledge and experience in the fabrication of modular steel structures. Working closely with their engineers and in their fabrication shop helped in the development process of the modular system presented in this project.

I would also like to extend my thanks to Eng. Abdullah Bugshan and Hadhramout Foundation for the financial funding and the social and technical support provided from day one and throughout the whole program.

Finally, I would like to thank my parents, who were always by my side, supporting me from my first step. Thanks to my siblings, who always cheered me and believed in me. I can't forget thanking my lovely wife for all of the love and support she surrounded me with through the challenging days.

Table of Contents

List of Tables

List of Figures

Chapter 1: Introduction

1.1 Modular construction and its benefits

Modularization is a construction technique that involves constructing repetitive structural units (i.e., modules) off-site. Modularization can be divided into three main categories:

- Singular elements such as beams and columns with shop-welded connection plates and bolt holes to ease assembly on-site. Figure 1.1 shows beams with welded connection plates.
- Planar modules like wall assemblies, precast slabs, and frames. These often have a load-bearing system and sometimes include cladding and windows (Figure 1.2)
- Three-dimensional (volumetric) units that contain most of the structural elements like columns, beams, and slabs. In some cases, the units come fully finished and ready for use (Figure 1.3).

Figure 1.1: Prefabricated beam with connection plates

Figure 1.2: Planar module (Ibrahim 2019)

Figure 1.3: Volumetric building module (Modern Steel Construction 2014)

Modules are divided into two categories in terms of the load-supporting system: load-bearing modules, where walls of the modules transfer the loads through the structure, and corner-supported modules where loads transfer through the steel frames (Lawson and Richards 2010). In the past, modular construction techniques were limited mainly to portable or temporary buildings similar

to portable washrooms or project site offices. Later in the 90s, off-site techniques gained more attention from engineers to be used for building structures, particularly cellular-type buildings such as schools, hotels or even hospitals (Lawson et al. 2014).

The interest toward modular construction methods is increasing every year due to the advantages it offers. Advantages of modularization can vary from one project to another, yet the main advantages obtained from modularization can be listed as:

- Project duration reduction: One of the key advantages modular approaches bring to projects is shortening the project schedule. With proper planning and management, the modular project duration can be cut to half. (Lawson et al. 2014)
- Cost reduction: The cost of a structure is determined by many factors. Labour and workforce influence the total project cost. Modularisation can help reduce costs, for instance, by reducing the number of labourers needed on site.
- Factory quality production: Modules are built inside special fabrication units that facilitate high-quality control. The closed environment enhances the safety of workers due to the availability of cranes and tools in hand, safety measures applied, and the elimination of weather impacts, especially in cold and rainy regions. This makes it easier and safer for workers day or night, summer or winter.
- Green construction: Modular solutions provide better waste management and less noise and disturbance to the surrounding neighbourhood because of the reduced construction time and limiting heavy work to the factory, leaving mainly bolting and simple jobs on-site.
- Maintenance and movability: Modules are usually connected using bolts on-site, which allows faster construction and even faster disassembly for maintenance or moving purposes without the need for a complicated demolition process.

1.2 Problem statement

With all of the benefits modularization offers, a dramatic shift in construction methods cannot be spotted yet. The 2019 Modular Building Institute (MBI) annual report revealed the market share for permanent modular construction in North America as compared to all construction starts by year, as can be viewed in Table 1.1 (Modular Building Institute 2019). Although relocatable buildings can include residential buildings, hotels, or even multi-family residential buildings, they are not included in the provided percentages as they are not comparable to conventional structures. An increase in the market share can be noticed through the years. However, the percentage is still considered minor. The low percentage can be a reflection of the barriers and constraints reducing the move toward more modularization in the construction industry. These constraints and barriers can be the result of different factors, yet this research will state the problems and needs that can be controlled from a civil and structural engineering perspective, the principal ones being:

- the lack of extensive research, testing, and information on the structural response of modular steel framed structures under vertical and lateral loads, creating a state of uncertainty for designers;
- the need for an innovative multi-storey modular steel structural system that provides modularization benefits of reducing time and cost and improving productivity, while offering desirable structural performance;
- some of the current modular steel systems require special design methods that, in some cases, are only applicable to specific conditions similar to what was examined in the scientific publications. This creates the need for either a system that can be designed using current building codes or applying extensive studies to provide design guidelines for different design cases of the modular system; and
- the need for a modular steel lateral load resisting system (LLRS) that can be integrated with the modular system to help in speeding the construction, in particular in high seismic regions. Figure 1.4 shows a modular building that uses a concrete core, wherein the steel modules of the building cannot be assembled until the concrete core has cured, which creates delays in construction time.

Figure 1.4: Modules assembly for ALT Hotel in Calgary, Alberta (Cappis 2017)

Table 1.1: Permanent modular construction market share in North America (Modular Building Institute 2019).

Year	Permanent modular construction (PMC) market share
2015	2.43%
2016	3.18%
2017	3.27%
2018	3.67%

1.3 Objectives

This research project aims to develop an innovative modular steel structural system for multi-storey buildings. The specific objectives of this research are as follows:

- to conduct a literature review on current modular steel systems and connections;
- to develop a new and innovative modular steel structural system for multi-storey buildings, with an integrated lateral load resisting system to provide vertical and lateral stability under

both gravity and lateral loads, considering the constructability of the system, the transportation of modules to site, the total cost of the project, and the architectural flexibility and interior spaces of modules;

- to contemplate the simplicity in the fabrication of the new system's connections and assure the compliance of the design process with current building design codes; and
- to evaluate the construction efficiency and structural behaviour of the proposed modular system under both gravity loads (dead, live and snow) and lateral loads (seismic).

1.4 Methodology

In order to accomplish the research objectives, the following four steps were taken:

Step 1: Development of a good understanding of modular steel structures through a review of the existing literature related to modular steel systems. Scientific publications with the focus on the structural behaviour of innovative modular steel systems and modular connections were collected and summarized.

Step 2: Development of an innovative modular steel system for multi-storey buildings that offers modularization benefits, flexibility for use in different types of buildings, and desirable structural performance under gravity and lateral loads.

Step 3: Structural design of two prototype buildings in accordance with Canadian building codes NBCC (National Research Council of Canada 2015) and CSA S16 (CSA 2019). One of the structures is built with the developed modular steel system, and the other building is designed as a conventionally-constructed steel building. A comparison between the two buildings in terms of the steel tonnage required and the number of on-site connections is made.

Step 4: Development of a detailed numerical model of the frame connection assembly using the finite element method and performing a nonlinear static analysis to understand the structural behaviour under gravity and lateral seismic loads.

Chapter 2: Literature Review

This chapter's purpose is to review past research studies pertaining to modularization and innovative modular systems. First, samples of research studies assessing the economy and benefits of modularization are discussed. Then, the chapter describes studies on the global structural response of innovative systems, especially under lateral loading. Further, studies focused on developing new connections for modular structures are presented. Lastly, the seismic provisions and design process for one of the widely-used lateral load resisting systems (LLRS), concentrically braced frames (CBFs), is described.

2.1 Constructability and economic feasibility

Modular construction methods have recently become more popular around the world, mainly for structures where on-site construction time is the main concern. Engineers and researchers have started to show more interest in other benefits modularization could bring to the industry. A 2007 survey on modular construction, with over 1100 engineering firms and general contractors in the US participating, was done to reflect the thoughts and experience of industry on prefabrication. According to the survey, there was agreement on off-site construction benefits such as: reducing the construction period, providing more efficient quality control, increasing labour productivity, maintaining a safer construction environment, and cutting the construction cost (Lu 2007). The book *Design in Modular Construction* (Lawson et al. 2014) put an eye on different modular construction methods and their structural design procedures for most of the main structural materials in use. The book also revealed study cases on different modular techniques, modular building examples, and construction time and cost. One of the cases compared construction duration for a six-storey building using either modular or on-site construction methods; the study predicted up to 50% reduction in project time from start to handover to the owner, as shown in Figure 2.1 (Lawson et al. 2014).

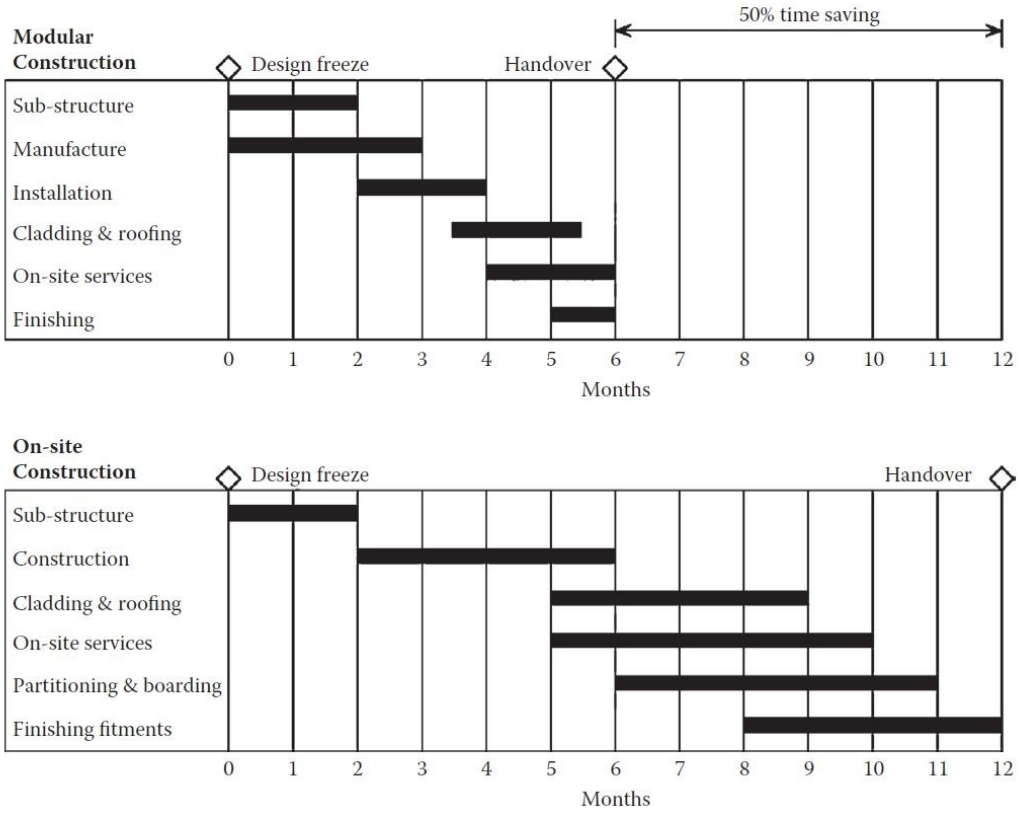

Figure 2.1: Construction periods for a six-storey building with modular and on-site methods (Lawson et al. 2014)

Modular construction methods have shown that they can have many benefits over conventional methods. A study with an objective to compare the environmental impacts of modular and conventionally built structures found superiority of off-site built structures in sustainability and life cycle performance (Kamali and Hewage 2016). Cost-wise, a study was conducted to compare two similar single-family houses, one built with full volumetric modules (similar to Figure 1.3) in Vancouver, Canada, and the other built with a panelized modular method (similar to Figure 1.2) in Bethel, Connecticut, USA. The study revealed the costs of both the modular process, excluding taxes, and transportation due to the different locations of the two buildings. The building cost with the volumetric modular method was 103.6 CAD/ft^2, around 12.4 CAD/ft^2 less than the house built with the planar modular method (Lopez and Froese 2016).

2.2 Structural seismic behaviour of modular structures

Although modularization offers an efficient construction technique, it brought new challenges to the industry. As the need for mid-rise and high-rise modular buildings grew in recent years, several questions have been raised regarding the structural response of such structures under lateral wind and seismic loads. There is limited supporting information including experimental data that can confirm the satisfactory response of new modular structural systems or connections under extreme loads, which leaves a state of uncertainty regarding the structural performance of modular systems. There have been several barriers reported in the past that explain the reasons associated with the slow adoption of modular methods in the steel construction industry. Some of them are a lack of a good understanding of the structural response, strict connection tolerances, fabrication, transportation, and installation challenges (Ramaji and Memari 2013). Several studies into the various aspects of modular steel systems have been carried out, including the evaluation of the global response of the structure under extreme loading conditions and the assessment of the local behaviour of modular connections. These studies and their results are discussed in the following sections: first, the global seismic response of modular systems is introduced. Then, the focus is on the connections specially developed for modular systems. Finally, a brief review of the Canadian code design provisions is provided.

2.2.1 Global seismic response of modular structures

During the past few years, different innovative modular systems were presented as a result of researchers' effort to develop and lead the current construction methods into safer and more efficient techniques. One of the earliest research programs conducted on modular steel structures in Canada was a study on the seismic performance of modular steel buildings (MSB) with a braced frame system using finite element analysis and experimental testing (Annan et al. 2007). The study focused on a clustered modular concentrically braced frame (CBF), depicted in Figure 2.2. The results from experimental and numerical analysis confirmed that unique detailing is required to prevent undesirable limit states, especially in the connections between the floor beam and the roof beam of two connected modules where eccentricity is developed (Annan et al. 2009).

Another study on the same type of MSB used numerical simulation to evaluate a full three-dimensional building and a two-dimensional frame (Fathieh and Mercan 2016). The objective of the study was to understand the behaviour of a full modular building under earthquake events and the connections between the units. The results gave an understanding of the response of connections and found a concentration of inelasticity on the first floor due to limitations of internal force redistribution.

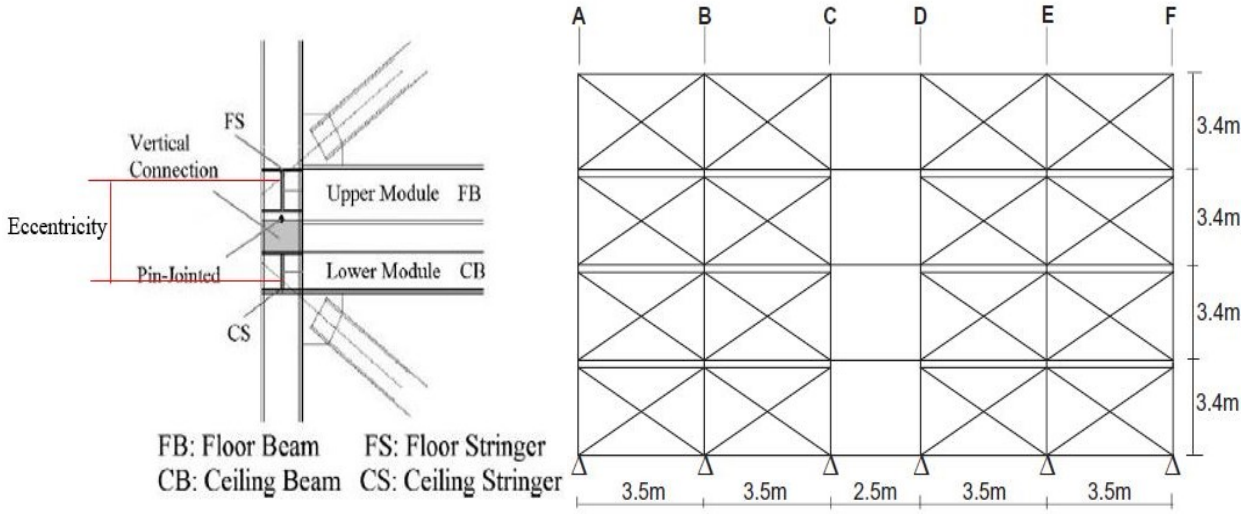

(a) (b)

Figure 2.2: (a) MSB vertical connection (Fathieh and Mercan 2016); (b) Side-view of MSB investigated (Annan et al. 2009)

The modular design of high-rise buildings with a focus on light steel modules (Figure 2.3) and C-section columns was discussed by Lawson and Richards (2010). The study discussed some of the modular technologies at the time and presented a design method for modular structures taking initial eccentricities and second-order moments into account. Laboratory experiments on lightweight C-section columns revealed that the stiffness of columns could be increased when attached with fascia boards (Lawson and Richards 2010).

Figure 2.3 Lightweight steel modules (LifeTec 2020)

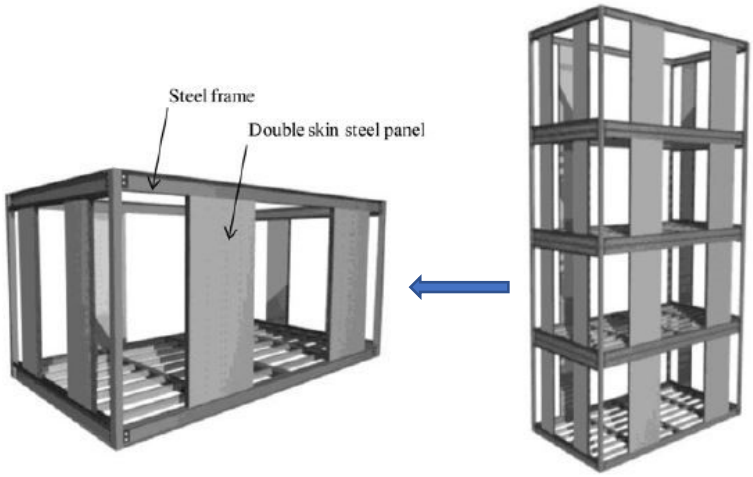

Figure 2.4: Modules with double-skin lightweight steel panels (Hong et al. 2011).

Researchers have focused on developing innovative modular systems to accommodate the need of improving the seismic behaviour of modular systems (Hong et al. 2011). Employing the behaviour of steel plate shear walls, an innovative framed modular system with double-skin lightweight steel panels integrated into walls was presented and investigated (Figure 2.4). The innovative system uses the steel panels as an LLRS. A full-scale experiment was conducted, and it has proven the efficiency of the system in resisting lateral loads.

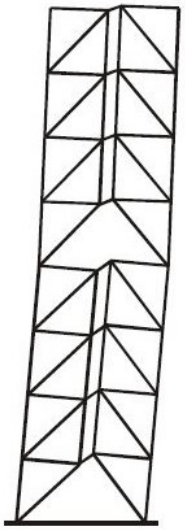

Figure 2.5 Modular tied eccentrically braced frame (Chen et al. 2012)

A modular tied eccentrically braced frame, illustrated in Figure 2.5, was developed from a conventional tied braced frame to reduce seismic forces on members and increase the structural efficiency under lateral forces together with providing benefits from the modular construction method. The system succeeds in fulfilling its objective of reducing seismic forces on frame members. However, an increased story drift and link rotations were noticed to be bigger compared to conventionally built frames (Chen et al. 2012).

Trying to develop solutions for fast-erected high-rise buildings, a unique prefabricated steel frame structural system with inclined braces (Figure 2.6a) was proposed to improve constructability, as well as global and local connection response (Liu et al. 2015). The proposed system was proven by experimental test and finite element analysis to have a desirable failure mode by developing plasticity in the truss beam while other members remain elastic. In an accompanying study, a full numerical model for a 30-storey hotel in China built with the modular steel frame with an inclined bracing system was simulated using finite element analysis software, as shown in Figure 2.6b. The results from the model under dynamic and push-over analysis were satisfactory and led to the development of a design specification for the system (Liu et al. 2018).

(a) (b)

Figure 2.6: (a) Prefabricated system under construction, (b) FEA model of the system. (Liu et al. 2018)

Corner-supported modules with pretensioned columns were presented to provide a stronger vertical connection between modules. The proposed system will have concrete-filled HSS and use special connections and steel pretensioning strands. A full-scale test was done to assure the ability of connections between columns to work as a rigid connection under lateral loads. When contact bonding between concrete and the connection assembly was accounted for in the design, the results demonstrated good lateral stiffness and ductility (Chen et al. 2017).

A research project of testing full-scale steel braced modular structures was conducted to examine the seismic response and the failure sequencing of the structure's members, flooring system, and connections. The yielding sequence of the members and joints was clarified, and the end-plate beam-to-column joint (Figure 2.7a) was found to provide good ductility and lateral stiffness (Shi et al. 2018).

The global response of the structure together with a prefabricated composite slab was investigated during the experimental test of a 3-storey modular assembly, shown in Figure 2.7b, and the system gave satisfactory behaviour under lateral loading (Shi et al. 2018).

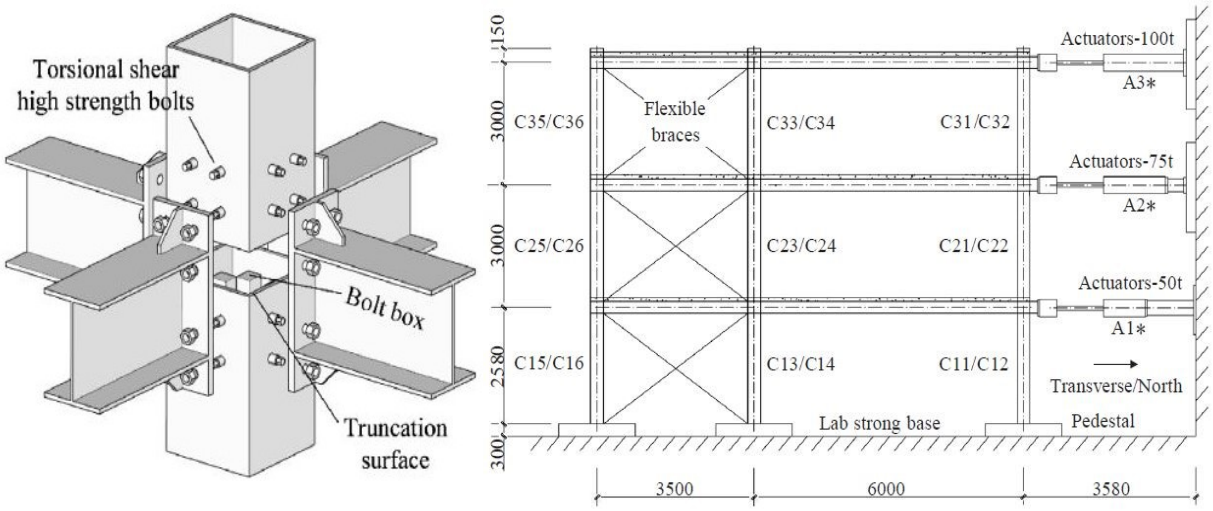

(a) (b)

Figure 2.7: (a) End-plate connection, (b) elevation of test assembly of modular structure (Shi et al. 2018)

An innovative damped H-frame system that consists of an H-shaped moment-resisting frame using buckling-restrained braces (BRB) was proposed with the intension of providing an innovative modular frame with capabilities to resist seismic forces (Figure 2.8). The proposed system had a unique shape and connection-level at mid-storey height to reduce the moment demand on the connections. Dynamic analysis results of the system exposed its ability to dissipate the seismic energy by yielding of the BRB and keeping other frame members elastic under high seismic actions (Etebarian and Yang 2018).

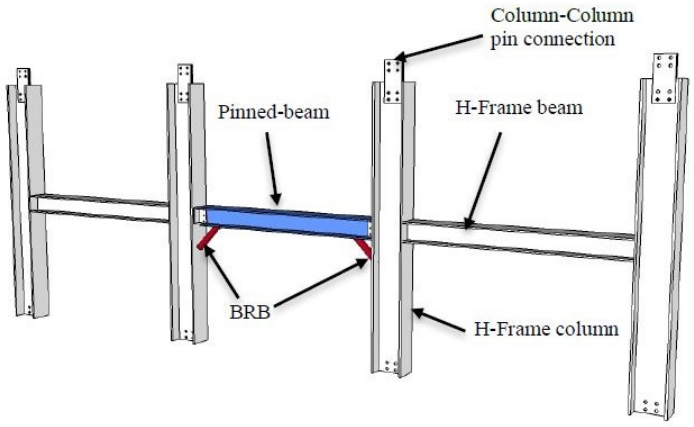

Figure 2.8: Damped H-frame system (Etebarian and Yang 2018)

2.2.2 The response of connections in modular systems

Connections, in general, play a key role in the structural performance of modular structures. Among all connections in the system, vertical module-to-module connections can be critical, especially to the behaviour of the lateral-force resisting system. This is why a lot of studies were focused on developing and improving connection rigidity and stability, especially those used in lateral force-resisting systems in modular structures. With the aim of developing a good understanding of the vertical column splice behaviour of moment frames under lateral loading, a parametric study was conducted (Shen et al. 2010). The seismic demand of column splices of 4-, 9- and 20-storey buildings was investigated under 20 different ground motions. An example of the 4-storey prototype building is shown in Figure 2.9. The study results showed agreement with design provisions (AISC 2010) of the need to design splices to the flexural strength of the smaller column.

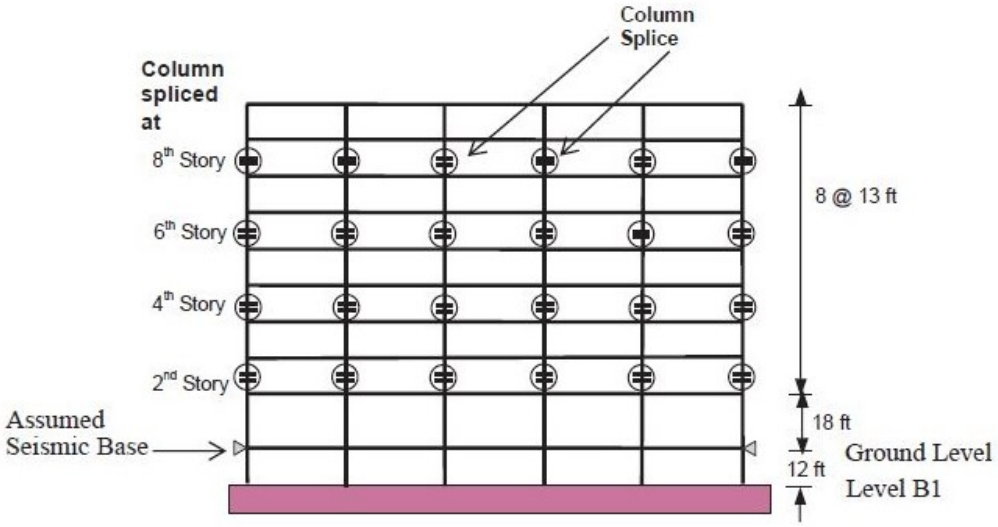

Figure 2.9 Four-storey prototype moment frame with column splice tested (Shen et al. 2010).

Connections between modules, especially the vertical connections, influence the speed of the construction and the structural response of the building. Hence, a considerable number of research studies were done on developing new modular connections between the building units. With the main objective of developing simple and quick connections for modular steel moment frames, a

series of studies was directed to obtain the best design for modular moment frame connections. An innovative welded joint for modular steel structures underwent experimental testing to understand its structural performance. The connection pictured in Figure 2.10a showed an undesired fracture of the weld under static and quasi-static loading. Providing auxiliary plates between the column base and truss angle flanges helped to change the failure mode to local buckling of the truss beam (Liu et al. 2015). More modifications were added to the welded connection to replace the use of welds with bolts (Fig 2.10b). The modified column-column-beam connection was investigated, and it demonstrated a preferred energy dissipation mechanism of bolts slipping before the yielding of the truss beam. The study also suggested design guidelines for this type of connection (Liu et al. 2018). Concurrently, the research team also worked on a similar type of connection that can be used with H-shaped beams instead of the beam trusses, as displayed in Fig 2.11a. The connection for H-shaped beams showed good results in dissipating the energy and increasing ductility through the bolts slipping. Additionally, the study indicated that the number of bolts and their spacing is the main factor in controlling the strength of the connection (Liu et al. 2017).

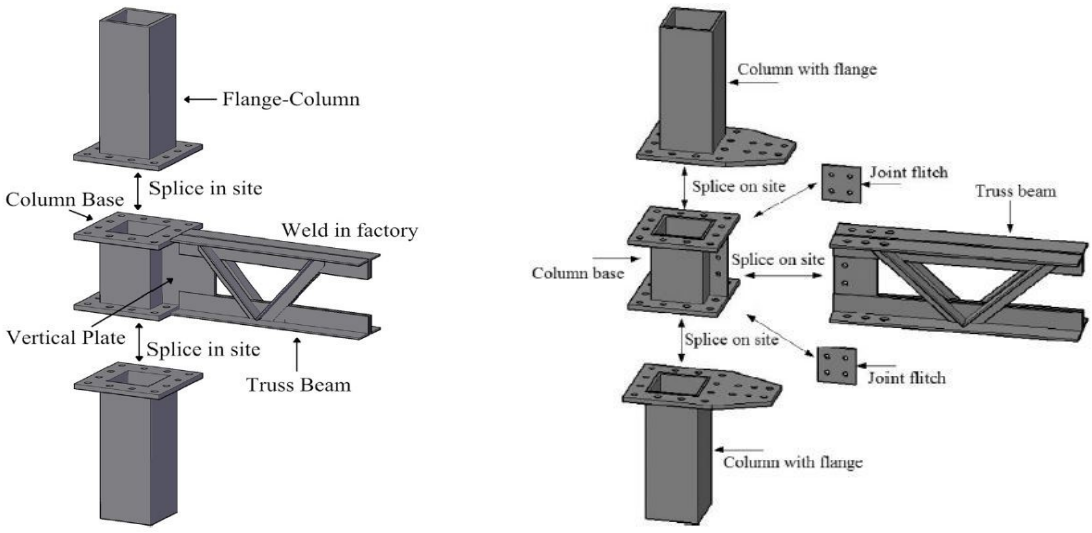

(a) (b)

Figure 2.10: a) Modular welded joint (Liu et al. 2015); b)Modular bolted truss-to-column connection (Liu et al. 2018)

Alongside the development of column-column-beam connections, the Chinese research center worked on investigating the column-to-column bolted-flange connection, illustrated in Figure 2.11b, to understand its bending and shear performance. The study succeeded in identifying the key parameters that affect the behaviour of the connection. Increasing the thickness of the flange plate helped reduce the yielding of the plate, thus helping to direct the force to tension in the bolts. This bolted connection can be applied to a wide range of modular systems (Liu et al. 2018).

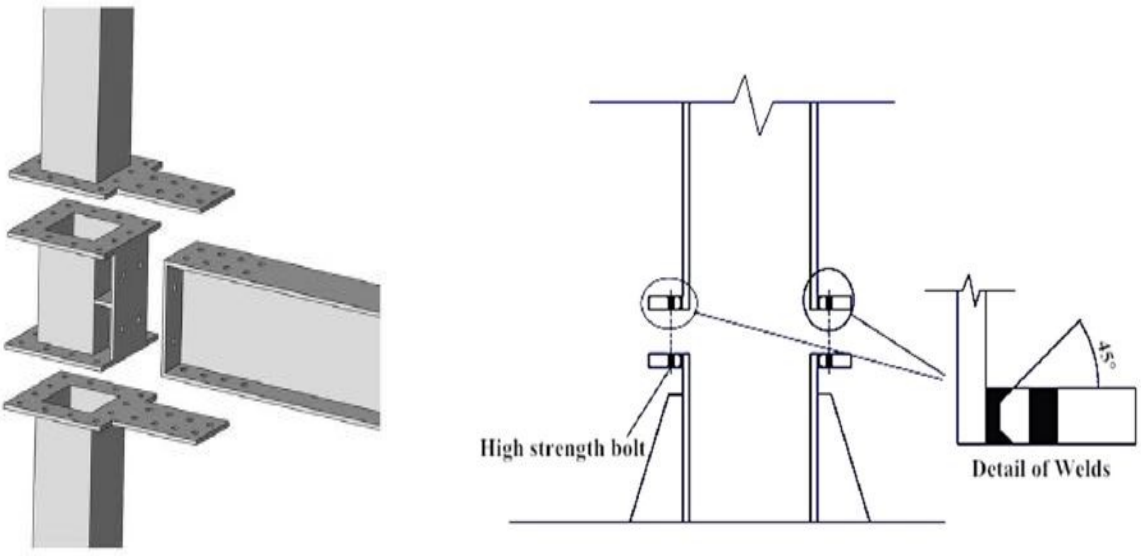

(a) (b)

Figure 2.11: a) H-section beam to HSS column connection (Liu et al. 2017), b) column-to-column bolted-flange connection (Liu et al. 2018)

An innovative interior connection for modular buildings was presented by Chen et al. 2017. The connection was proposed to replace the use of plates in connecting modular volumetric units, as using plates causes construction difficulties, especially for inner connections, as in Figure 2.12. The results of the experimental test of the connection concluded that the connection had good flexural ductility and stiffness. Nevertheless, the connection failed to tie all units to work as one building. Instead, units diverge under dynamic lateral loads and move independently. Therefore, this type of connection is not suitable for use in modular structures built in seismic zones.

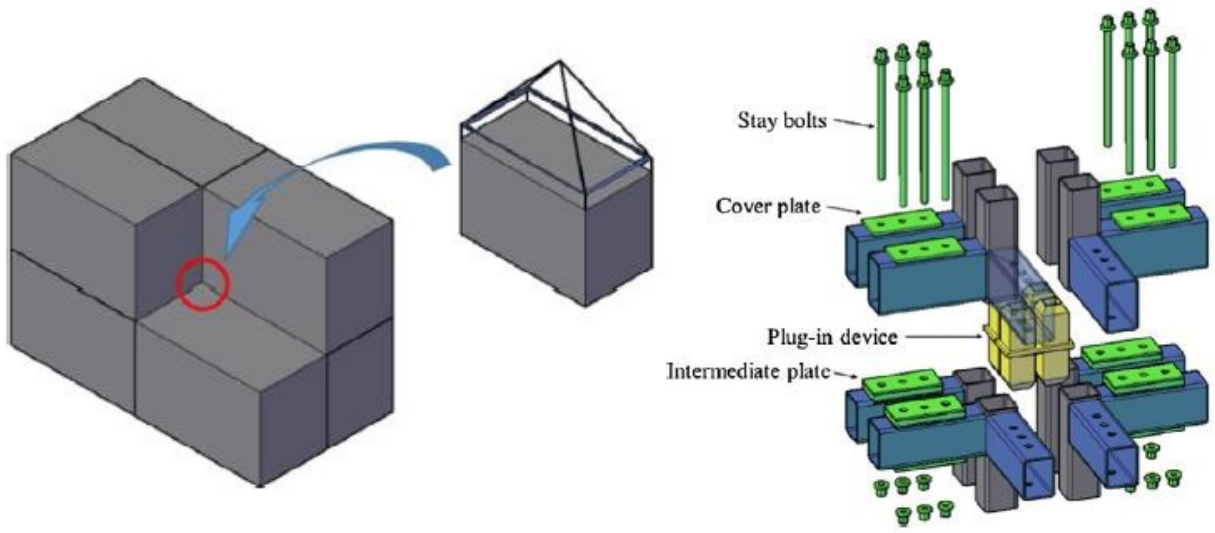

(a) (b)

Figure 2.12: a) inner connection region, b) proposed interior connection (Chen et al. 2017).

Previous studies showed that modular braced steel frames need special detailing, particularly at their vertical column-to-column connections (Annan et al. 2009). A study on the use of Superelastic Shape Memory Alloy bolts in vertical connections of modular braced steel frames—similar to Figure 2.2a—was conducted to improve behaviour under seismic loading. The vertical connections showed a good response, as it helped in reducing the residual drifts of the frame. In low earthquake intensity, maximum inter-storey drift, which is the difference in drift between the top and the bottom of each storey, increases. On the other hand, in higher intensity earthquakes, the drifts are reduced compared to frames using normal steel bolts. Overall, the use of Superelastic Shape Memory Alloy bolts improved the behaviour of the structures, mainly in high seismic intensity (Sultana and Youssef 2018).

2.2.3 Design and seismic behaviour of concentrically braced frames (CBFs)

The concentrically braced frame (CBF) is a common steel lateral load resisting system that is widely used in Canada, especially for low-rise buildings, due to its simplicity in design and fabrication. CBFs are built from beams, columns, and diagonal members (braces). Under lateral loads, the braces act as the structural fuse; yielding and buckling of the braces act as an energy

dissipation mechanism that protects the structure from collapse or permanent damage to gravity load-bearing system members. Having the braces act as structural fuses, other frame members and connections should remain elastic. Therefore, all beams, columns, and connections are designed based on capacity design requirements to remain elastic under lateral loads (Metten and Driver 2015).

Based on ductility, which is the ability of the system to deform inelastically to dissipate the energy from the lateral loads, CBFs are categorized as either limited ductility (LD) or moderate ductility (MD) in S16. The design process for CBFs starts with calculating the base shear of the building and finding the loads on braced frame bays, including notional loads, so the load on each level can be found after that. Design requirements for MD-CBF can be found in Clause 27.5 in S16. Brace sections should be picked to resist assigned loads while meeting the slenderness ratio requirements of Clause 27.5.3.2 in S16. Beams, columns, and connections are designed based on the maximum tensile force (T_u) and expected compressive force (C_u) calculated with the probable yield stress (R_yF_y) of the brace member defined in Clause 27.1.7.

Under high lateral forces and as the frame starts moving laterally, the tension brace starts to elongate and yield. Simultaneously, the brace under the compressive force buckles when it reaches its buckling capacity, as can be seen in Figure 2.13. A full-scale test of a CBF with rectangular HSS braces showed the deformed shape of the frame after quasi-static loading; the deformed shape showed good agreement with the design assumptions (Figure 2.14) (Tremblay et al. 2003). The buckling of braces forms rotational points at the end of the braces. To allow the formation of hinges, a distance of at least two times the thickness of the gusset plate is recommended to remain clear (Figure 2.15) (Sabelli et al. 2013).

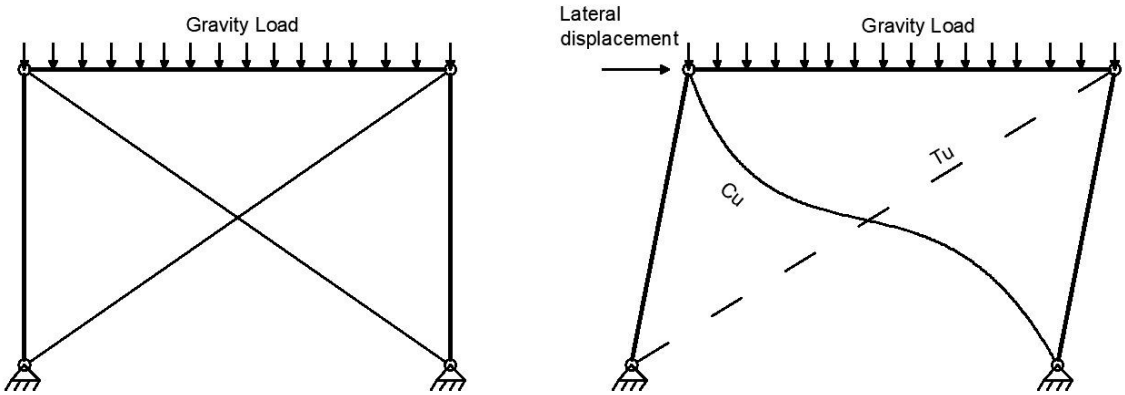

(a) (b)

Figure 2.13: (a) Undeformed frame, (b) deformed frame under lateral displacement

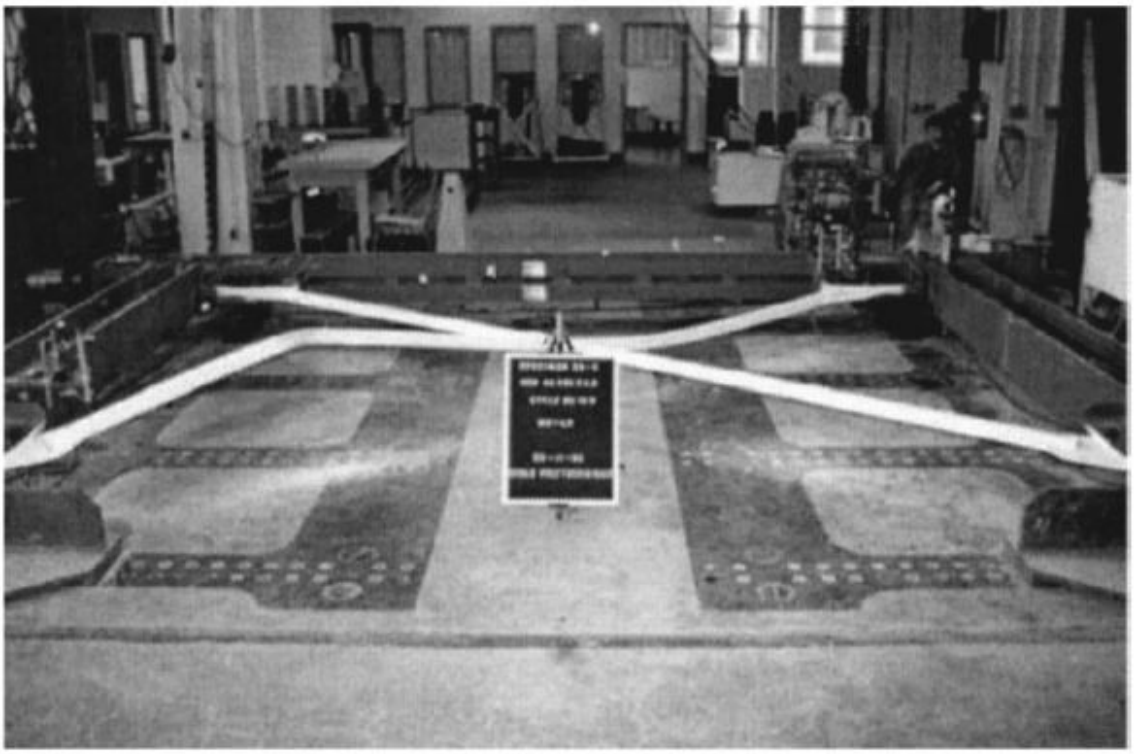

Figure 2.14: Full-scale CBF after applying lateral displacement (Tremblay et al. 2003)

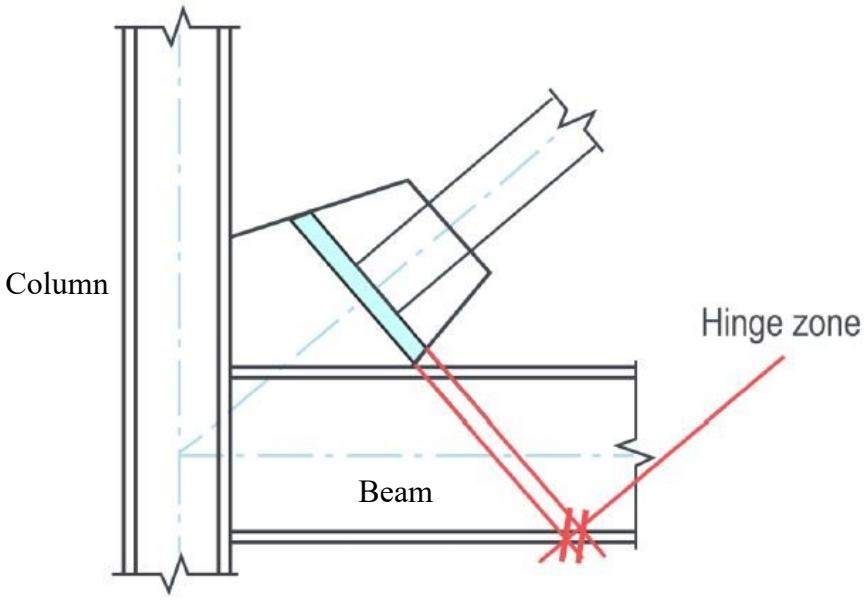

Figure 2.15: Hinge zone at gusset plate (Sabelli et al. 2013)

Chapter 3: Proposed modular steel system

In this chapter, the proposed modular steel system is introduced. First, the key parameters and constraints that led to the selection of the modules are discussed. Then, the structural components of the proposed modules, including members and connections, are presented. Finally, the constructability of the system and how it can be configured to accommodate different building plans being presented.

3.1 Dimension and geometry considerations

Several constraints that dictate the dimensions of the proposed modules were considered that include the transportation of modules, module size, column spacing, fabrication, and assembly. Shipping modules from the fabrication shop to the construction site is one of the major limitations that control the dimensions and the weight of structural modules. Although large modules (e.g., up to 7.3 m wide) can be transported by applying extra requirements and obtaining special permits, the process will not necessarily be the most economical choice, especially if the modules need to be hauled in streets or highways (WF Steel & Crane 2019). Therefore, the dimensions of the proposed modules were obtained using the requirements prescribed in "Module 4: Weight and Dimensions" by the Government of Alberta (2018), to ensure a safe transportation process while minimizing the need to acquire additional safety permits. Table 3.1 from this document shows the safety requirements and restrictions for the transportation of oversized loads.

Table 3.1: Over-dimensional safety requirements acquired from (Government of Alberta 2018)

Vehicle dimensions	Requirements
Over 2.60 metres wide (8’ 6”)	• Vehicle equipped with flags by day. • Vehicle equipped with warning lights by night or during adverse weather conditions.
Over 3.05 metres wide (10’)	• As above plus 2-dimension signs at the front and back of the vehicle in a manner that is clearly visible to approaching traffic.
Over 3.35 metres wide (11’)	• As above plus 1 or more flashing lights.
Over 3.85 metres wide (12’ 6”)	• As above plus 1 pilot vehicle behind when on 4-lane road or 1 pilot vehicle in front when on 2-lane road. • No movement from 3:00 pm until midnight on a Friday or a day preceding a statutory holiday. • No movement on a Sunday or a statutory holiday.
Over 4.45 metres wide (14’ 7”)	• Vehicle equipped with flags, signs, and flashing lights. • On 2-lane road, need 1 pilot and 1 trailing vehicle. • On 4-lane road, vehicles up to 5.5m wide (18’) need 1trailing vehicle. • On 4-lane road, vehicles over 5.5m wide need 1 pilot and 1 trailing vehicle. • No operation on highway from 3:00 pm until midnight on a Friday or a day preceding a statutory holiday. • No operation on highway on Sunday or a statutory holiday. • Travel during daylight hours only.
Over 5.5 metres wide (18’)	• As above plus other conditions as specified on the permit. • Stopping on provincial highways only permitted at designated truck pull-outs (except for emergencies and power line lifting). • Travel during daylight hours only.
Over 5.3 metres high (17’ 4”)	• Notify power and telephone companies. • Travel during daylight hours only

3.2 Proposed structural modules

Proposed modules involve only the structural components including beams, columns and diagonals that form a volumetric structural unit. The modules are expected to be used in multi-storey residential, commercial, and office buildings. Therefore, the dimensions were selected to provide comfortable interior spaces for building occupants. Large clear spans between columns provide more flexibility in using the space inside the modules. Thus, the spans between columns were chosen, such that it gives the architectural designers more open space to design partitions based on the building occupancy and owner needs.

The proposed modules include gravity and braced modules. The former is used to carry gravity loads; however, the latter consists of steel concentrically braced frames (CBFs) and is designed to carry both gravity and lateral loads, including earthquake or wind load. The concept of the lateral load-resisting system proposed here is independent seismicity level of the building site and whether the wind or seismic load governs the structural design of the braced module. Special detailing to ensure the ductility capacity of steel braces are required when the braced modules are designed to resist seismic loads.

The three-dimensional view and elevation view of the proposed gravity modules that include beams and columns are given in Figures 3.1 and 3.2, respectively. Figures 3.3 and 3.4 show, respectively, the three-dimensional view and elevation view of the proposed braced modules that include beams, columns, and X-bracing. Temporary lateral bracing are proposed to be used in the bays without steel diagonals to ensure the lateral stability of modules during loading, transportation, unloading and assembly. Such bracing systems can also help efficiently assemble the modules on site.

The height of each module was set equal to 3.6 m, and the width of the modules was limited to 3.5 m centre-to-centre on columns. The span of each bay of the module was set to be 7 m, which gives a total length of 14 m for the whole module.

The total height of the multi-storey building structure made of the proposed modular system may be controlled by the height limit imposed by building codes for the braced modules stacked along the height of the structure (e.g., 40m limit when Moderately Ductile steel Concentrically Braced frame system is used to carry lateral seismic loads) and the construction challenges such as controlling the stack effects.

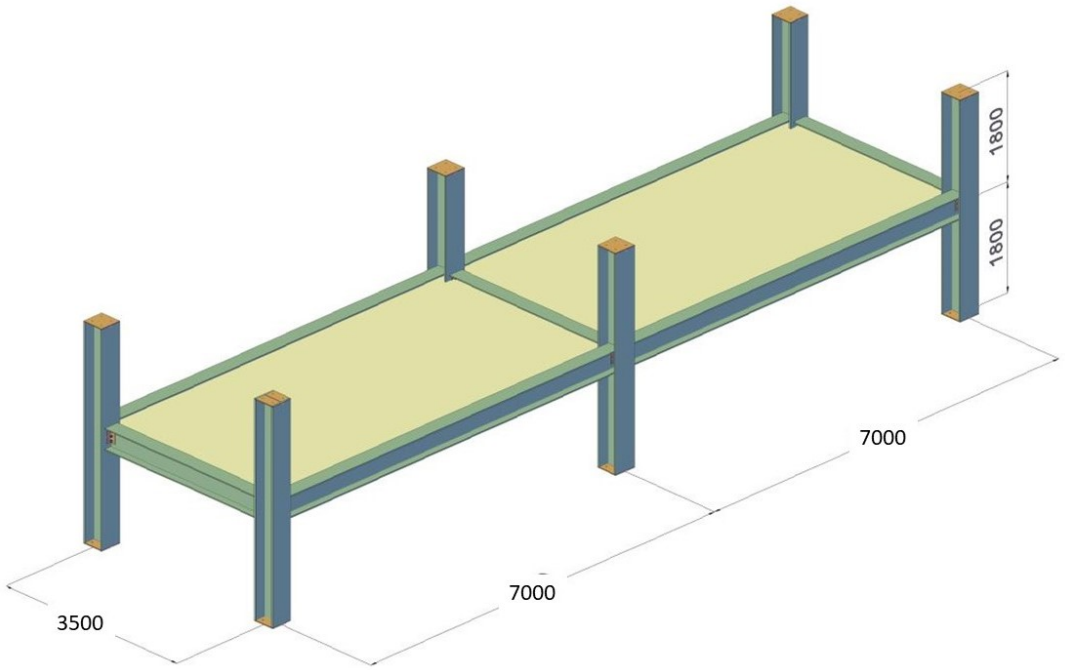

Figure 3.1: Gravity module (dimensions in mm)

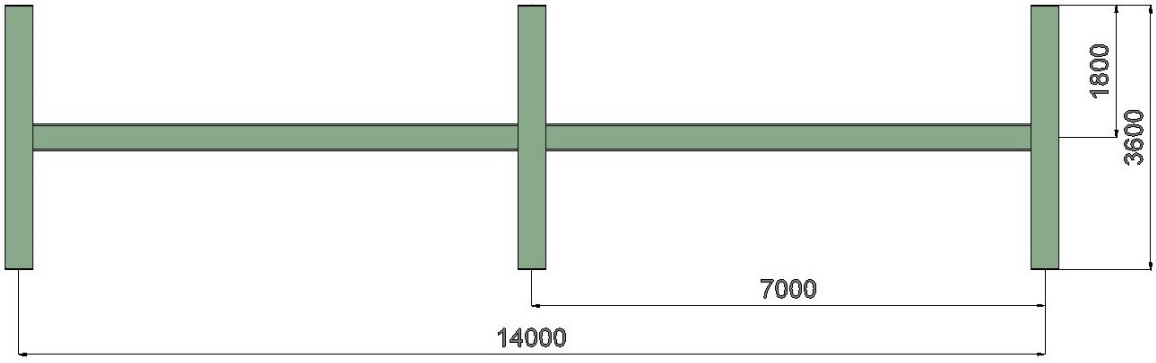

Figure 3.2: Elevation view of gravity module (dimensions in mm)

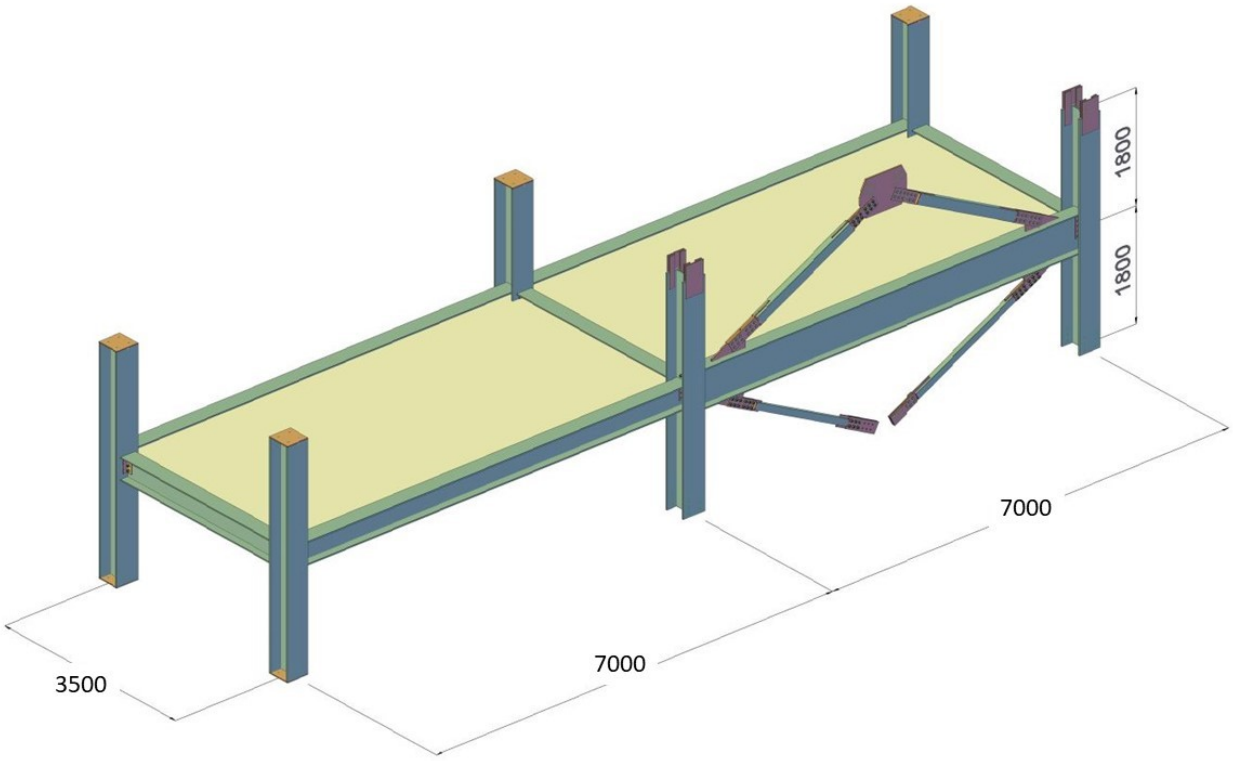

Figure 3.3: Braced module (dimensions in mm)

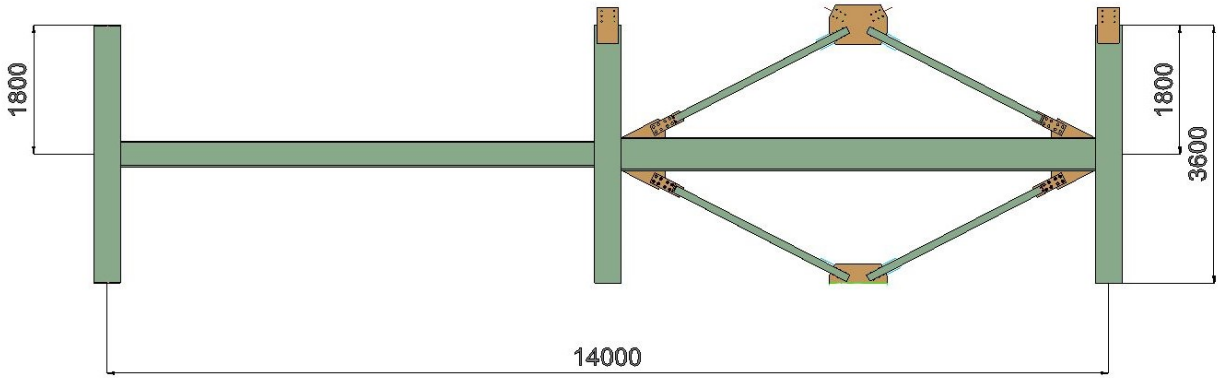

Figure 3.4: Elevation view of the proposed module (dimensions in mm)

3.3 Structural components of proposed modules

The modular structural system is constructed using structural steel because it is wildly available, reusable, and eco-friendly, and possesses high strength and ductility. Wide-flange (W-shape) members were selected for the columns and beams. For the lateral load resisting system (LLRS), integrated concentrically braced frames (CBFs) are used. CBFs are one of the most common LLRSs with relatively easy fabrication as compared to other conventional LLRSs. For the bracing members, rectangular hollow structural sections (HSS) were selected due to their higher compressive strength (Davaran et al. 2015). The columns of the braced frame are oriented on their weak axis in-plane.

The modules are developed, such that each creates half of the storey below the floor plus half of the storey above; the modules are connected at the mid-height of each storey. This arrangement avoids the eccentricity that might take place between modules stacked on top of each other, similar to that in the system proposed by Annan (2009), shown in Figure 2.2. Moreover, splicing modules at mid-height facilitates the assembly and bolting. Finally, such an arrangement can ease the maintenance and disassembly of the structure (WF Steel & Crane 2019).

The first vertical connection level is proposed to be situated at the second storey. Therefore, the total height of the first storey modules is from the base plates of columns to the mid-height of the second storey. With the height of all storeys to be identical, the total height of the first module would be 1.5 times the height of the other modules (Figure 3.5). The transportation of higher first-story modules is expected to add to transportation cost because of safety requirements associated with such taller modules; however, it is expected that avoiding column splices in this module contributes to reducing construction time.

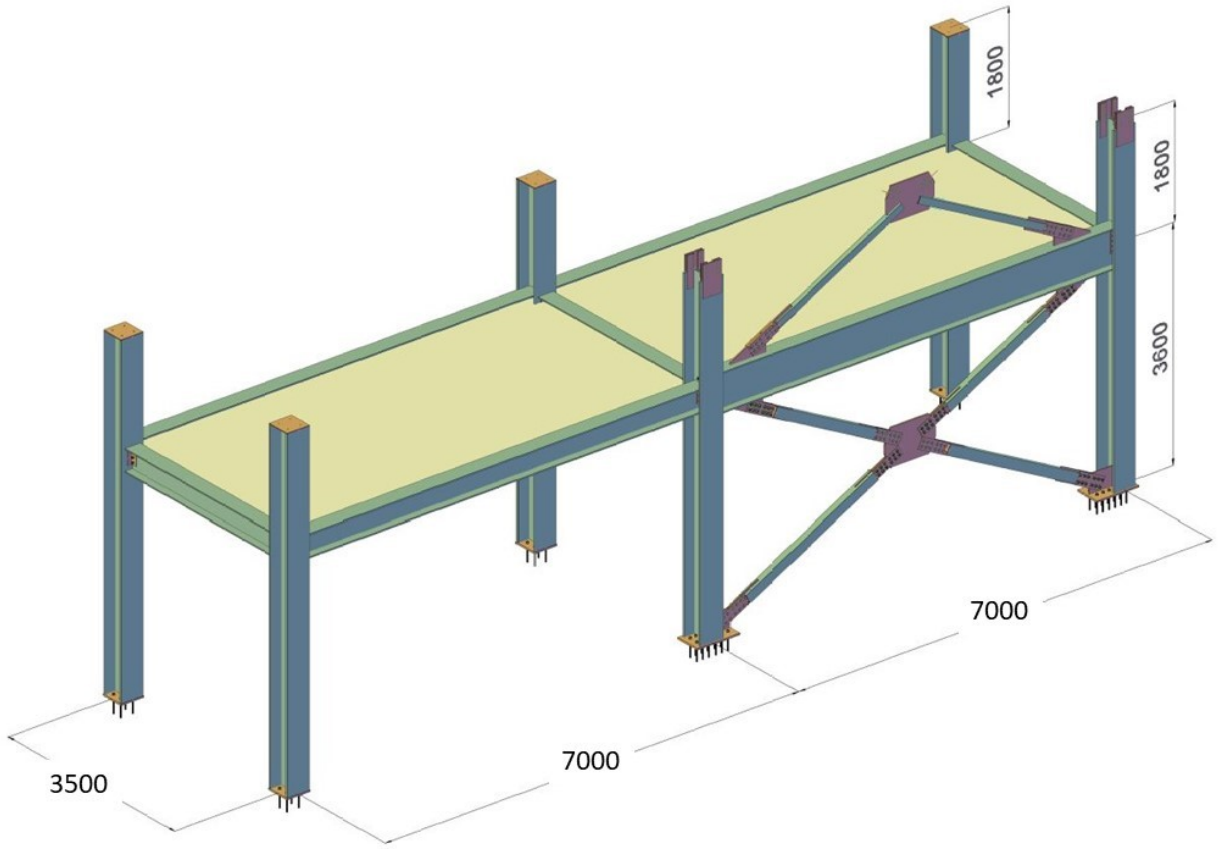

Figure 3.5: First storey braced module (dimensions in mm)

It is proposed that a floor system be used that can accommodate various types of prefabricated slabs such as hollow-core precast concrete, mass timber panels, steel joist slabs or any similar modular flooring system. The selected slab system should be designed and detailed taking into account a safe lateral load transfer to the lateral load-resisting system of the modular structure. An example of a flooring system that can be used with the proposed modular system is the innovative modular steel floor system developed by (Zhuo 2018) (Figure 3.6).

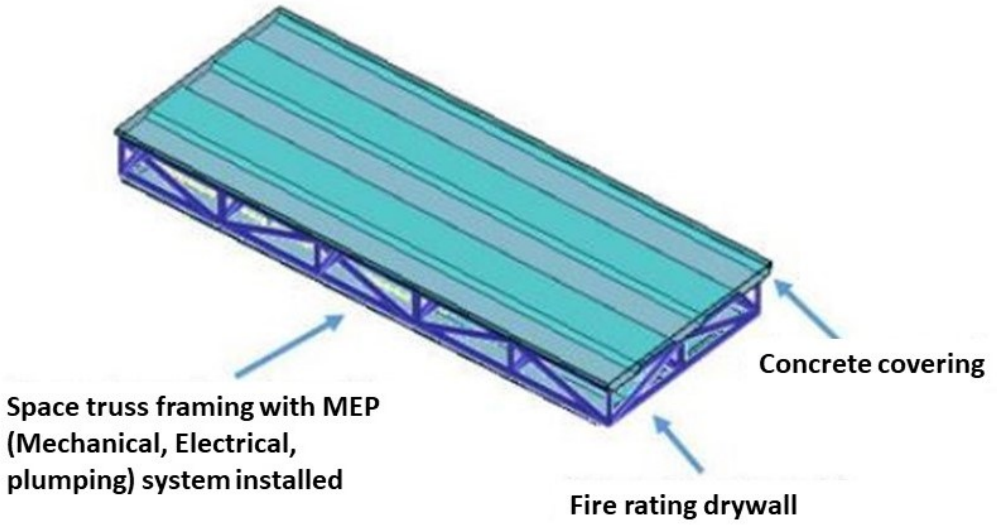

Figure 3.6: Modular steel flooring system (Zhuo 2018)

3.4 Connections

The connections proposed for the modular system were selected to minimize installation efforts and time while enhancing the fabrication process in the shop. Discussions with a leading modular steel fabricator in Alberta helped refine the proposed connections (WF Steel & Crane 2019).

Bolted connections are commonly used by most contractors as they do not need skilled iron-workers, as opposed to welded connections. Thus, most of the module connections, particularly those to be erected on-site, were chosen to be bolted. Although welding is still required for some connections, all the welds must be performed in the shop and only bolted connections are allowed at the construction site.

With the selected geometry of the braced frame module, the corner gusset plates are only connected to the beam's flange to avoid complex joint connections. The proposed module braces are connected to the corner gusset plates, which are, in turn, welded to the beam (Figure 3.7). Single or double knife plates are welded into slotted HSS braces at one end and bolted to the corner gusset plates at the other. Adding to the ease of fabrication and assembly, the braces are bolted to the

corner gusset plate to account for maintenance or rehabilitation of the structure in case of a major seismic event.

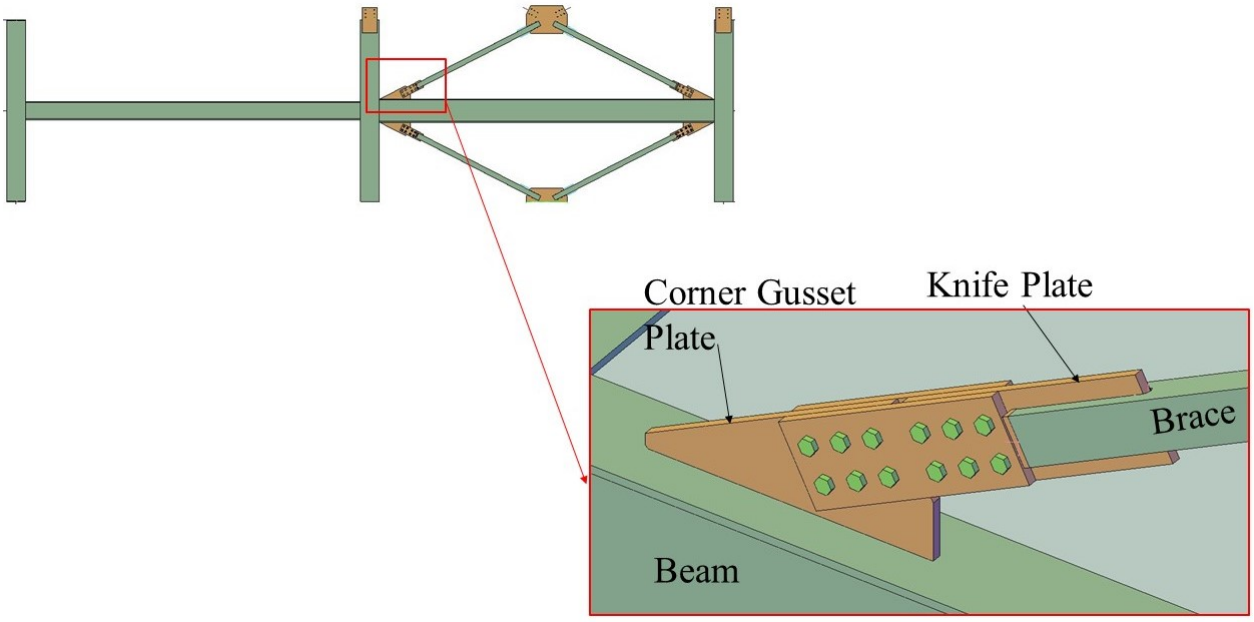

Figure 3.7: Corner gusset plate connection

The beams of the frame are connected to columns via bolted double-angle shear connections. Double angles are connected to the web of the beam and to the column flange or web, based on the column orientation, through bolts. Both sides of the angles can be bolted or just the side connecting to the beam (Figure 3.8). This type of connection is widely used in steel buildings to connect beams to columns, especially when loads transferred through connections are relatively high.

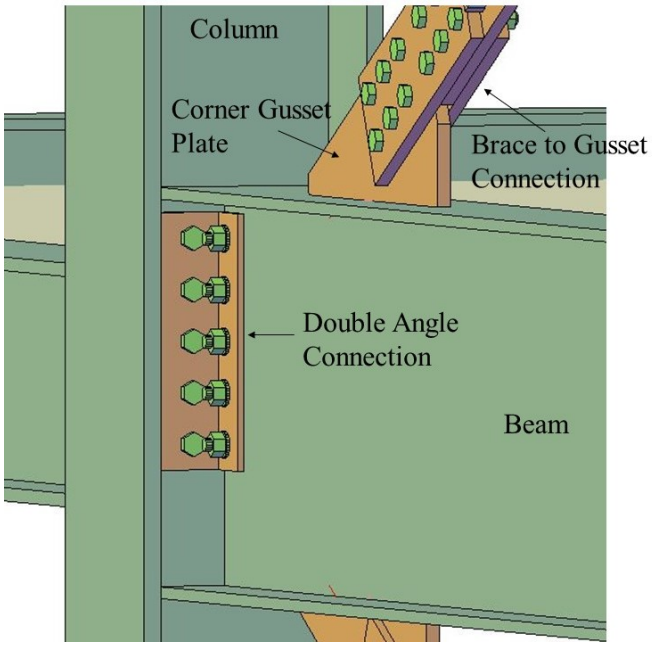

Figure 3.8: Bolted double angle beam-to-column connection

Modules are connected vertically through three types of connections: 1) gravity column splices; 2) braced frame column splices; and 3) middle gusset plate splices, as illustrated in Figures 3.9 and 3.10.

Columns that are not part of the CBF are designed under gravity loads only. End-plate splices are used to transfer the axial loads through the columns to the base of the building. End plates are welded to the ends of columns and then bolted together on-site (Figure 3.9a). End-plate splices are very common as they are fast to erect on-site. Columns of CBFs undergo both axial tension and compression during seismic events; therefore, cover-plate splices are used to connect the columns. As shown in Figure 3.9b), double plates are used on column flanges to increase the shear capacity of bolts. The plate can be welded to the lower module columns and bolted to the upper column or be bolted to both modules.

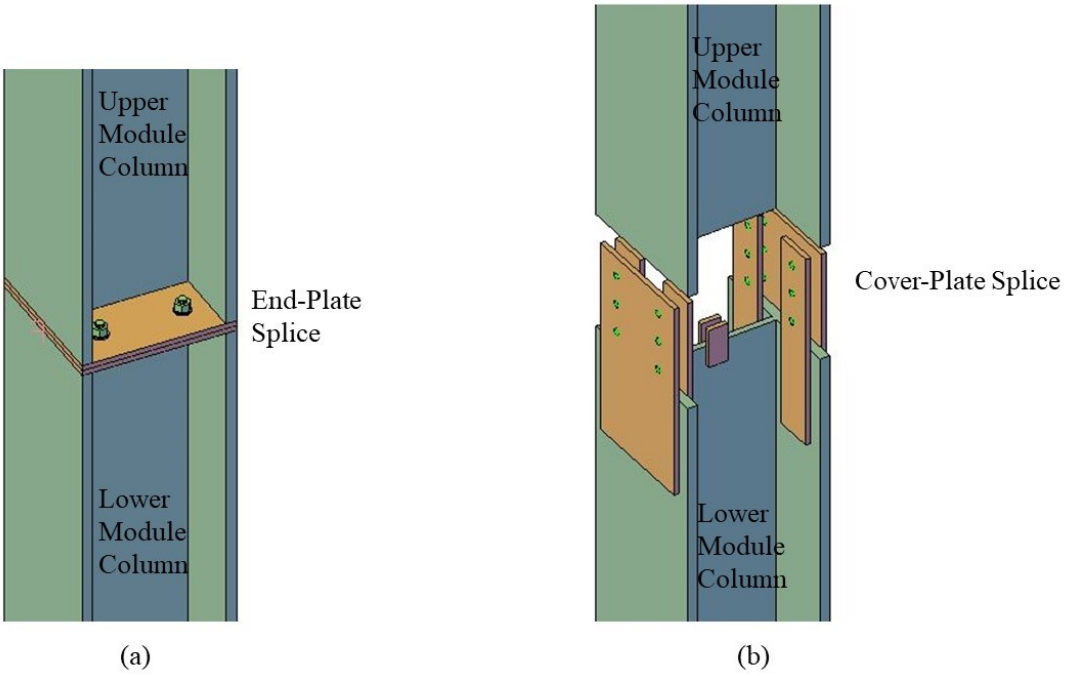

Figure 3.9: a) Gravity column splice, b) CBF column splice

In the proposed modular system, braces are connected at the storey's mid-height, which means that both braces are discontinuous and connected on-site through a middle gusset plate. The middle gusset plate is bolted to the lower module in the shop, which leaves only the braces of the top module to assemble on-site (Figure 3.10 and 3.11). To connect the braces to the middle gusset plate, knife plates are welded into the brace at one end and bolted to the middle gusset plate at their other end (Figure 3.10 and 3.11).

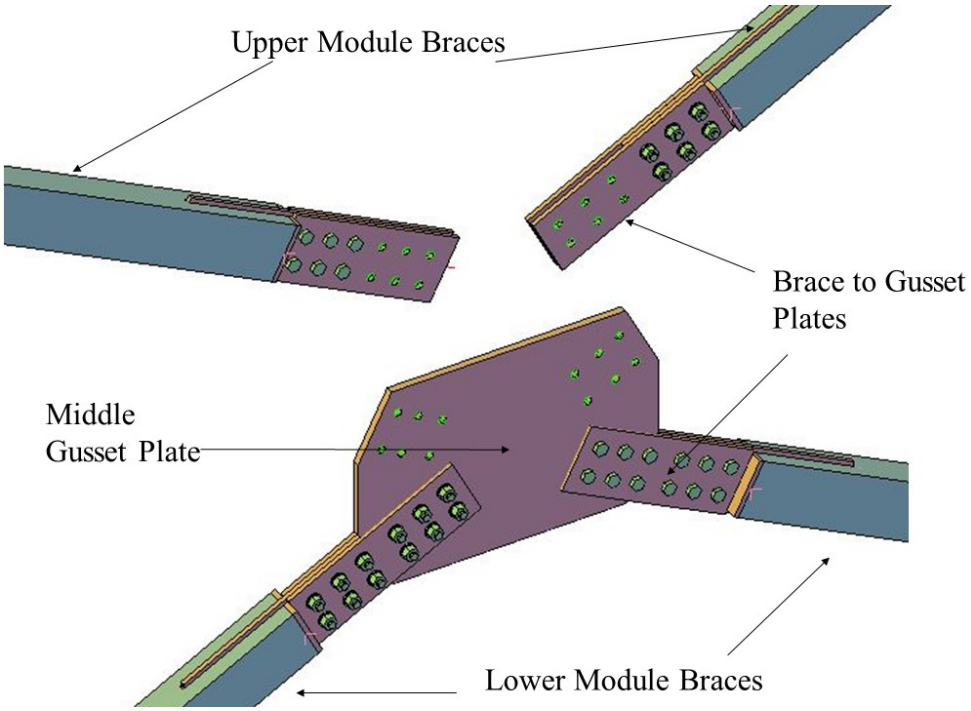

Figure 3.10: Middle gusset plate connection (before the assembly of the top module)

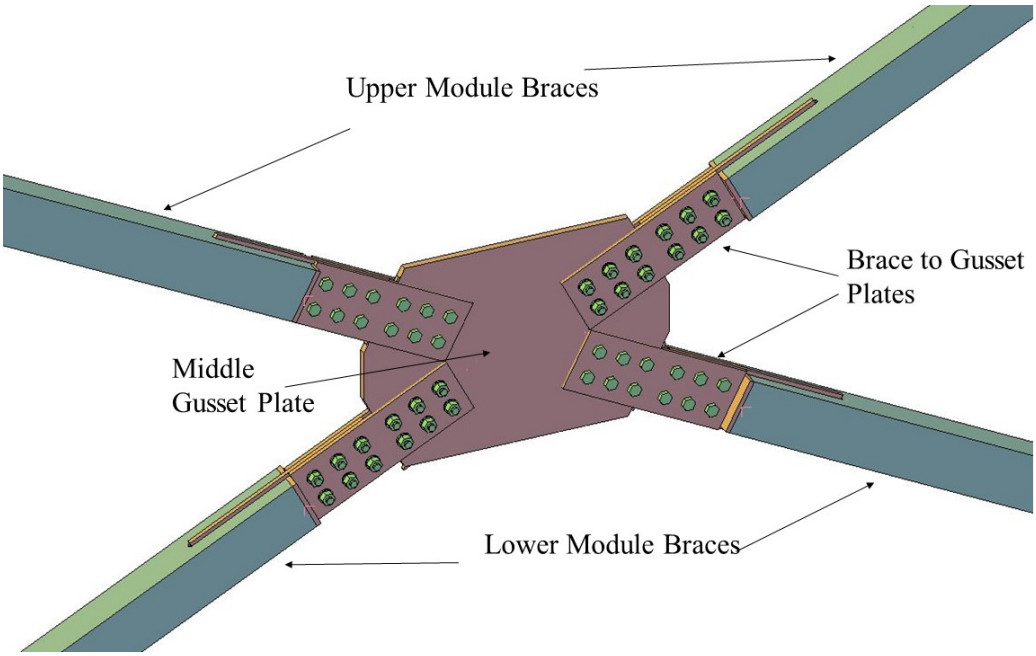

Figure 3.11: Middle gusset plate connection (after the assembly of the top module)

3.5 Module arrangement and construction sequence

The connections between modules are first described, followed by various building configurations that can be achieved using the proposed modular system. A prototype building is used for this purpose. Finally, the construction sequence for a six-storey building is presented.

3.5.1 Lateral load resisting system of the modular frame

When the braced modules are stacked on top of each other, the upper half-braces of the lower module are connected to the lower half-braces of the upper module to create an X-bracing panel. Figure 3.12 shows an example of the second (in green) and third (in blue) modules connected vertically. The red line shows the X-bracing that is finally formed in the frame.

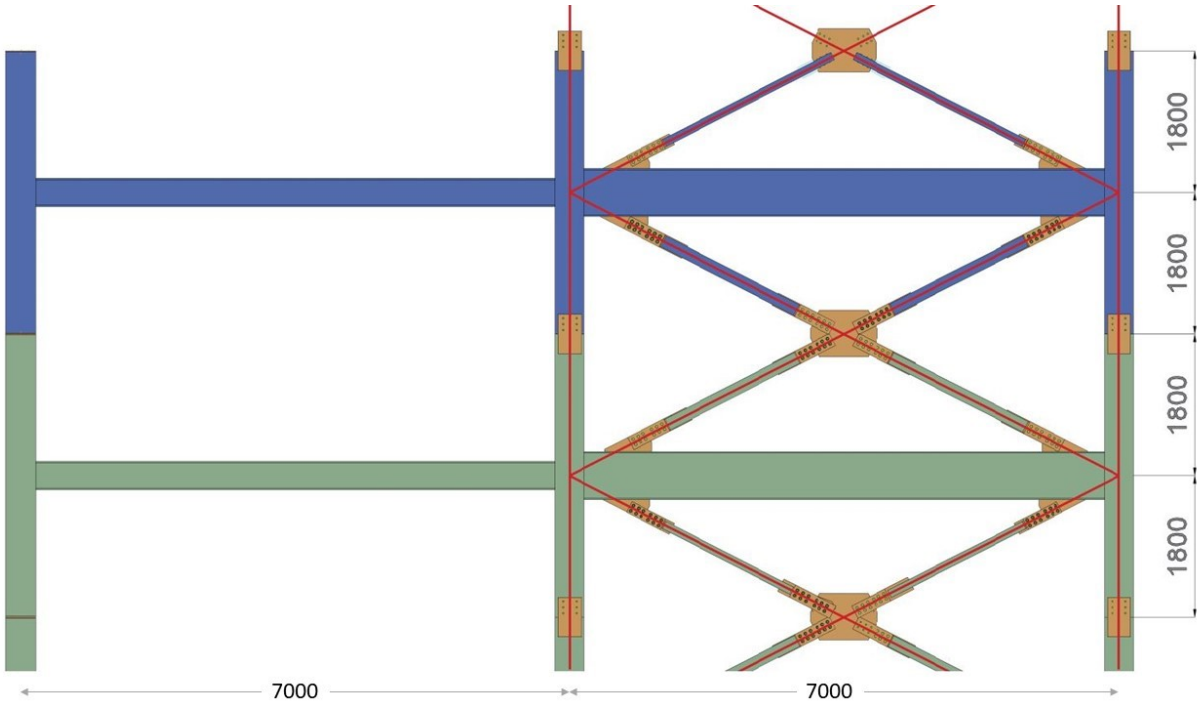

Figure 3.12: Braced module assembly including second storey (green) and third storey (blue) modules (dimensions in mm)

3.5.2 Module Configurations

The proposed structural modules were designed such that they can be used to create various building shapes. The geometry of the modules can also vary to efficiently achieve the anticipated shape. Figure 3.13 shows the module's arrangements used to produce three different building shapes. In this figure, the modules are represented using the black hatched area. The beams to be assembled on-site to connect modules laterally are represented using the blue lines. The crossed red areas show the slabs to be assembled on-site.

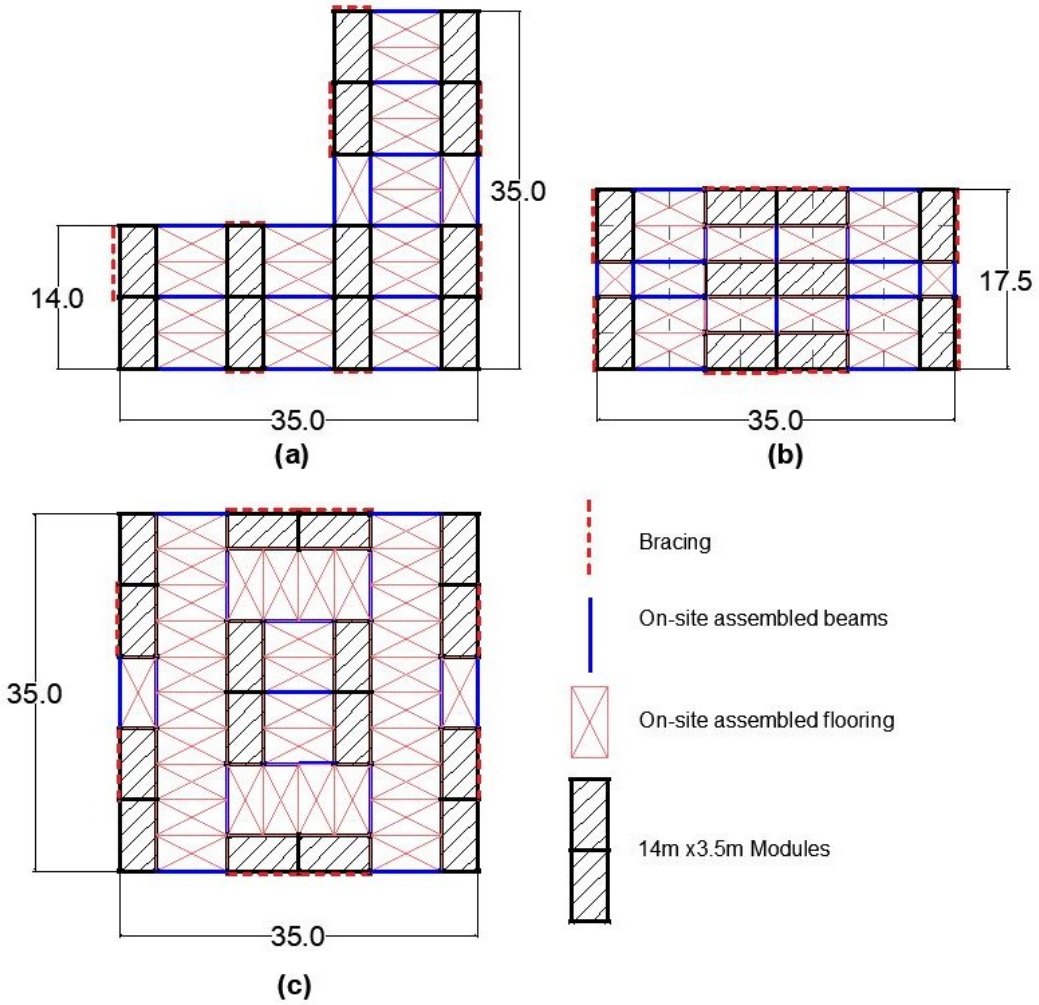

Figure 3.13: Module layouts forming various building geometries (dimensions in m)

To better understand the effect of module arrangements on construction time, a prototype building with plan dimensions of 35 m × 35 m was chosen. Five different module arrangements were evaluated and compared based on the following parameters:

- Number of columns
- Number of volumetric modules
- Percentage of slab area assembled on site
- Number of beams assembled on-site

The selected parameters are compared in Table 3.2 for the five module arrangements illustrated in Figure 3.14. The parameters are indicators of the cost and construction time. The number of columns and beams used can reflect the cost and speed of the construction; the more members (columns and beams) used in the buildings, the more steel needed and a higher number of connections to be assembled on-site. The on-site slab assembly percentage shows the area to be covered on-site with respect to the total area of the floor. Comparing different arrangements resulted in the selection of arrangement C as the best alternative out of the five arrangements compared. Note that there are several other parameters such as transportation, crane capacity, the geometry of the building, etc. that can also influence the selection of the arrangement. These parameters are not studied here.

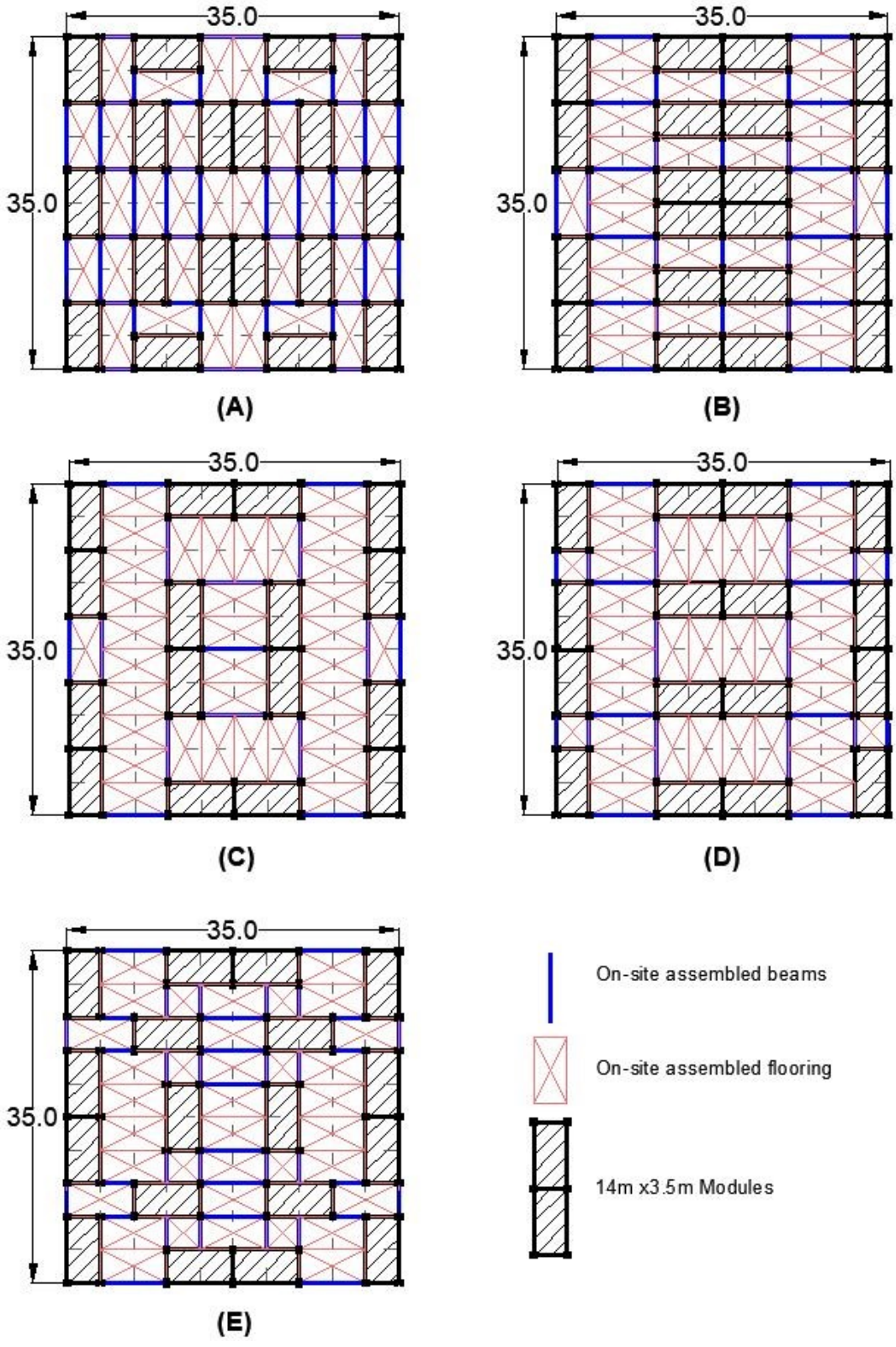

Figure 3.14: Module arrangements for a square prototype building (dimensions in meters)

Table 3.2: Comparison of module arrangements for the prototype building

Module Layout	Module and member dimensions			No. of Columns	No. of 3D Modules	On-site Slab Assembly (%)	No. of On-site Beam Assembly
	Modules (m^2)	Beams (m)	Slabs (m^2)				
A	7 × 3.5	7 & 3.5	7 × 3.5	72	18	64	44
B	14 × 3.5	7 & 3.5	7 × 3.5	60	10	60	28
C	14 × 3.5	7	7 × 3.5	48	8	68	15
D	7× 3.5 & 14 ×3.5	7 & 3.5	7 × 3.5 & 14 × 3.5	52	10	68	22
E	7 × 3.5 & 14 × 3.5	3.5	7 × 3.5 & 14 × 3.5	68	16	64	38

3.5.3 Construction sequence

Figure 3.15 shows the construction sequence for the proposed modular system. Once the earthwork and foundations are completed, first storey modules are set in place (Figure 3.16). Then, the beams connecting the modules are assembled (Figure 3.17). This is followed by installing modular slab units (Figure 3.18). Once the first storey is complete, the modules of the second storey are placed on top of the first-storey modules (Figure 3.19). The beams between the modules are then installed in a similar manner as the first-storey modules. Once this step is completed, the slabs are installed to form the second storey floor. These steps are repeated until the last storey is constructed (Figure 3.20). It is worth noting that assembling units vertically may involve several erection and

construction imperfections such as vertical staking effects, settlements, or out-of-plumpness of modules, which can negatively affect construction time and costs.

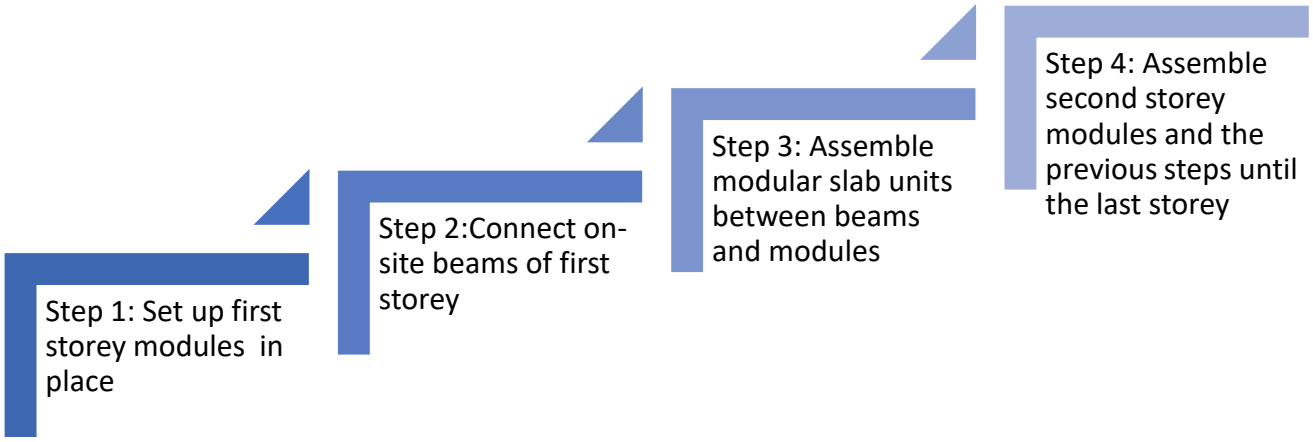

Figure 3.15: Construction sequence for the proposed modular system

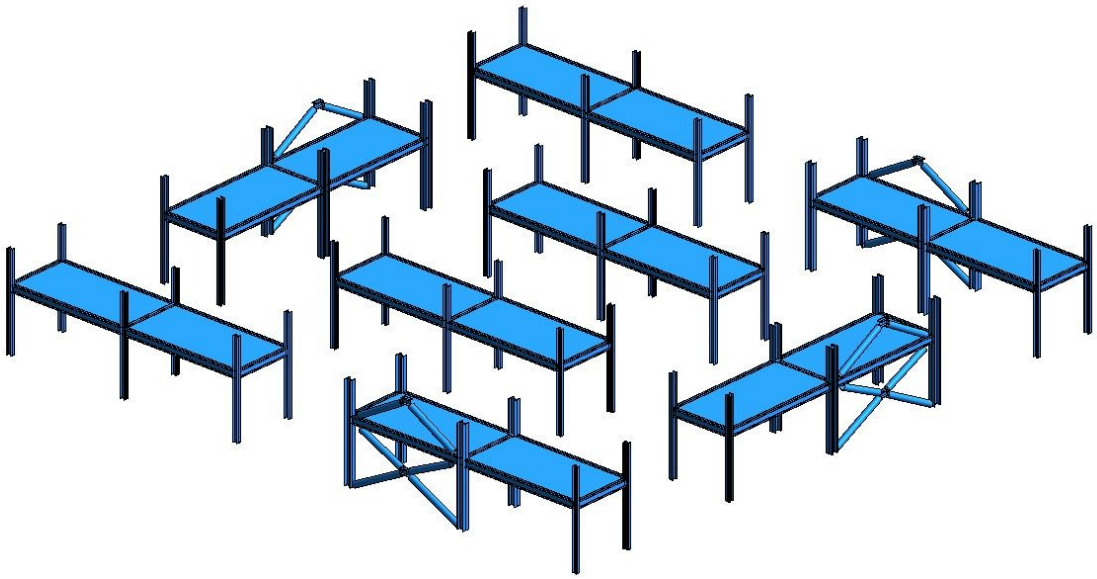

Figure 3.16: Construction sequence Step 1: Setting first storey modules (shown in blue) in place

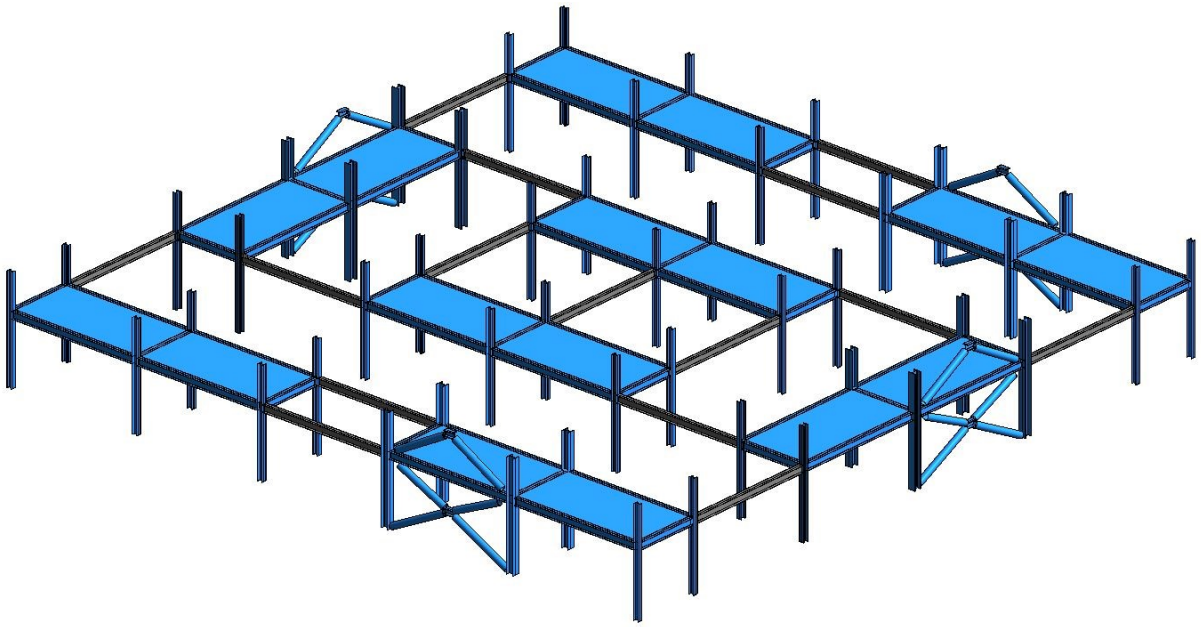

Figure 3.17: Construction sequence Step 2: Assembling first storey beams (shown in grey) between modules

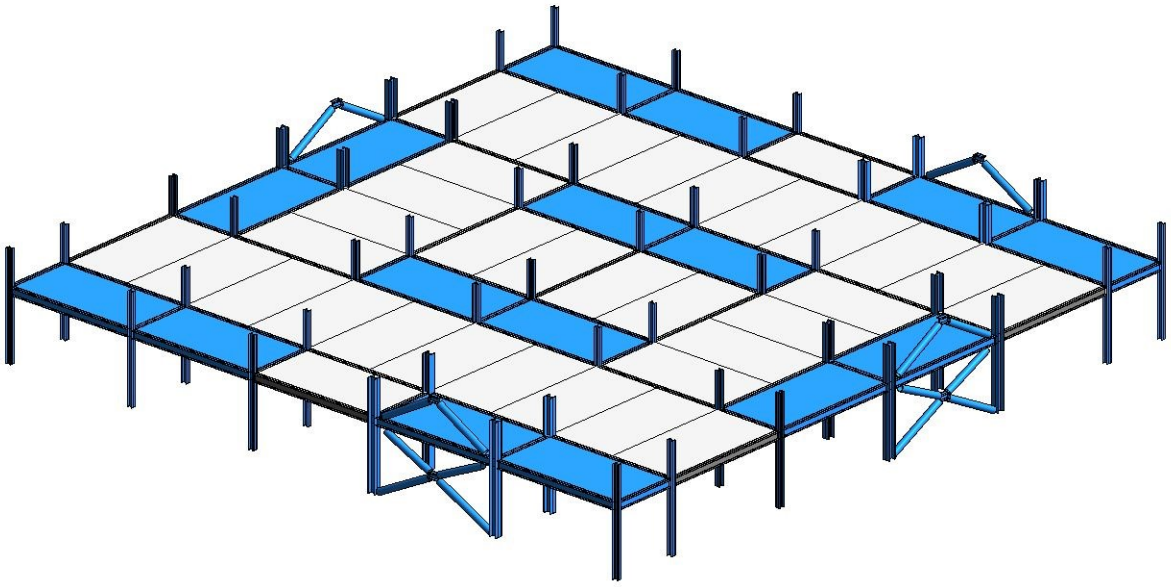

Figure 3.18: Construction sequence Step 3: Assembling slab units of the first floor (shown in light grey)

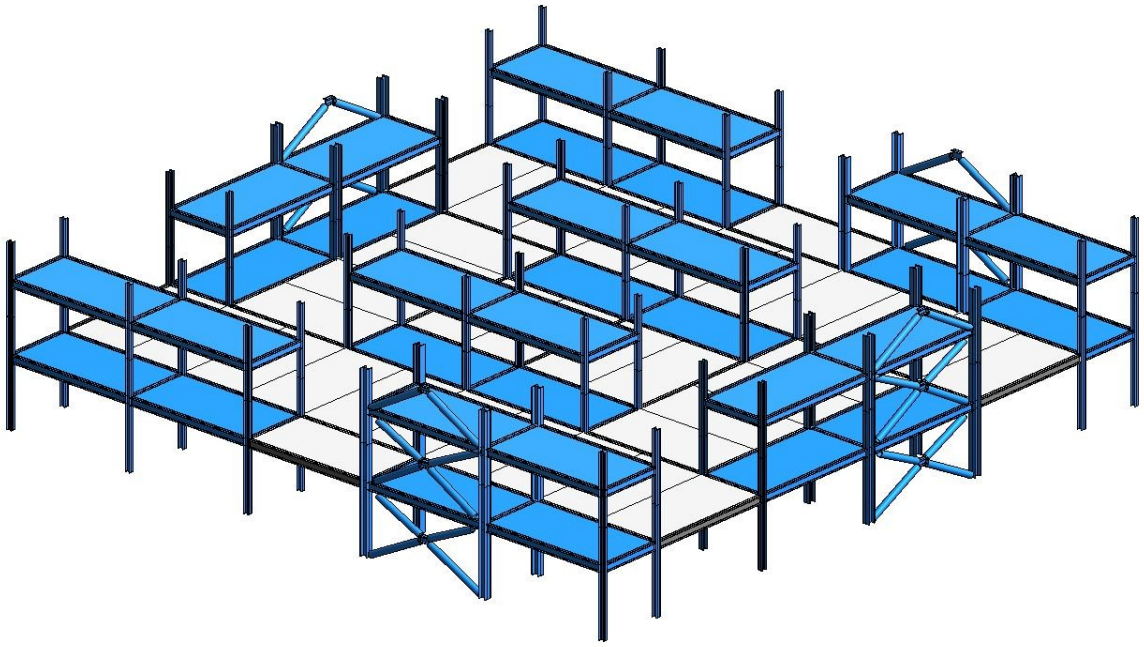

Figure 3.19: Construction sequence Step 4: Stacking second-storey modules on top of existing first-storey modules

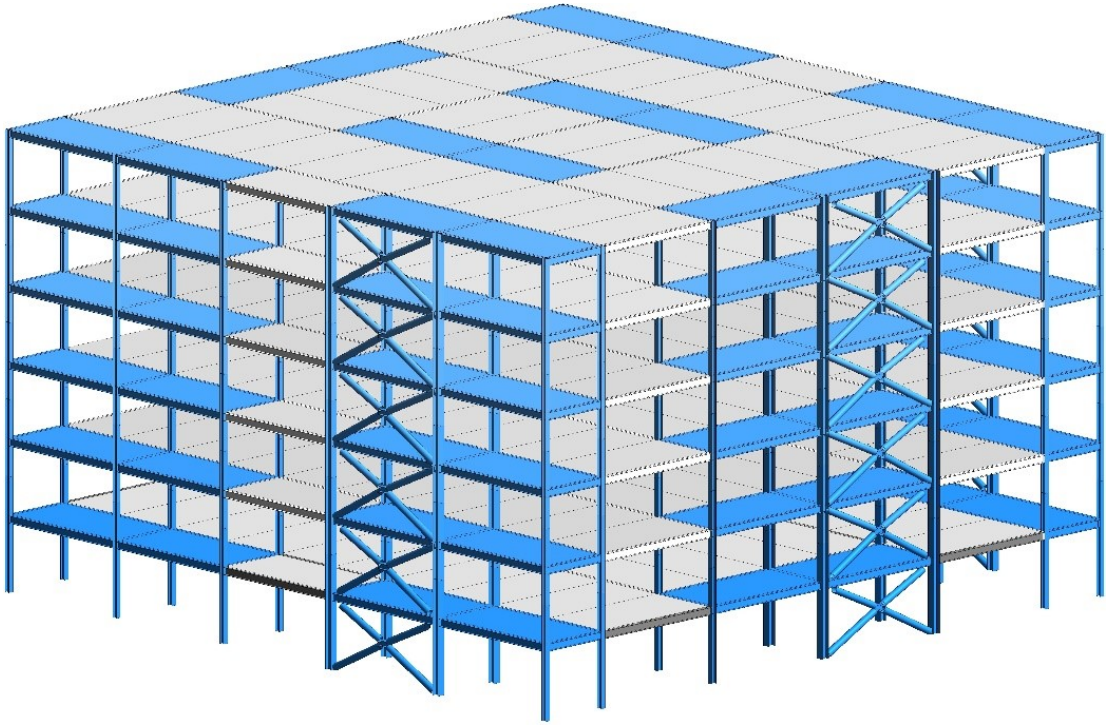

Figure 3.20: Final assembled structure of a prototype six-storey building built using the proposed modules

3.6 Summary

A new modular steel system and its components are introduced in this chapter. The module dimensions were selected based on both transportation limits and maximizing column spacing. The system consists of two types of modules: braced modules to carry lateral and gravity loads, and gravity modules to carry gravity loads only.

The structural members of the new system were developed with steel members due to the structural properties, availability, and the fact that steel is a recyclable material. Bolted connections were suggested for on-site assembly. The mid-height of the storey was selected as the level of connecting modules vertically; connecting modules at the mid-height of the storey helps enhance the assembly process. Collaboration with a local modular steel fabricator helped with the validation of the selected connections.

A prototype building plan was selected to compare the effect of module layouts on the cost and speed of the modular project. The number of members was used as an indicator of the cost and construction time. Finally, the chapter reviewed the suggested construction sequence of the new modular system and the final look of the modular building.

Chapter 4: Structural design of the modular system

This chapter presents the structural design of the proposed modular system performed in accordance with the Canadian loading code and steel design standard. Loading and design are illustrated for the six-storey prototype building of Chapter 3. Geometry and loads are first presented, followed by gravity and seismic analyses. The member's design is then provided. Finally, the design and detailing of connections are presented.

4.1 Prototype building

The prototype building chosen for the design example is a six-storey office building with plan dimensions of 35 m x 35 m (Figure 4.1). The module arrangement for the selected building complies with the most efficient arrangement of those in Table 3.2. The storey height is 3.6 m for all storeys. . In order to examine the behaviour of the proposed modular system, in particular the braced modules, under lateral seismic loads, the building is assumed to be located in a high seismic region of Canada, Vancouver, British Columbia. The soil type is Type C (very dense soil). Moderately Ductile (Type MD) steel Concentrically Braced Frames (CBFs) were selected to resist the lateral seismic load. Four CBFs are located in each principal direction of the building.

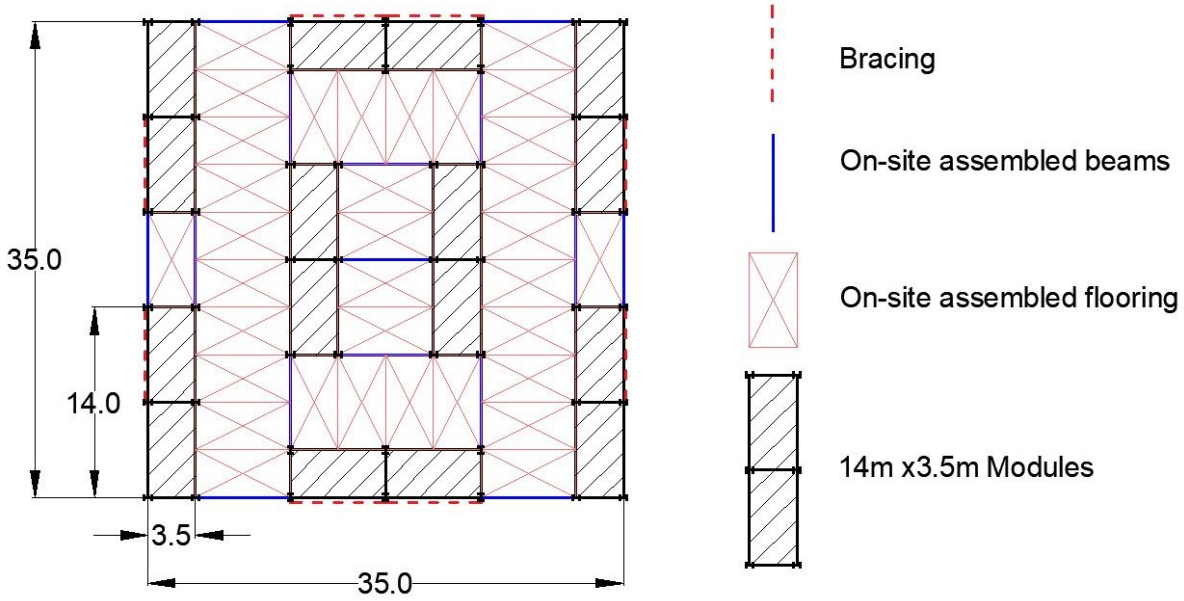

Figure 4.1: Prototype building plan

4.2 Loads

Structural loads, including gravity, wind and seismic, were calculated in accordance with the national building code of Canada (NBCC) (National Research Council of Canada 2015). The gravity loads are summarized in Table 4.1.

Table 4.1: Gravity Loads

Load	Magnitude (kPa)
Floor Dead Load	4.6
Roof Dead Load	3.4
Floor Live Load	2.4
Roof Live Load	1.0
Snow Load	1.64
Exterior Wall Load	1.5

Section 4.1.7 of NBCC 2015 was used to calculate wind loads on the prototype building. The assumptions used in the calculations are as follows:

- Reference velocity pressure, q = 0.45 kPa for Vancouver (City Hall)
- Importance factor: I_w = 1.0
- Exposure factor, $C_e = 0.7*(h/12)^{0.3} = 0.83 \geq 0.7$, ($h$ is the building reference height)
- Topographic factor, C_t = 1.0 (building not on hill)
- Gust effect factor, C_g = 2.0
- External pressure coefficient, $C_p = 0.27(H/D + 2) = 0.71$ for windward side and, $C_p = -0.27(H/D + 0.88) = -0.40$, for leeward side. ($H$ is height and D is width of building)
- External pressure P (combined)= $I_w.q.C_e.C_t.C_g.C_p$ =|0.53| kPa (windward) + |-0.3| kPa (leeward) = 0.83 kPa

According to the NBCC load combination, 1.25D (Dead load) +1.4W (Wind load) +0.5S Snow load was used to compute member forces under gravity and wind loads. The factored wind base shear calculated per CBF V_w/frame = 201 kN.

4.3 Seismic analysis

To calculate the seismic base shear, the equivalent static force procedure (ESFP) is employed as it is permitted by the NBCC for the prototype building (regular building with the height $h_n < 60$ and fundamental period $T_a < 2.0$ s.

Based on Section 4.1.8.11(3) of NBCC, the fundamental period is calculated as $T_{emperical} = 0.025$ $h_n = 0.54$ s < 2.0 s in both principal directions of the building. NBCC permits the modal analysis method to compute the design period T_a, taking into consideration the building's stiffness and mass. The period obtained from the modal analysis shall be less than two times the empirical value to be used in design; otherwise, $2 \times T_{emperical}$ should be used. SAP2000 was used to compute the analytical period (Figure 4.2) (CSI Computers and Structures Inc 2009), which resulted in $T_{analytical}$ = 0.98 s. This value is less than $2 \times T_{emperical,}$ and thus it is used as the design period of the building: T_a = 0.98 s. The calculations of the fundamental period and seismic forces are taken for the X-direction only.

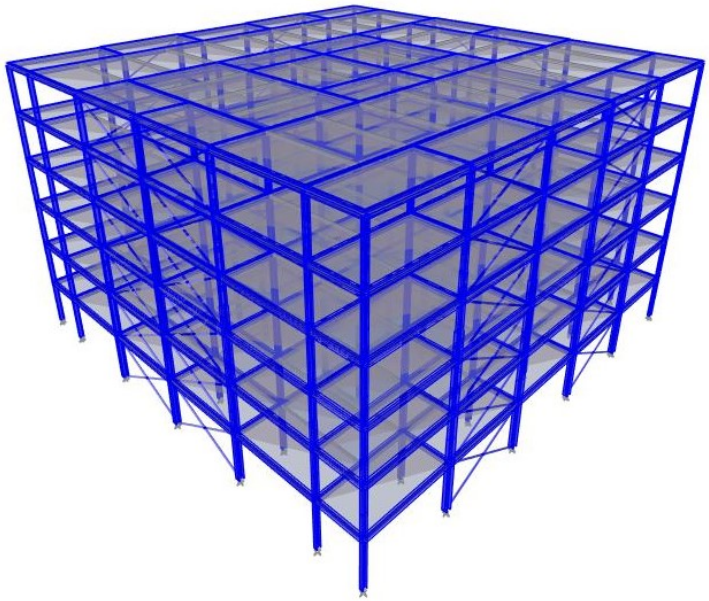

Figure 4.2: 3D model of the prototype building in SAP2000

The design spectral response acceleration *S(T)* is calculated using site coefficient *F(T)* = 1 for Type C soil, as defined from Table 4.1.8.4. This gives the value of site coefficients F_a and F_v = 1. Values of design spectral response acceleration *S(T)* are illustrated in Figure 4.3.

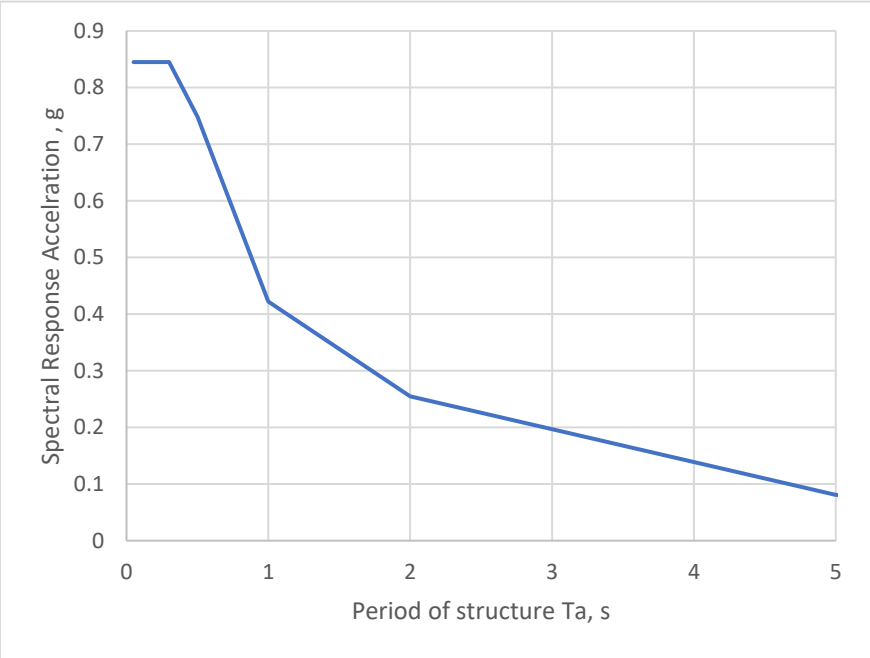

Figure 4.3: Spectral Response Acceleration for Vancouver (Soil Type C)

Based on Section 4.1.8.11, seismic base shear (*V*) is calculated as follows:

$$V = W.\ S(T_a).M_v.I_E/R_d.R_o \quad (1)$$

where

W: seismic weight of the building = dead load + 1.25 snow load= 36951 kN

$S(T_a)$*:* design spectral response acceleration = *S(0.98s)* = 0.44 g

M_v: higher mode factor = 1 for $T_a < 1$

I_E*:* Importance factor = 1

$R_d.R_o$*:* ductility and over-strength modification factors for Type MD-CBFs are $R_d = 3$ $R_o = 1.3$.

The total design base shear for the building in one direction is V= 4144 kN. This load is then compared with V_{min} and V_{max} defined as:

$V_{min} = W.\ S(2).M_v.I_E/R_d.R_o$ = 2416 kN.

$V_{max} = max\ (W.(2/3)S(0.2).I_E/R_d.R_o\ \&\ W.S(0.5).I_E/R_d.R_o)$ = 7087 kN.

The NBCC Section 4.1.8.12 permits calculating the seismic design load using a dynamic analysis procedure to obtain a more realistic seismic base shear (V_d) and lateral load distribution (F_x). The modal response spectrum analysis (MRSA) method was used to find the base shear using SAP2000. As per NBCC, this base shear should be compared with that calculated using ESFP to obtain the design base shear using the dynamic analysis method.

V_e elastic base shear obtained from the model = 14532 kN.

V_{ed} design elastic base shear = $max(\ 2S(0.2)/3S(T_a)\ \&\ 2S(0.5)/S(T_a)) \leq 1 \times V_e$ = 14532 kN.

V_d design base shear = $max\ (V_e.\ I_E / R_d.R_o\ \&\ 0.8\ V)$ = 3726 kN

Base shear obtained from MRSA (V_d) is only 80 % of base shear obtained from equivalent static force procedure (V). V_d= 3726 kN was used as the design total base shear in the X-axis direction of the building. The design seismic base shear of each frame (V_x) is then calculated, including accidental torsion, P-Delta, and notional load effects, as summarized in Table 4.2. The maximum base shear per frame is 1035kN, which is greater than the wind base shear per frame 201 kN. The NBCC seismic load combination of 1.0D (dead) + 1.0E (seismic) + 0.5L (live) + 0.25S (snow) is therefore used to design the CBFs.

Table 4.2: Seismic base shear per braced frame

Storey	Height (m)	Area (m^2)	Floor weight (kN)	V notional (kN)	V_d (for building in x) (kN)	Accidental torsion percentage	U_2	V_x/ frame (kN)
6	3.6	1225	5609	28	942	0.275	1.03	266
5	3.6	1225	7861	39	1870	0.275	1.02	524
4	3.6	1225	7861	39	2612	0.275	1.02	728
3	3.6	1225	7861	39	3169	0.275	1.01	881
2	3.6	1225	7861	39	3541	0.275	1.01	984
1	3.6	1225	7861	39	3726	0.275	1.01	1035

The lateral seismic load per braced frame was used to calculate the design axial compressive forces in the braces (C_f) in the X-direction, as summarized in Table 4.3.

Table 4.3: Design forces in braces

Level	V_x/frame (kN)	Storey height (m)	Bay width (m)	Angle between brace and beam(°)	Brace design force C_f (kN)
6	266	3.6	7	27.22	150
5	524	3.6	7	27.22	295
4	728	3.6	7	27.22	409
3	881	3.6	7	27.22	496
2	984	3.6	7	27.22	553
1	1035	3.6	7	27.22	582

4.4 Brace design

Rectangular HSS were selected for the bracing members due to the available range of sizes. The braces were designed to satisfy the strength, global slenderness, and width-to-thickness ratio provisions of CSA S16. An example of the design check of one brace is given here.

HSS127×101×7.9 section is used for the first-storey module and is oriented to buckle out-of-plane about its weak axis. First, the global slenderness ratio $70 \leq KL/r \leq 200$ is checked. KL was taken as the exact brace length, and the buckling resistance (C_r) of the braces was calculated according to section 13.3 of S16 and checked against the design force (C_f). Finally, the width-to-thickness ratio (b_o/t) was verified for the section to be $\leq 330/\sqrt{F_y}$, for $KL/r \leq 100$. The design summary for braces is given in Table 4.4.

Table 4.4: Brace design check

Module	Section	Load C_f (kN)	F_e (MPa)	λ	KL/r	C_r (kN)	C_f/C_r Check	b_o/t	$330/\sqrt{F_y}$
4-6	HSS127×76×6.35	409	353	0.98	74.8	434	0.94	16	17.77
1-3	HSS127×101×7.9	582	355	0.98	74.6	604	0.96	12	17.77

4.5 Design of braced module beams and columns

Beams and columns of the braced frame modules are designed to resist the probable brace resistances plus gravity loads. Probable tensile resistance (T_u), probable compressive resistance (C_u), and probable post-buckling compressive resistance (C'_u) of the braces were calculated according to Section 27.5.3.4 of CSA S16 and using the probable yield stress R_yF_y (Table 4.5). The seismic loads from brace resistances were combined with gravity loads to verify the member strength and stability. Design loads of beams and columns are summarized in Table 4.6. Design checks are summarized in Tables 4.7 and 4.8. Members' sections were selected to be identical every three storeys for the fabrication economy.

Table 4.5: Probable design forces developed in braces

Module	T_u (kN)	C_u (kN)	C'_u (kN)
4-6	1067	661	213
1-3	1481	920	296

Table 4.6: Design loads of beams and columns in braced module

Module	*Columns*		Beams		
	Moment (M_{fbc}=0.2 M_{py})(kN.m)	Axial force C_{fbc} (kN)	Moment (M_{fbb}) (kN.m)	Shear force V_{bb} (kN)	Axial force C_{fbb} (kN)
4-6	46	2358	157	26	759
1-3	150	5858	157	26	1054

Columns were checked for all beam-column limit states and class of flange and web. Member strength was calculated based on the interaction equation in Section 13.8.2 of S16.

$$\frac{C_f}{C_r} + \frac{0.85U_{1x}M_{fx}}{M_{rx}} + \frac{\beta U_{1y}M_{fy}}{M_{ry}} \leq 1 \qquad (2)$$

Axial resistance, moment resistance, width-to-thickness ratio (at least class 2), cross-sectional strength, overall member strength, and lateral–torsional buckling (LTB) strength are checked in accordance with section 13.8.2 and Table 2 of CSA S16 (CSA 2019). Since the columns of the braced module are oriented on their Y-axis in-plane, Design moments on the X-axis of columns are considered equal to zero. This modifies the equation (2) as follows:

$$\frac{C_f}{C_r} + \frac{\beta U_{1y} M_{fy}}{M_{ry}} \leq 1 \qquad (3)$$

where

$\beta = 0.6 + 0.4\lambda_y \leq 0.85$

U_1 is specified in Clause 13.8.4 of S16.

C_r and M_{ry} are determined as defined in S16 for every limit state.

Table 4.7 summarises design checks for the braced module column.

Table 4.7: Braced frame column design checks

Module		1-3	4-6
Section		W360×216	W360×110
Flange class		1	1
Web class		1	1
Axial strength	(C_{fbc}/C_r)	0.84	0.72
Cross-sectional strength	$(C_{fbc}/C_r)+(\beta U_{1y} M_{fybb}/M_{ry})$	0.82	0.67
Overall member strength		0.87	0.88
Lateral-torsional buckling		0.87	0.88
Bending	M_{fybb}/M_{ry}	0.22	0.22

Beams of the braced frames are checked for width-to-thickness ratio (at least class 2), shear strength, deflection, cross-sectional strength, and overall member strength. LTB strength does not

govern the design due to lateral support of the beams through anchorage to the slabs. Moments on beams act only on the strong axis of the beam, which makes the design check equation as follows:

$$\frac{C_f}{C_r} + \frac{0.85U_{1x}M_{fx}}{M_{rx}} \quad (4)$$

Design checks for braced frame beams are given in Table 4.8. Shear yielding governs in both beams due to the high reaction shear force coming from the braces connected to the beam. Axial components of probable brace resistances from braces connected to the top and the bottom of the beam have to be transferred to the column by the beam web. Shear resistance of the beam $V_r = \phi. A_w.F_s$, where A_w area of the web, *and* $F_s = 0.66F_y$ for $h/w \leq (1014/\sqrt{F_y})$.

Table 4.8: Braced frame beams design check

Module		**1-3**	**4-6**
Section		W610×113	W530× 74
Flange class		at least class 2	at least class 2
Web class		at least class 2	at least class 2
Cross-sectional strength	$(C_{fbb}/C_r) + (0.85 U_{1x}.M_{fxbb}/M_{rx})$	0.41	0.51
Overall member strength		0.43	0.53
Shear strength	(V_{bb}/V_r)	0.9	0.89
Deflection /(*L*/240)		0.17	0.31

4.6 Design of gravity module beams and columns

Structural members outside the CBF are designed under gravity loads. Gravity columns experience axial load combinations (C_{fgc}) acting on the tributary area of the column. The load combination case used to calculate the axial load is *(*1.25 *D* + 1.5 *L* + 1.0 *S)*, which provides the worst-case loading on gravity columns. Loads are checked against the compressive resistance of the columns (C_{rgc}), as summarized in Table 4.9.

Table 4.9: Gravity columns design check

Module	Section	C_{fgc} (kN)	C_{rgc}(kN)	C_{fgc}/C_{rgc}
4-6	W310×60	1282	1446	0.89
1-3	W310×79	2199	2351	0.94

Gravity beams are designed as simply supported members under a distributed load q_f due to the load combination *(*1.25 *D* + 1.5 *L* + 1.0 *S)* (Table 4.10). The designed members are selected to be identical for all storeys.

Table 4.10: Gravity beams design check

Module	Section	q_f (kN/ m)	q_{sls} (kN/m)	M_{fgb} (kN.m)	M_{rgb} (kN.m)	M_{fgb} / M_{rgb}	Shear strength (V_{gb}/ V_r)	Deflection /(*L*/240)
1-6	W360×91	72	49	442	505	0.88	0.81	0.99

4.7 Design of connections

Module connections are designed to remain elastic under seismic and gravity loads. The probable resistances of the braces were used to obtain the design forces. Corner and middle gusset plate dimensions were chosen based on the geometry of the frame and the angle between the brace and the beam. Both gusset plates and knife plates connecting the gusset plates to the braces, shown in Figures 4.4 and 4.5, were designed in accordance with AISC Design Guide 24 (Packer et al. 2010). Figure 4.5 shows the middle gusset plate connection for the first-storey module. Connection length is referred to as L_c (Figure 4.4), and it is measured from the end of the compression brace to the tension restrained area displayed as the red shaded area. Connection length (L_c) and width (w) were used to find the Euler buckling resistance of the plate between brace end and tension restrained area in the middle gusset (illustrated as the blue shaded area in Figure 4.4). The equation used for calculating the compressive resistance of the middle gusset plate (P_r) is as follows:

$$P_r = \frac{1}{\frac{1}{P_C}+\frac{4e}{9M_C}}, \text{ when } \frac{P_r}{P_c} \geq 0.2 \quad (5)$$

P_c is the compressive buckling strength of the plate calculated based on the slenderness ratio (KL_c/r) and cross-sectional area (A) of the plate. e is the out-of-plane eccentricity between the gusset plate and the knife plate welded into the brace. M_c is the moment resistance of the plate around its weak axis. P_r is checked to be bigger than the probable brace compressive resistance (C_u). Table 4.11 gives the design checks for the middle gusset plate. Single or double knife plates can be used to connect braces to the gusset plates. Double plates are preferred in design as the eccentricity effect is eliminated. A single knife plate was used in this case to simplify the numerical modelling of the frame to be conducted in Chapter 5. The knife plate will have the same thickness as the gusset plate, as the connection length (L_c) represents both the gusset and the knife plate (Packer et al. 2010). The plate thickness (t) of 35 mm was found to be sufficient for the middle gusset plate and the knife plates to remain elastic.

Table 4.11: Middle gusset plate design check (single knife plate)

Parameter	Value	Unit/Ratio
w	260	mm
L_c	430	mm
t	35	mm
e	35	mm
K	1.2	
KL_c/r	51.1	
C_r/A	251	MPa
P_c	2284	kN
M_c	25	kN.m
P_r	945	kN
P_r/P_c	0.4	>0.2
C_u	920	kN
C_u/P_r	0.97	≤1.0

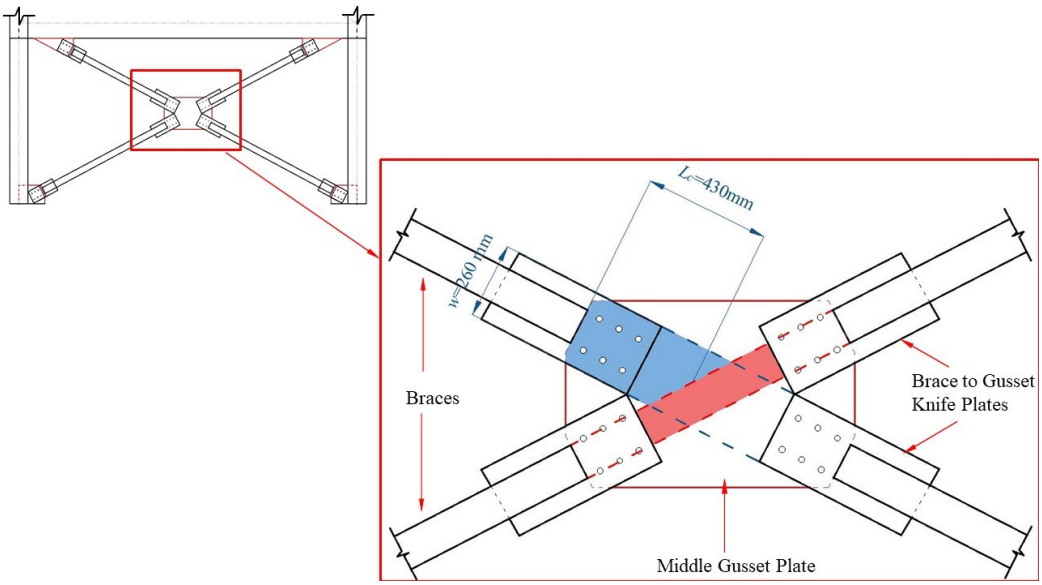

Figure 4.4: Middle gusset plate connection for the first-storey braced module

In the case of using double knife plates, the plate resistance (P_r) is equal to the buckling resistance (P_c). The design check for gusset plates and knife plates in the case of using double knife plates is listed in Table 4.12.

Table 4.12: Middle gusset plate design check (double knife plate)

Parameter	Value	Unit/Ratio
w	260	mm
L_c	430	mm
t	24	mm
e	0	mm
K	1.2	
KL_c/r	74.5	
C_r/A	194	MPa
P_c	1211	kN
M_c	11.8	kN.m
P_r	1211	kN
P_r/P_c	1	>0.2
C_u	920	kN
C_u/P_r	0.76	≤1

The connection length (L_c) of corner gusset plates is smaller than the middle gusset plate connection, but the same plate thickness is used for consistency and simplicity in fabrication. A plastic hinge region equal to two times the plate thickness ($2t$), as prescribed by S16, is designed to provide ductile rotational behaviour out-of-plane (Figure 4.5).

Knife plates connected to the braces experience tensile forces and are checked under brace tension resistance (T_u). The resistance of the plate, bolts, and welds are checked against T_u. The design check for the case of double knife plates is summarized in Table 4.13.

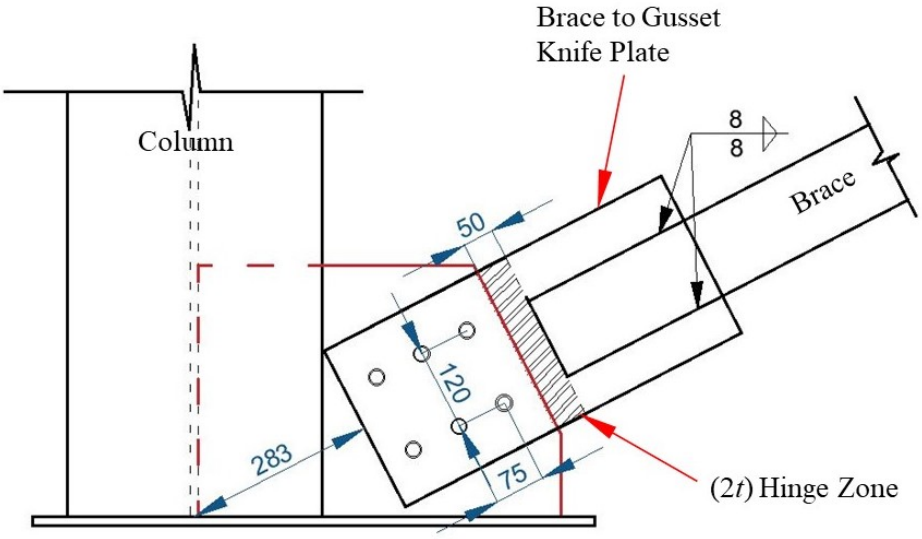

Figure 4.5: Base corner gusset plate connection for first-storey braced module (dimensions in mm)

Table 4.13: Knife plate design check (tension)

Parameter	Value	Unit
w	260	mm
L_c	500	mm
t	24	mm
Weld size	8	mm
Weld length ×4	300×4	mm
No. of bolts	6	
Bolt diameter	7/8	in.
F_y	345	MPa
T_u **(design force)**	1481	kN
T_r **(yielding)**	1938	kN
T_r **(net-section rapture)**	1610	kN
T_r **(block shear)**	2036	kN
T_r **(bolts)**	1693	kN
Bearing of bolt hole (B_r**)**	3421	kN
T_r **(brace welds)**	1721	kN
T_r **(base material)**	5818	kN

Bolted double angle connections are used to carry the shear and axial forces from the beam web to the columns (Figure 4.6). Table 3-34 of the CISC Handbook of Steel Construction (Canadian Institute of Steel Construction 2015) indicates the number of bolts and angle dimensions required to resist a given shear force. Connection details for connections of the beams of gravity and braced modules are listed in Table 4.14. The parameters used in the design check table (e.g., *L, w, g*, and *g1*) are shown in Figure 4.6.

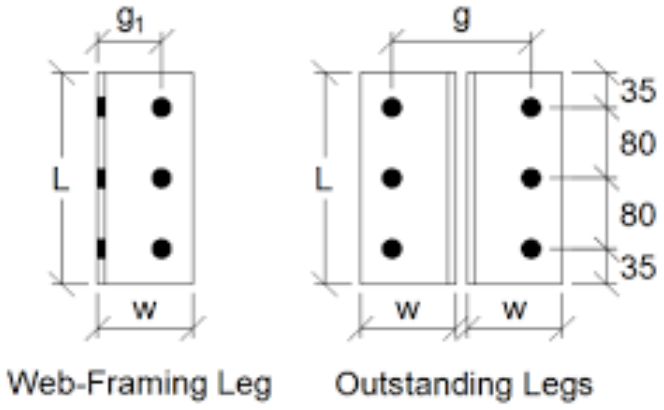

Figure 4.6: Design details for bolted double-angle beam-to-column connection (Canadian Institute of Steel Construction 2015)

Table 4.14: Bolted double angle beam connection design

Parameter	Braced module	Gravity module	Unit
Module	1-3	1-6	
Reaction force (*V*)	1187	504	kN
Beam depth	610	360	mm
Web thickness	11.2	9.5	mm
No. bolts	6	3	
Size of bolts	7/8	7/8	in.
Angle length (*L*)	470	310	mm
Angle width (*w*)	90	90	mm
g	130	130	mm
g1	60	60	mm
Connection capacity $V_r > V$	1260	630	kN

The splice cover plates for the columns of the braced module is shown in Figure 4.10. These plates are designed to resist both axial tension and compression forces that the columns experience under gravity and lateral loads. Two cover plates are welded to the lower module column and bolted on-site to the upper module column. The first-storey module splice is located at the mid-height of the

second storey. In the case of a downward compression force, the column bearing helps in transferring the axial load. However, in the case of uplift, the cover plate is designed to develop enough tensile resistance ($T_r \geq T_u$ column) to resist the load. Dimensions of the cover plates are shown in Figure 4.7. Table 4.15 gives the details of the limit states verified for the braced module splice plates.

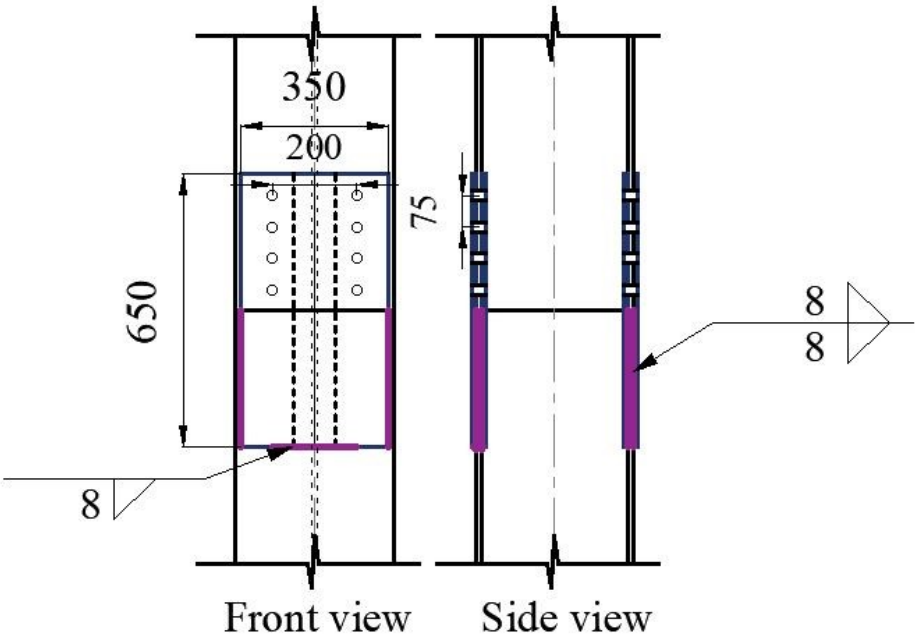

Figure 4.7: Cover-plate column splice (dimensions in mm)

Table 4.15: Design check of column cover plates splice

Parameter	Value	Unit
Width of outer plate	350	mm
Width of inner plate	120	mm
Half-length of plate	325	mm
Plate thickness	12	mm
Weld size	8	mm
Weld length (longitudinal)	325×8	mm
Weld length (horizontal)	200×2	mm
No. of bolts	16	
Size of bolt	7/8	in.
Design tension force ($T_{u\ column}$)	3381	kN
T_r (yielding)	4397	kN
T_r (net section)	4001	kN
T_r (block shear)	4546	kN
T_r (bolts)	4516	kN
Bearing of bolt hole (B_r)	4562	kN
T_r (welds)	5356	kN
T_r (base material)	6303	kN

Chapter 5: Construction Efficiency and Structural Response

This chapter presents the steel tonnage corresponding to the proposed modular system used to construct a multi-storey building as compared to the conventional structural system used to build the same building. The structural behaviour of a sub-assembly consisting of braced modules is then evaluated numerically under gravity and lateral loads.

5.1 Steel tonnage and construction time estimation

Steel tonnage was compared for the construction of a multi-storey building using the proposed modular system (modular construction) and that using the conventional method (conventional construction). The six-storey prototype building presented in Chapter 4 was selected for this comparison.

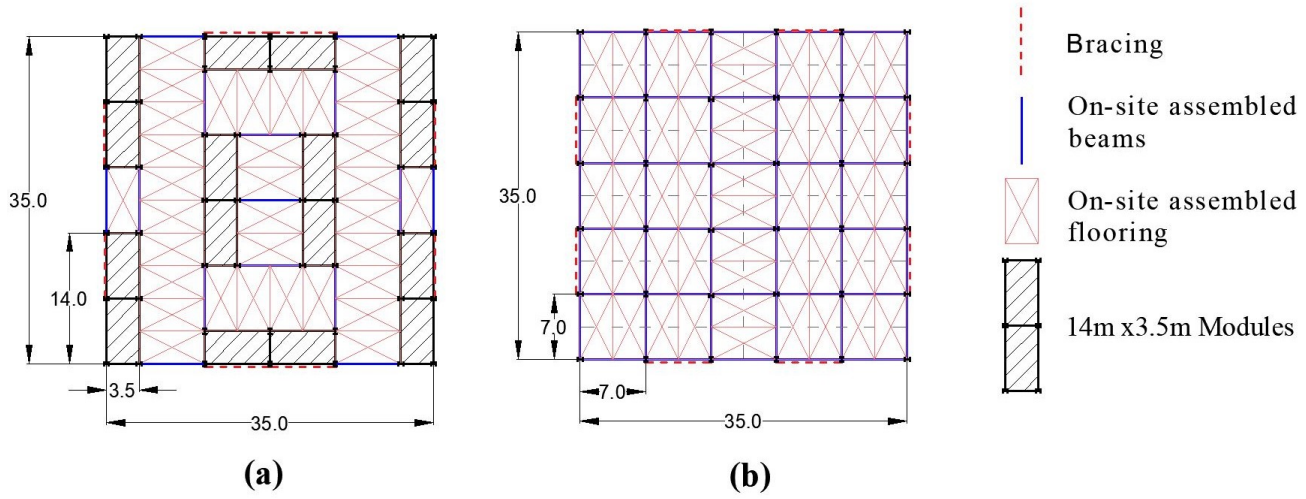

Figure 5.1: Plan view of the six-storey office building constructed using a) proposed structural modular system; b) conventional structural system (dimensions in m)

The steel tonnage of the main structural members (beams and columns) of both systems was used here as an approximate cost indicator, since the steel tonnage is often used by fabricators for the purpose of preliminary cost estimation and bidding (WF Steel & Crane 2019). Steel deck with cast-in-place concrete is usually used for conventional steel structures, which can add to the cost and time of construction, although it can more efficiently rigid diaphragm as compared to available

prefabricated slab systems. However, for simplicity, it is assumed that both buildings have the same slab system so that the contribution form of the slab can be ignored in the comparison. The weights bracing members were not included in the calculations as they were assumed to be identical for both systems for simplicity. Table 5.1 shows the steel tonnage for the two systems. As shown, the steel tonnage is nearly identical, which indicates that the application of the new modular system is not expected to add to the cost of the material, and in turn, steel fabrication. One key parameter in this table that can be used for this purpose is the number of connections to be assembled on-site. Although the number of these connections is not the only factor that affects the construction time, it can still provide a good indication to compare the construction time between the two systems. As given in Table 5.1, the number of such connections for the modular system is less than half of those for the conventional system. Although these numbers do not assure that the construction time will be reduced by two when using the proposed modular system, it suggests that the modular system can result in faster construction.

Table 5.1: Comparison of steel tonnage and no. of connections corresponding to main structural components for conventional and modular systems

Parameters	**Conventional method**	**Modular method**
Total weight of beams per storey	40 Tonnes	21 Tonnes
Total weight of columns per storey	19 Tonnes	39 Tonnes
Total steel tonnage per storey	58 Tonnes	59 Tonnes
Total steel tonnage for six storeys	350 Tonnes	356 Tonnes
No. of shear tab connections	624	0
No. of double-angle connections	96	180
No. of brace connections (corner & middle)	240	48
No. of end-plate column splices	20	170
No. of cover plate column splices	16	70
Total on-site connections	996	468

5.2 Structural response evaluation

5.2.1 Numerical model assumptions

To evaluate the structural response of the modular system, a finite element model of a two-storey sub-assembly of the braced module was developed in the Abaqus finite element program (Dassault Systèmes 2019). Abaqus is used due to its ability to simulate material, geometric, and loading nonlinearities. The assumed element types and material properties used in the modelling are described here.

All columns, beams, braces, and connection plates of the sub-assembly were developed using three-dimensional deformable quadrilateral (4-node) shell elements with reduced integration (S4R). The reduced integration helps with computational efficiency, as it requires only one integration point per element compared to four points with the full integration element, as shown in Figure 5.2 (Adeeb 2020). For a quadrilateral element with an 8 × 8 stiffness matrix, the number of computations needed with one integration point is one-fourth of that needed for full integration.

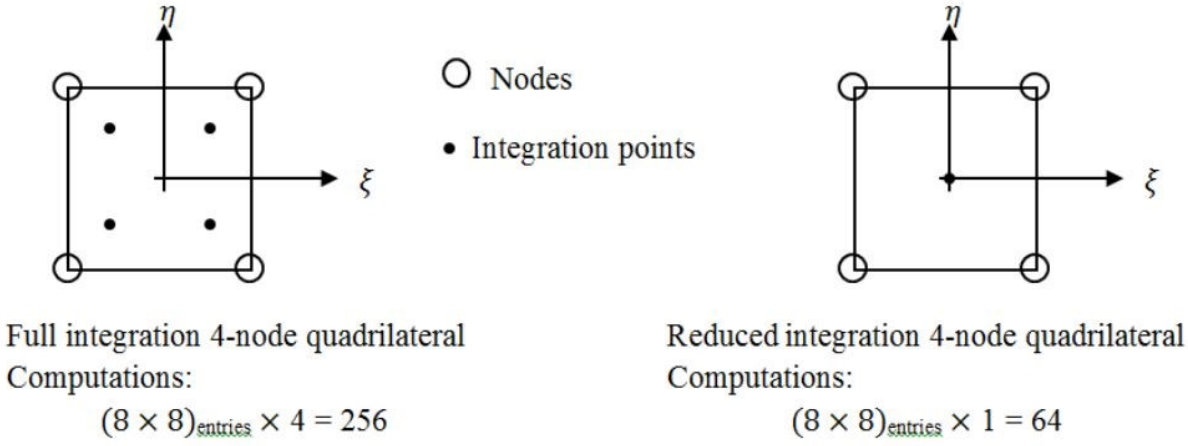

Figure 5.2: 4-node quadrilateral shell elements: full vs. reduced integration (Adeeb 2020)

The elastic properties of the steel material were simulated using Young's modulus of E = 200,000 MPa and Poisson's ratio ν = 0.3. A combined kinematic/isotropic material model was

chosen to simulate the plastic response of steel (Suzuki and Lignos 2015). The following parameters were used to define the combined hardening response of steel :

- F_y yield stress at zero plastic strain = 350 MPa for all members and connection plates
- R_yF_y = 460 MPa probable yield stress for braces
- C_1 initial kinematic hardening modulus = 3378 MPa
- γ the rate of decreasing of C_1 = 20
- Q_∞ the maximum change in the size of the yield surface = 90 MPa
- b rate of yield surface change with plastic deformation = 12

5.2.2 Model calibration

A 4.5-meter-long HSS 127×127×7.9 brace was selected to verify the finite element modelling assumptions used in this study. The HSS brace was part of a full-scale experiment conducted by Jiang (2013). In the numerical model, a uniform mesh with a size of 20 mm was used (Cano and Imanpour 2019). The yield stress F_y = 430 MPa, as obtained from the coupon tests, was assigned to the material in the model. A pinned restraint was selected at one end of the member, while the other end was free to rotate and move only parallel to the brace longitudinal axis. The HSS section was modelled using two methods: HSS with rounded corners, as shown in Figure 5.3a, and HSS with sharp corners, as shown in Figure 5.3b. Both had the same cross-sectional area, identical element sizes, and material properties.

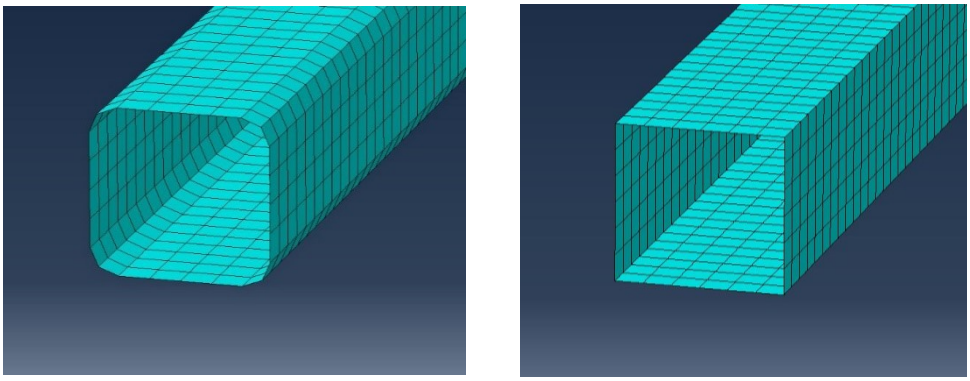

(a) (b)

Figure 5.3: HSS finite element model with a) rounded corners; b) right-angle square

Geometrical imperfections were applied to the numerical models in order to help the initiation of the global buckling in the brace when the compression load is applied. Eigen-bucking analysis was conducted to assign initial geometrical imperfections similar to the first buckling mode shape and with an amplitude of $L/1000$ in the middle of the brace (Figure 5.4). Residual stresses were ignored for simplicity.

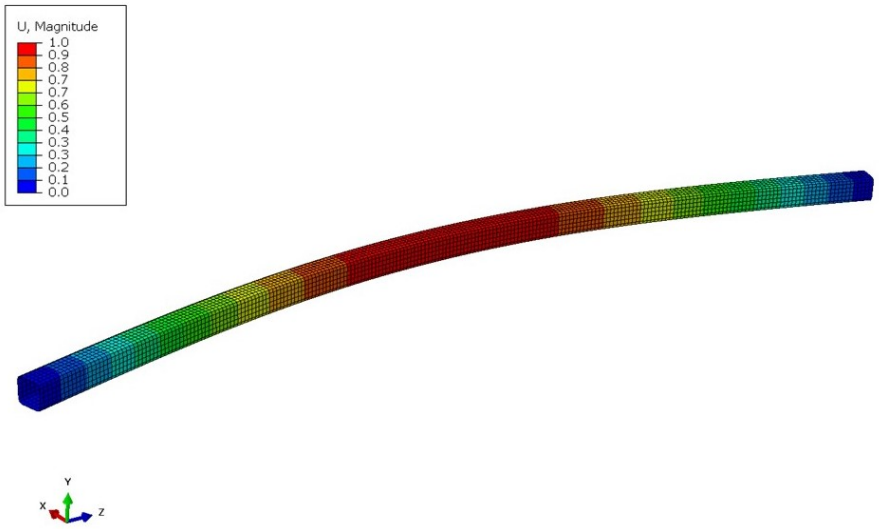

Figure 5.4: First buckling mode of brace used to apply initial geometrical imperfection of L/1000

The brace models were analyzed under the cyclic longitudinal displacement protocol used on the tested braces by Jiang (2013). The displacement protocol is shown in Figure 5.5. The results obtained from both numerical models were plotted against the experimental test data in Figures 5.6 and 5.7.

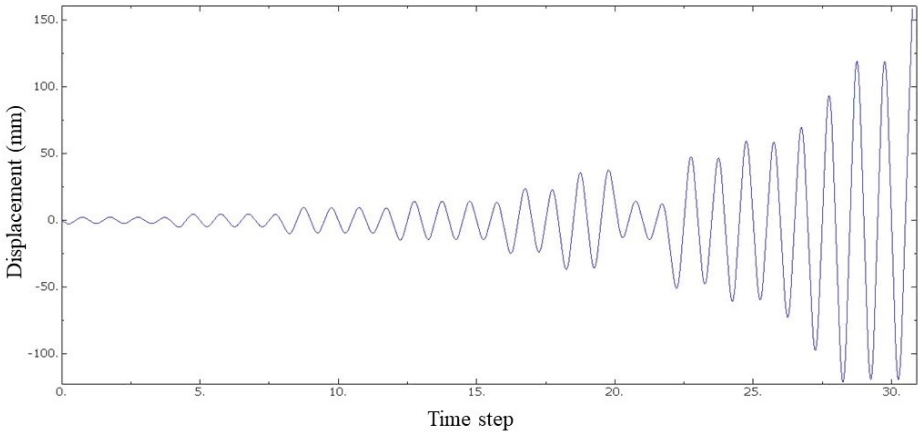

Figure 5.5: Isolated brace displacement history

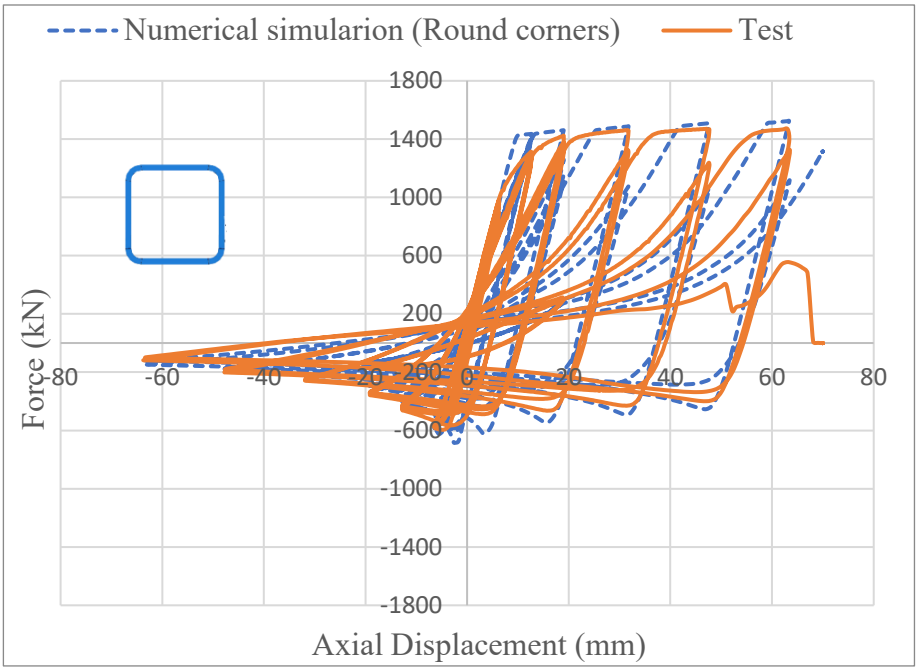

Figure 5.6: Hysteretic response of HSS 127x127x7.9 (round corners) against test data by (Jiang 2013)

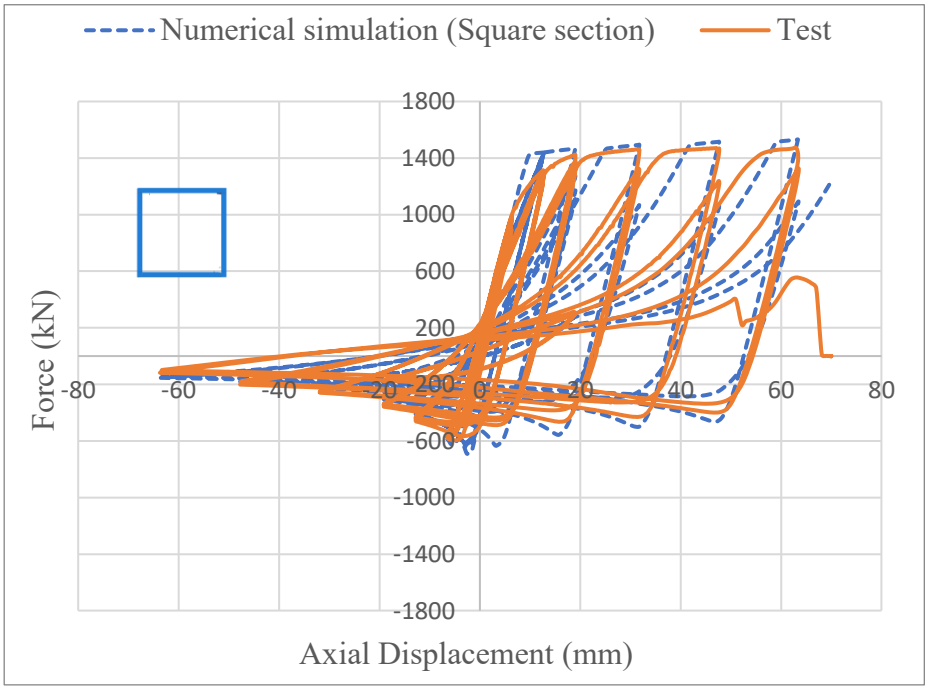

Figure 5.7: Hysteretic response of HSS 127x127x7.9 (right angle corners) against test data by (Jiang 2013)

The comparison between the hysteretic response of the finite element model and that of the test showed good correlation, which indicates that the nonlinear buckling and yielding response of the brace can be predicted well using the model developed here. The numerical model was able to simulate the plastic hinge formed in the middle of the brace under the cyclic load, as illustrated in Figures 5.8 and 5.9. Since both HSS models (rounded corners and right-angle corners) showed a similar hysteretic response, the right-angle corner HSS model is used to model the sub-assembly as it offers a faster modelling approach.

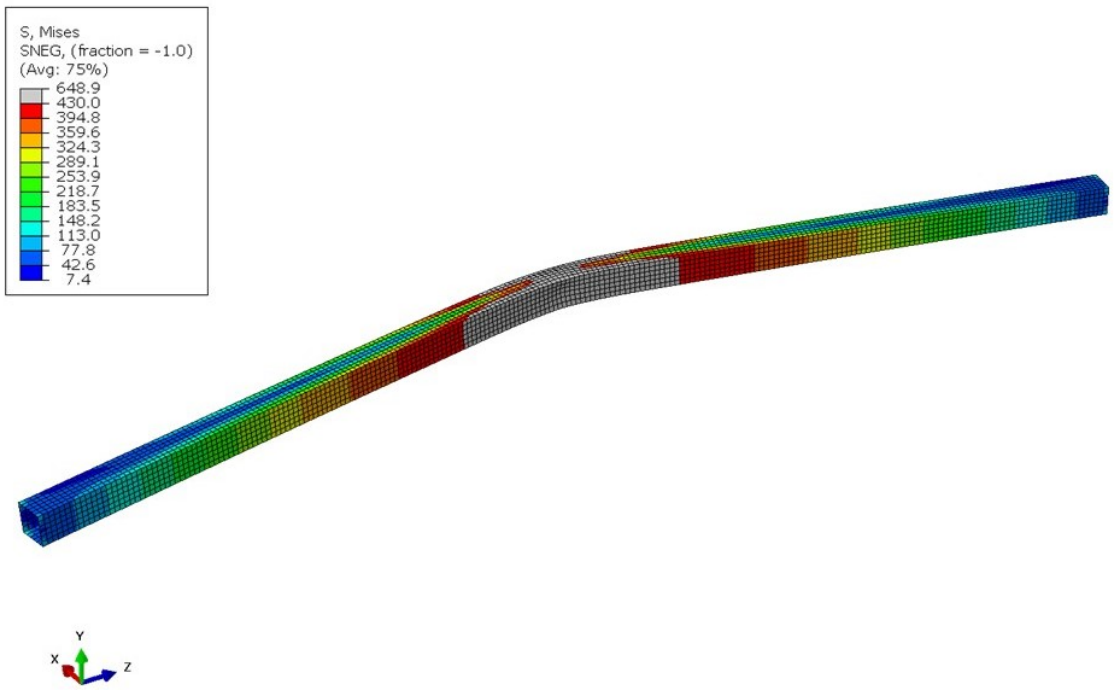

Figure 5.8: Deformed shape and von Mises stress (MPa) distribution for HSS 127×127×7.9 (right angle corner) at 60 mm axial displacement.

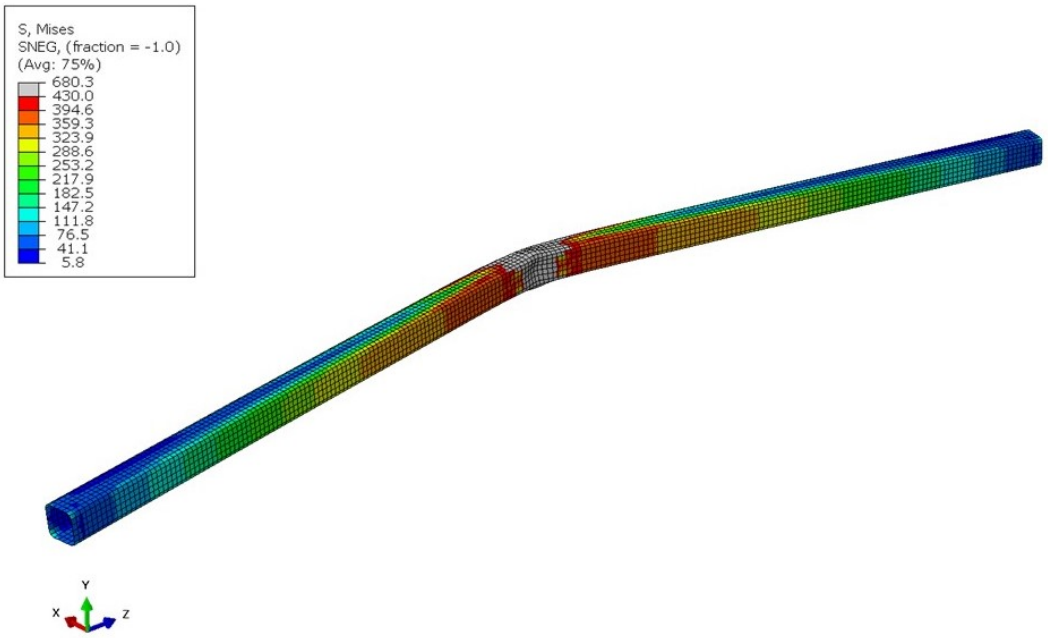

Figure 5.9: Deformed shape and von Mises stress (MPa) distribution for HSS 127×127×7.9 (round corner) at 60 mm axial displacement.

5.2.3 Development of the numerical model of the sub-assembly frame

The bottom two braced modules of one of the exterior wall braced frames of the six-storey prototype building of Chapter 4 were modelled. This model is referred to as the sub-assembly model, which consists of beams, columns, braces, and connections of these braced modules (Module 1 and Module 2). Figure 5.10 shows the two-storeys sub-assembly modelled as a part of the building. Module 1 is used to construct the first storey and half of the second storey, while the second module creates the remaining half of the second storey and the first half od the third storey, which is only used to load the subassembly.

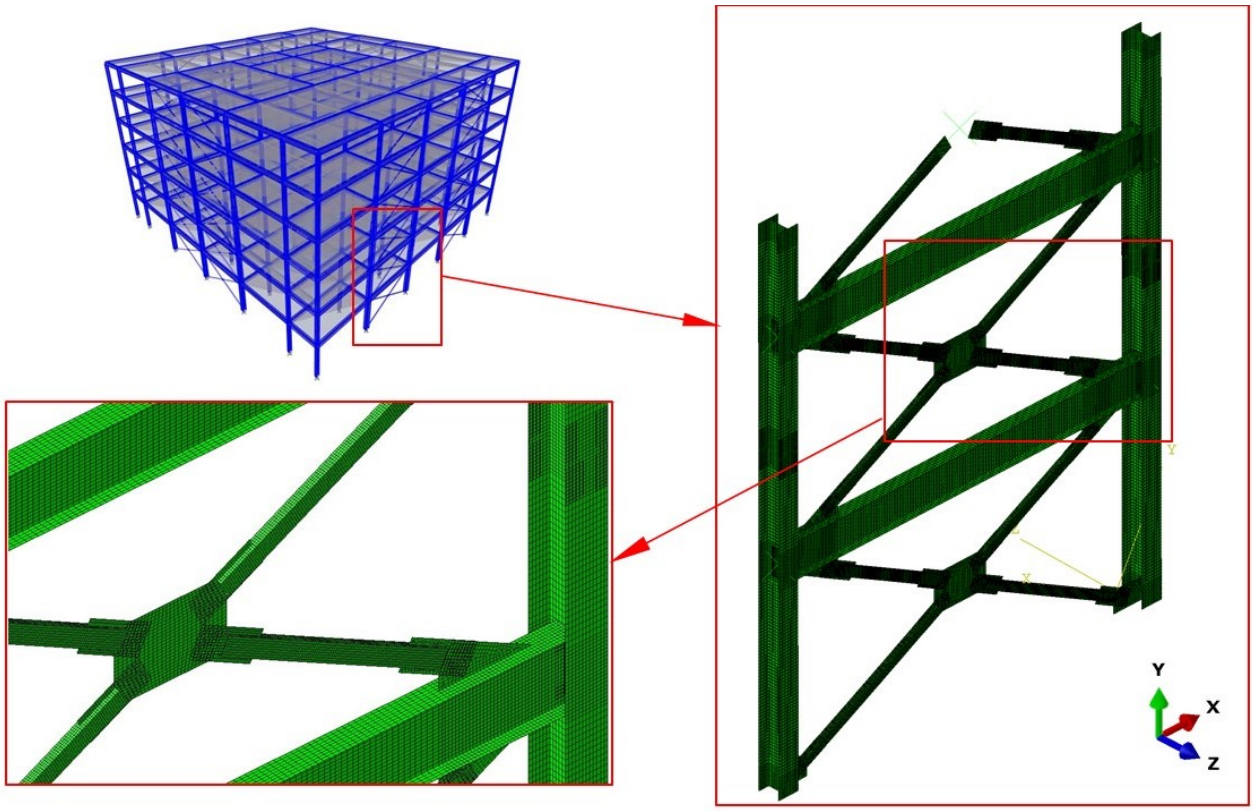

Figure 5.10: Modular braced sub-assembly model

The material properties previously validated in the calibration process were applied to the materials used to model the frame. However, the yield stress (F_y) parameter was changed to match design assumptions. The probable yield stress (R_yF_y) of 460 MPa was used for braces. All other members and connections were modelled with similar material properties except for F_y, which was selected to be 350 MPa.

The mesh size of the braces and connection regions was selected to be denser, with an element size of 20 mm, similar to the calibration process, whereas in regions that were not expected to undergo plastic deformation such as columns and beams, the mesh was selected to be coarser with elements size ranging between 30 mm to 50 mm to reduce computation time. The difference in mesh density can be seen in Figure 5.11. The storeys of the sub-assembly model are also defined in Figure 5.11.

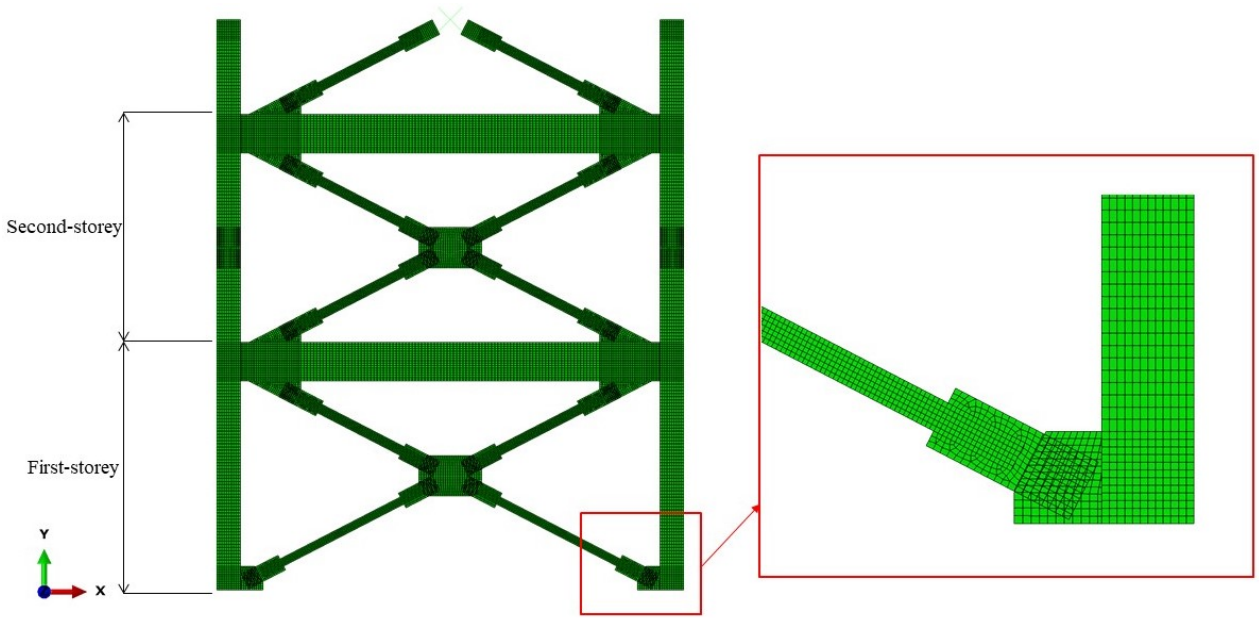

Figure 5.11: Elevation view of the sub-assembly model showing different mesh densities across the model

5.2.4 Boundary conditions

The boundary conditions of the sub-assembly frame were modelled to simulate the constraints as if it were part of the six-storey frame. Reference points were used to tie the nodes needed to be restrained; then, the boundary conditions were applied to the reference point. To simulate the pinned condition of the frame base, the column base and lower edges of the corner gusset plate were tied to a reference point (Figure 5.12c). The reference point is allowed to rotate in-plane (around the Z-axis) and out-of-plane (around the X-axis), while torsional rotation (around the Y-axis) and translational movements were restrained. The top of the frame was restrained as a rigid body at its middle to a reference point, as shown in Figure (5.12a). In this figure, the red shaded areas show the regions tied to the reference point. The rigid body was restrained from moving out-of-plane, yet the in-plane transition was allowed. Reference points were used to tie the column cross-section at the floor level (Figure 5.12b). Columns and beams were restrained in the out-of-plane direction to mimic the restriction of the slabs and perpendicular beams (shown as the red X in Figure 5.13). Figure 5.13 shows the boundary conditions applied to the sub-assembly.

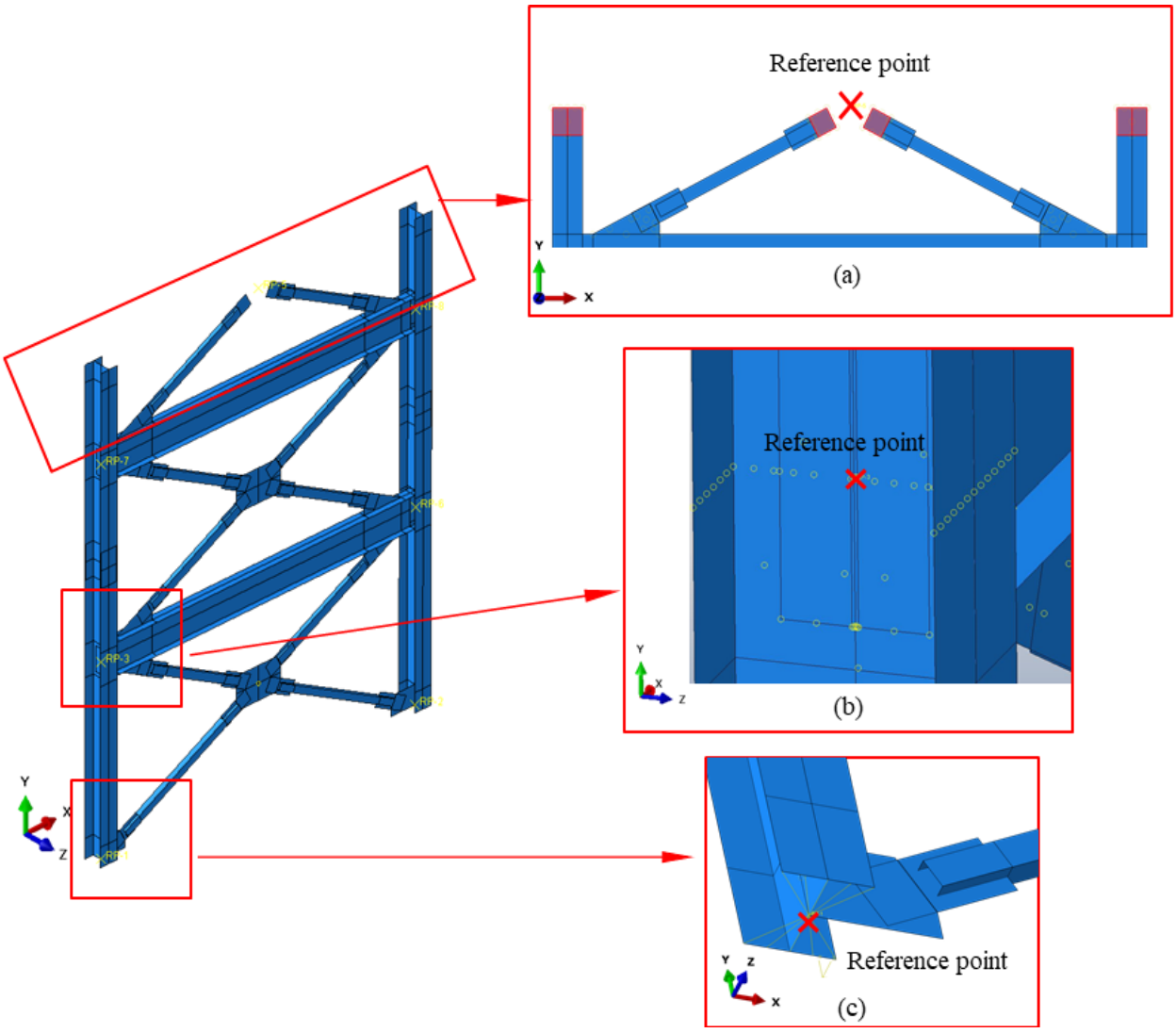

Figure 5.12: Couplings and ties defined in the sub-assembly model

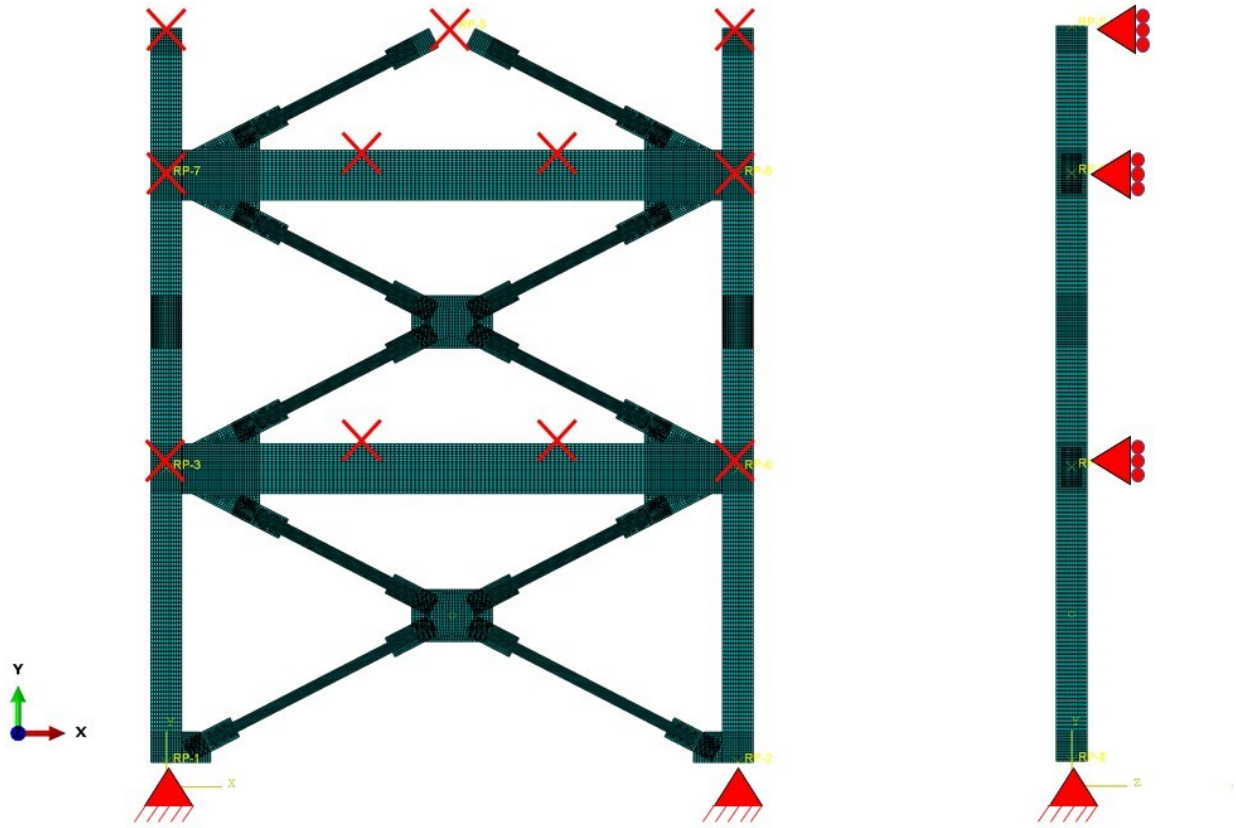

Figure 5.13: Boundary conditions assigned to the sub-assembly model

5.2.5 Initial Geometric Imperfections

An eigen-buckling analysis was performed to determine initial geometrical imperfections of braces in order to initiate global buckling of braces. The analysis was performed by applying a unit displacement in the X-direction (in-plane), at the top end of the model. The first ten brace buckling modes were combined to assign imperfections to the braces as initial conditions. The amplitude of the imperfection is equal to $L/500$ at the mid-length of the unsupported length, where L is the brace unsupported length. Figure 5.14 shows the first three buckling modes associated with the out-of-plane buckling of braces in the first-storey module. Geometrical imperfections were not applied to columns or beams as those members are not expected to become unstable.

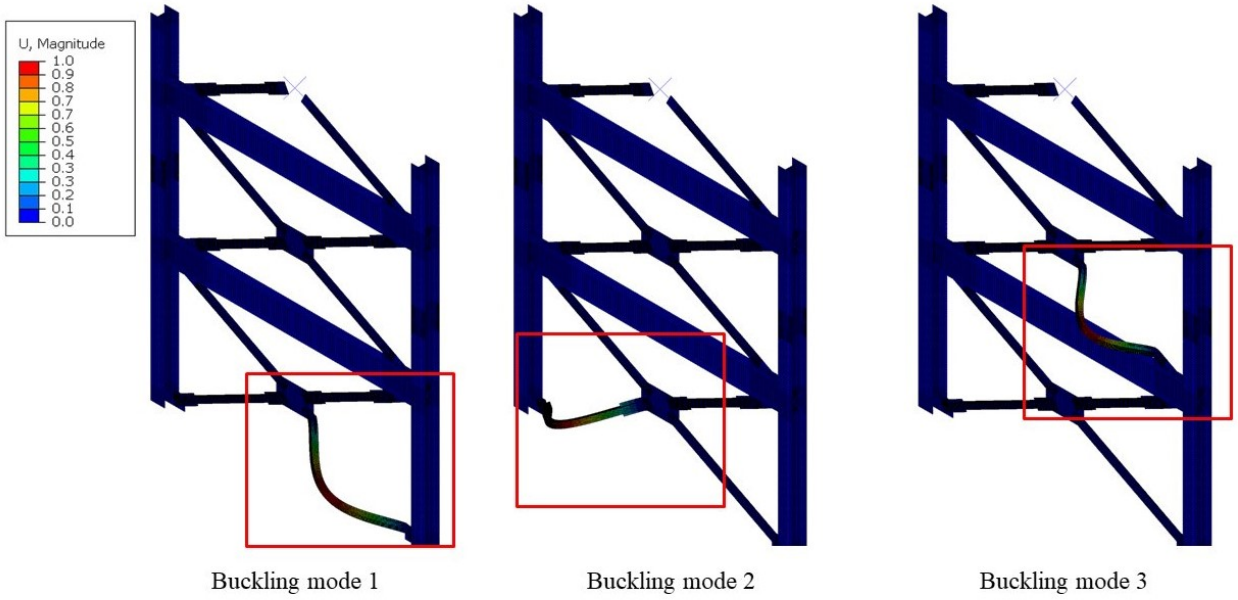

Figure 5.14: Samples of brace global buckling modes used to create initial geometric imperfections

5.2.6 Gravity and lateral load simulation

Loading was applied in two steps. The first step involves gravity loads applied to the model, which includes dead, live, and snow loads under the load combination $1D+ 1E+ 0.5L+ 0.25S$. Figure 5.15 shows the application of gravity loads on the sub-assembly model. Gravity loads tributary to the beams were applied on them as distributed loads, as shown in Figure 5.15. Axial load based on the tributary area of the second storey load was applied on the first storey column. For the second-floor columns, the loads applied were the accumulated gravity loads from all the storeys above (third storey up to the roof). Column axial loads were applied to the reference points as a concentrated load.

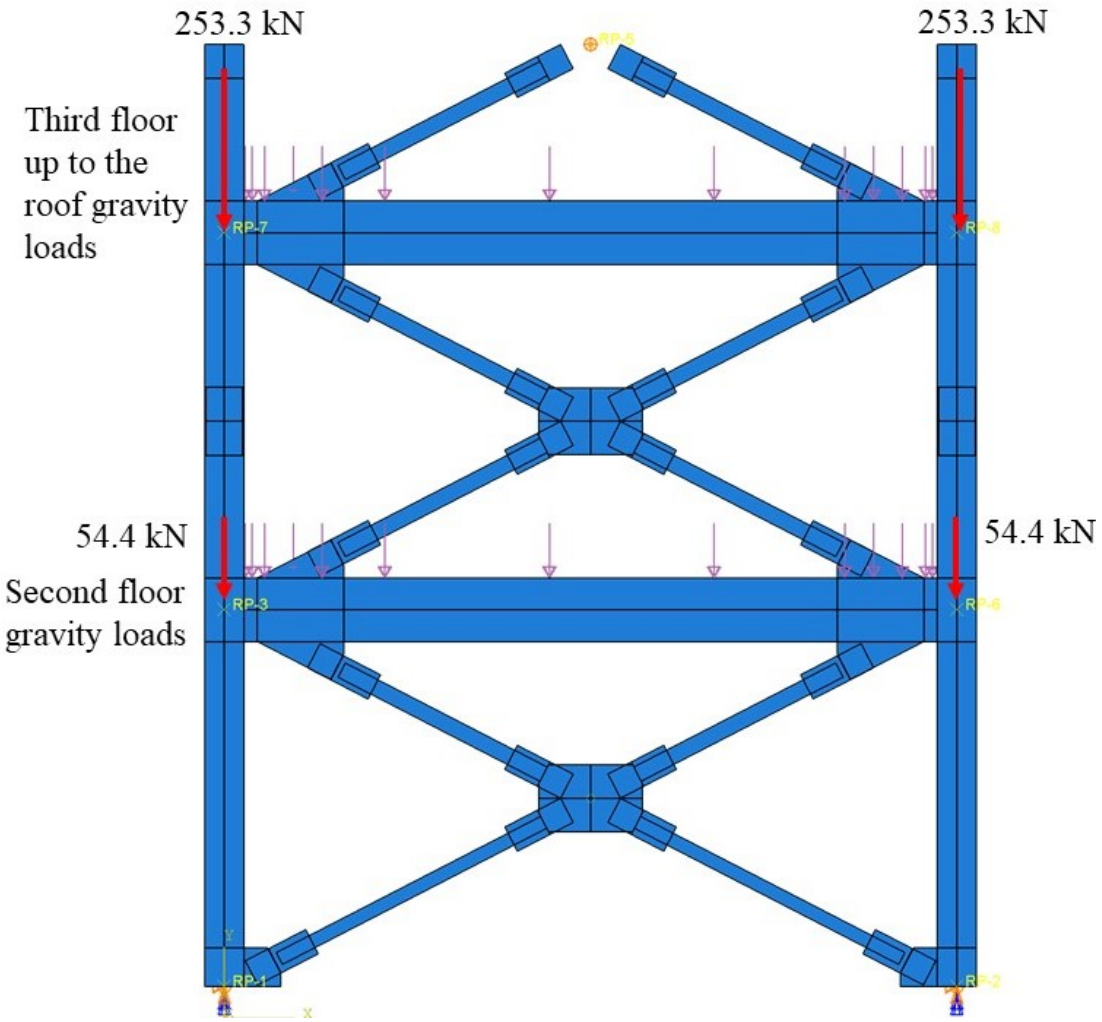

Figure 5.15: Gravity loads applied to the sub-assembly model

Once the gravity loads are applied, the lateral seismic load was simulated by imposing monotonically increasing lateral displacement in a nonlinear static (pushover) analysis step. The target displacement was set equal to 77.4 mm at the top end of the model. This is the lateral displacement that corresponds to the frame lateral deformation under seismic loads, as obtained from the modal response spectrum analysis (MRSA) performed on the 3-D model of the building in SAP2000. This pattern reflects the effect of accidental torsion and large P-delta effects. Figure 5.16 shows the points at which the deflections of the model were taken. Figure 5.17 shows the application of the lateral displacements to the sub-assembly model in Abaqus.

In order to account for the seismic forces of the upper braced storeys that were not modelled in the sub-assembly, equivalent axial loads, compression on one column and tension on the other were calculated using the probable tension and compression resistance (T_u *and* C_u) of the upper modules. The calculated seismic forces were then applied on the top end of the sub-assembly columns, as shown in Figure 5.17. Adding the seismic load helps to simulate the conditions of the sub-assembly model as a part of the full building. The axial seismic loads were applied simultaneously with the lateral drifts on the sub-assembly model.

The loads on the numerical models were applied as general static load steps with an increment size of 0.01 times the analysis time step. The minimum increment size was set as low as 10^{-15} to help numerical convergence in the case of sudden instability that is expected to take place in braces.

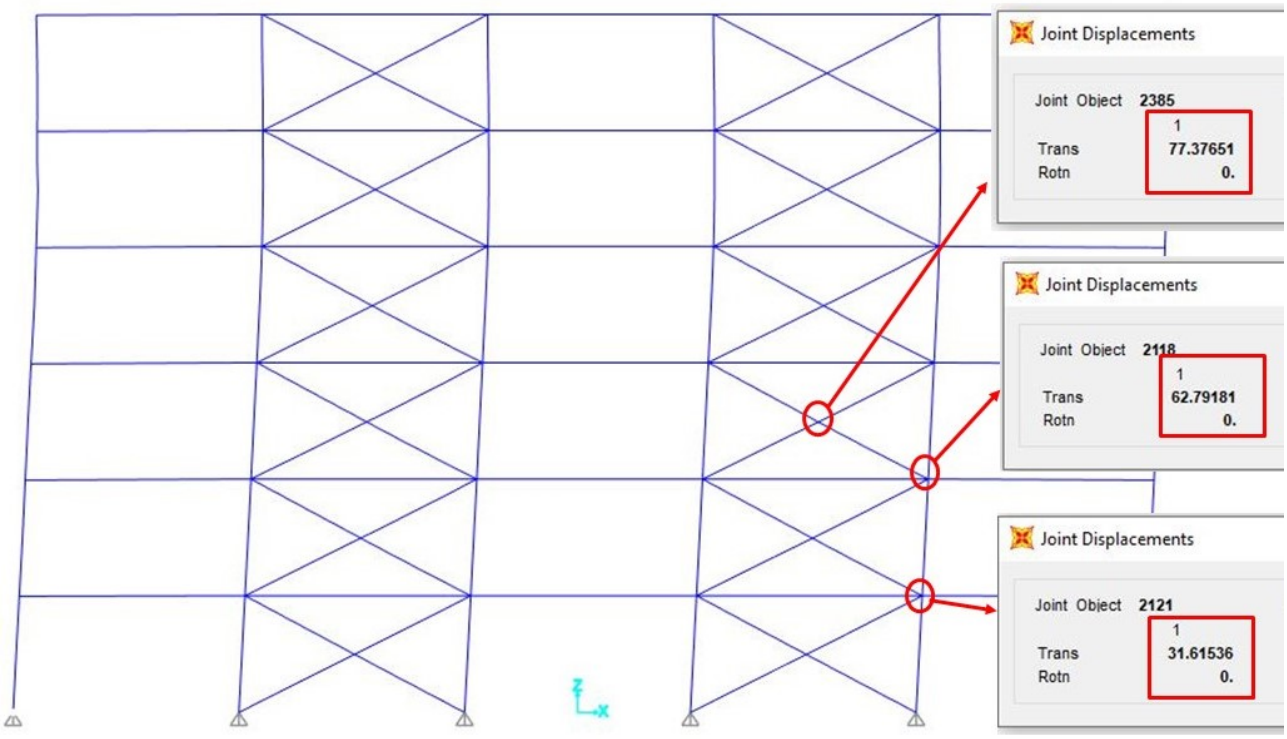

Figure 5.16: Lateral deformations as obtained from modal response spectrum analysis in the SAP2000 model

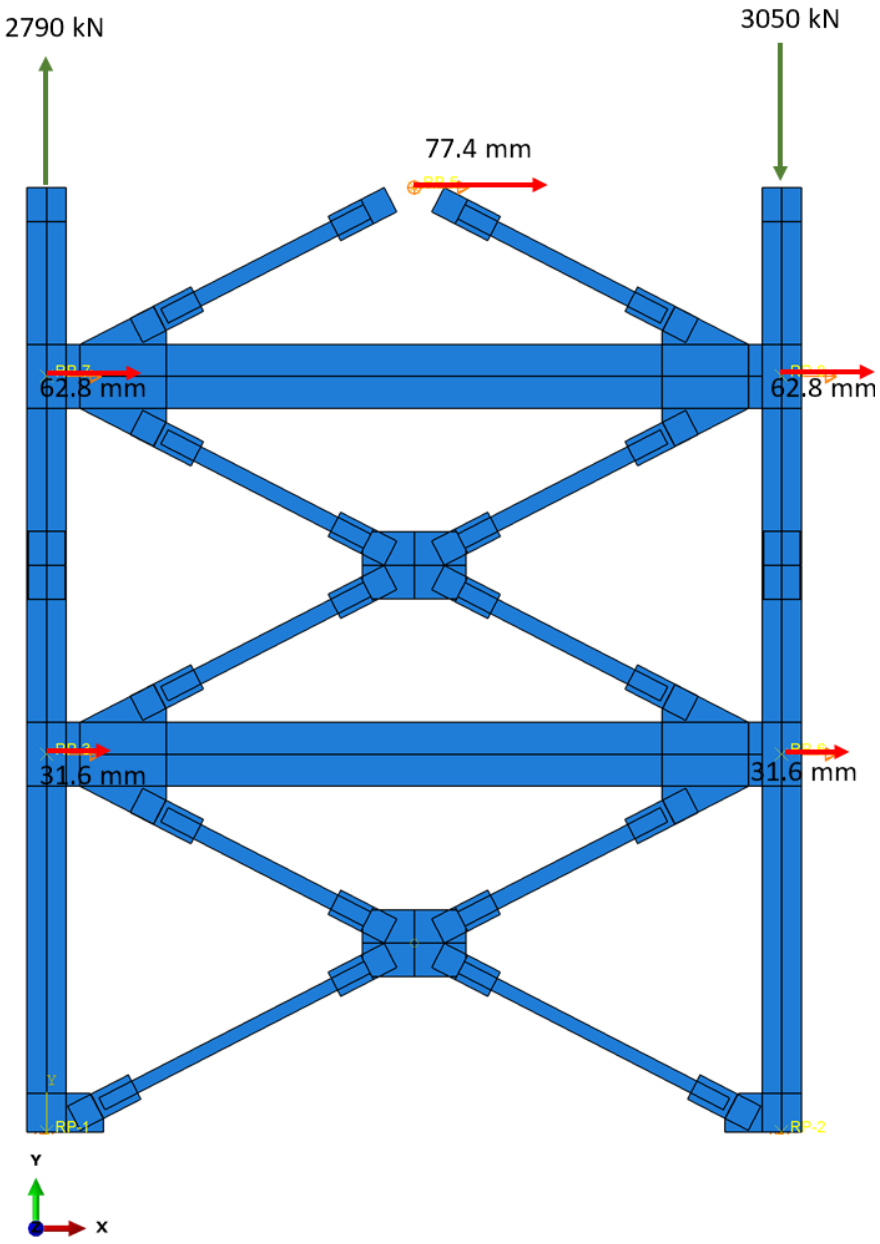

Figure 5.17: Lateral displacement obtained from modal response spectrum analysis and seismic forces as applied to the sub-assembly model in the pushover analysis step

Another sub-assembly module was examined using a nonlinear static pushover with a lateral displacement of 1.5% times the storey height applied at each storey level. This target displacement was examined to understand the behaviour of the frame when the lateral displacement exceeds the design storey drift predicted under the code-specified lateral seismic load. This can be the case

when the structure is subjected to a Maximum Considered Earthquake (*MCE*) level hazard. The model was pushed further to test if any members other than the braces would experience plastic deformation. The lateral displacement of 1.5% of the height was applied at three levels, as shown in Figure 5.18.

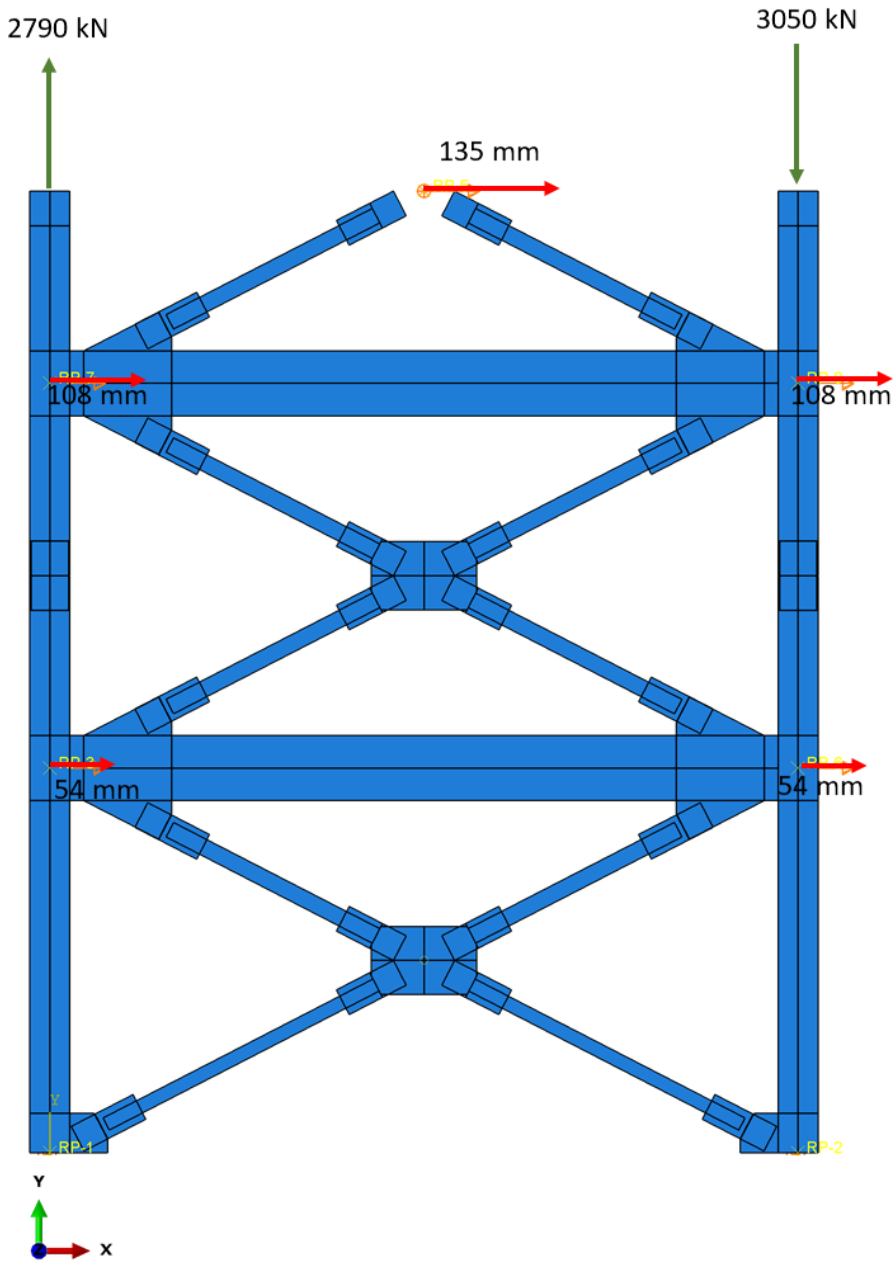

Figure 5.18: Lateral displacement corresponding to 1.5 % of the storey height and calculated seismic force as applied to the sub-assembly model in the pushover analysis step

5.3 Analysis results and discussion

The analysis results presented here focused on the global response of modules and their members. Under gravity loads, the frame elements deformed in the elastic range as expected. The deformed-shape and the stresses under gravity load are shown in Figure 5.19. After applying gravity loads to the model and under the lateral displacements simulating the seismic load, the frame deforms first in the elastic range of the material until the compression-acting braces buckle out-of-plane, as expected in design, and tension-acting braces yield in tension. Figures 5.20 and 5.21 demonstrate the deformed shapes of the frames and the corresponding von Mises stresses at the maximum drift obtained from the MRSA. The out-of-plane buckling of the braces at the same drift is shown in Figure 5.21.

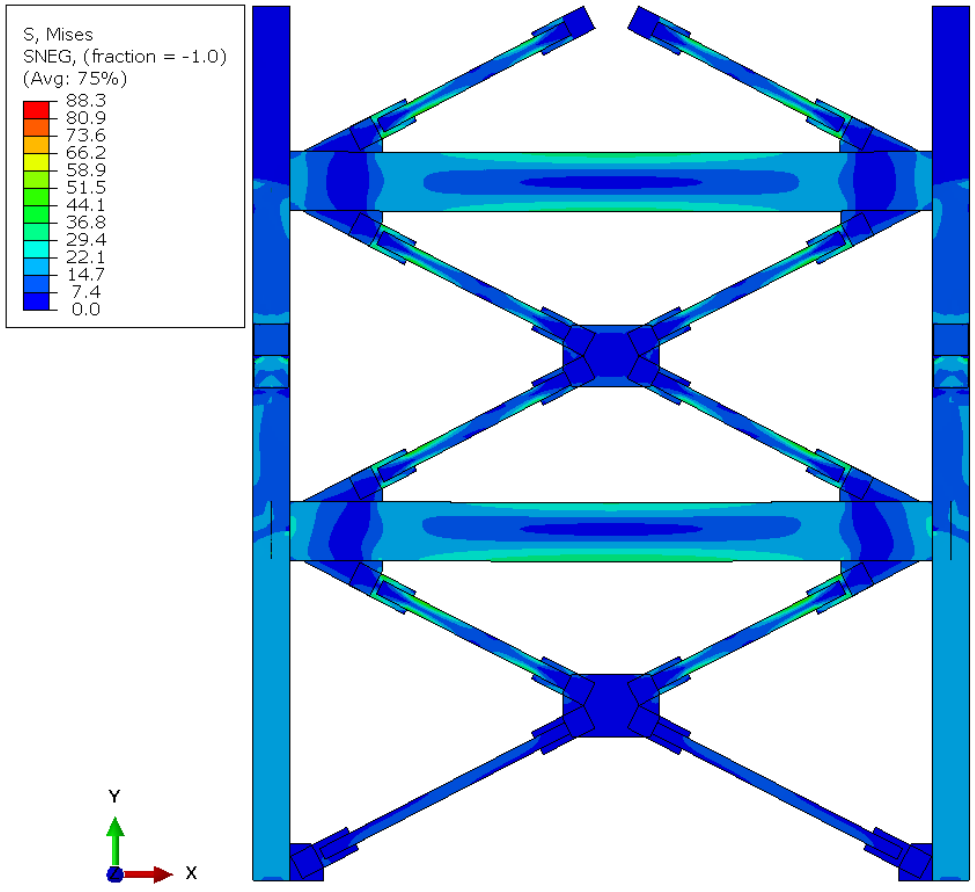

Figure 5.19: Deformed-shape and von-Mises stress contour under gravity loads (stresses in MPa)

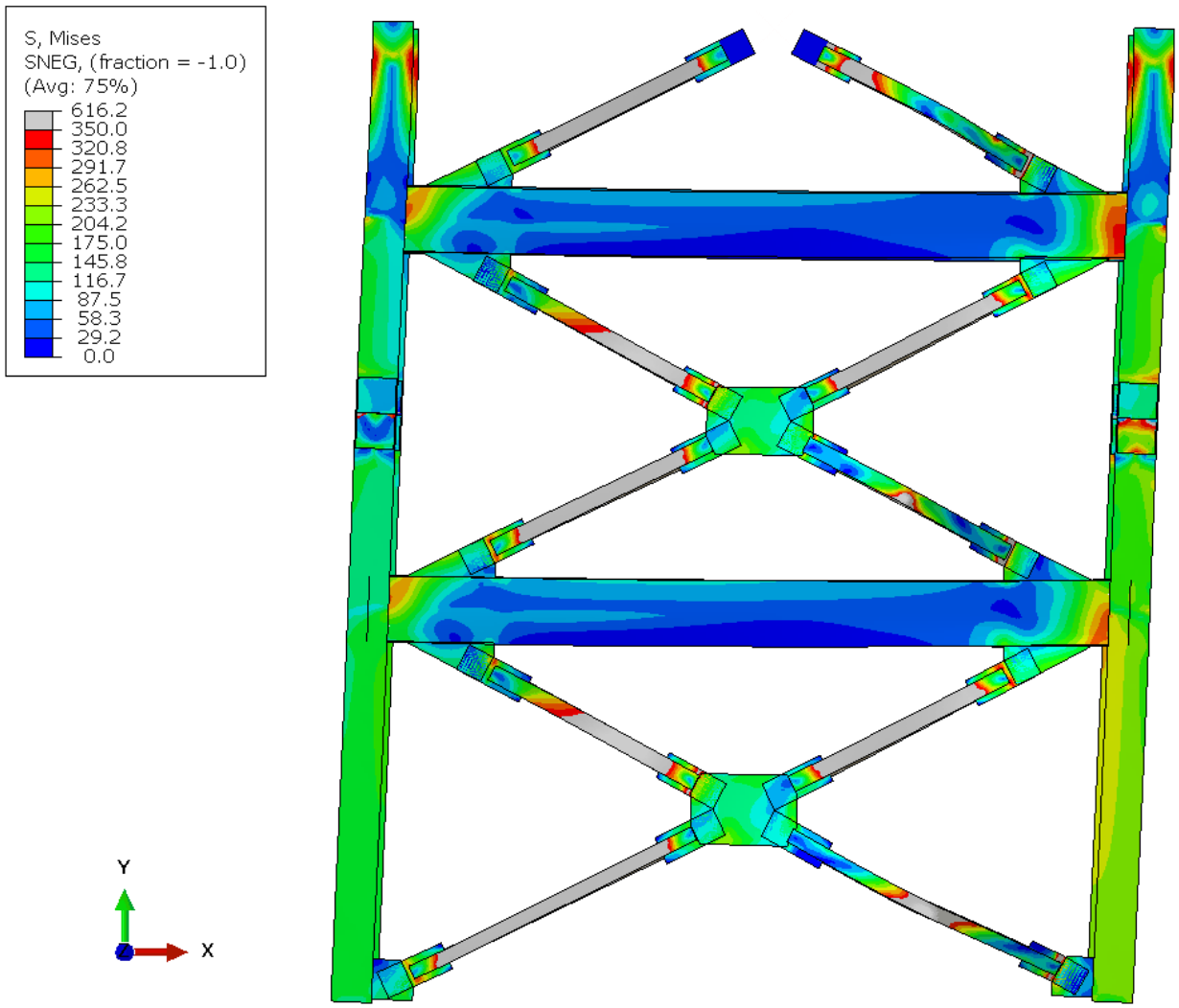

Figure 5.20: Deformed-shape pattern and von-Mises stresses (MPa) of the sub-assembly under MRSA displacement (deformation magnified x5)(elevation)

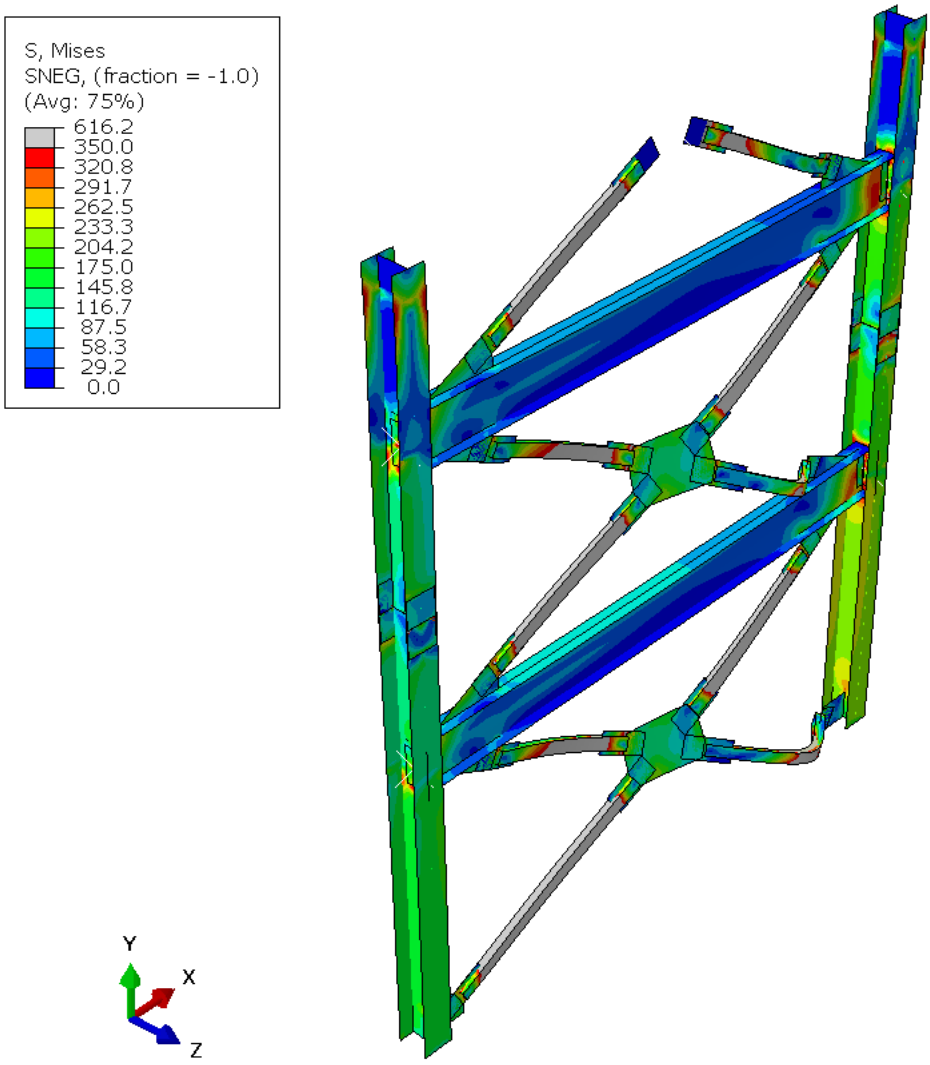

Figure 5.21: Deformed-shape pattern and von-Mises stresses (MPa) of the sub-assembly under MRSA displacement (deformation magnified x5)(3D)

Figures 5.22 and 5.23 reveal the deformed shape obtained from the pushover analysis under the displacement corresponding to the 1.5% times the storey height. The module response was nearly identical to that obtained from the MRSA displacement pattern. When the sub-assembly was pushed, the buckling of braces was initiated first, while other members deformed elastically without yielding. The brace forces kept degrading as the sub-assembly was pushed, as shown in Figure 5.25. No increase in stresses or yielding was noticed as the sub-assembly is pushed to the

target displacement. The yielded areas apparent at the top of the columns were due to the rigid body constraints at the top of the frame.

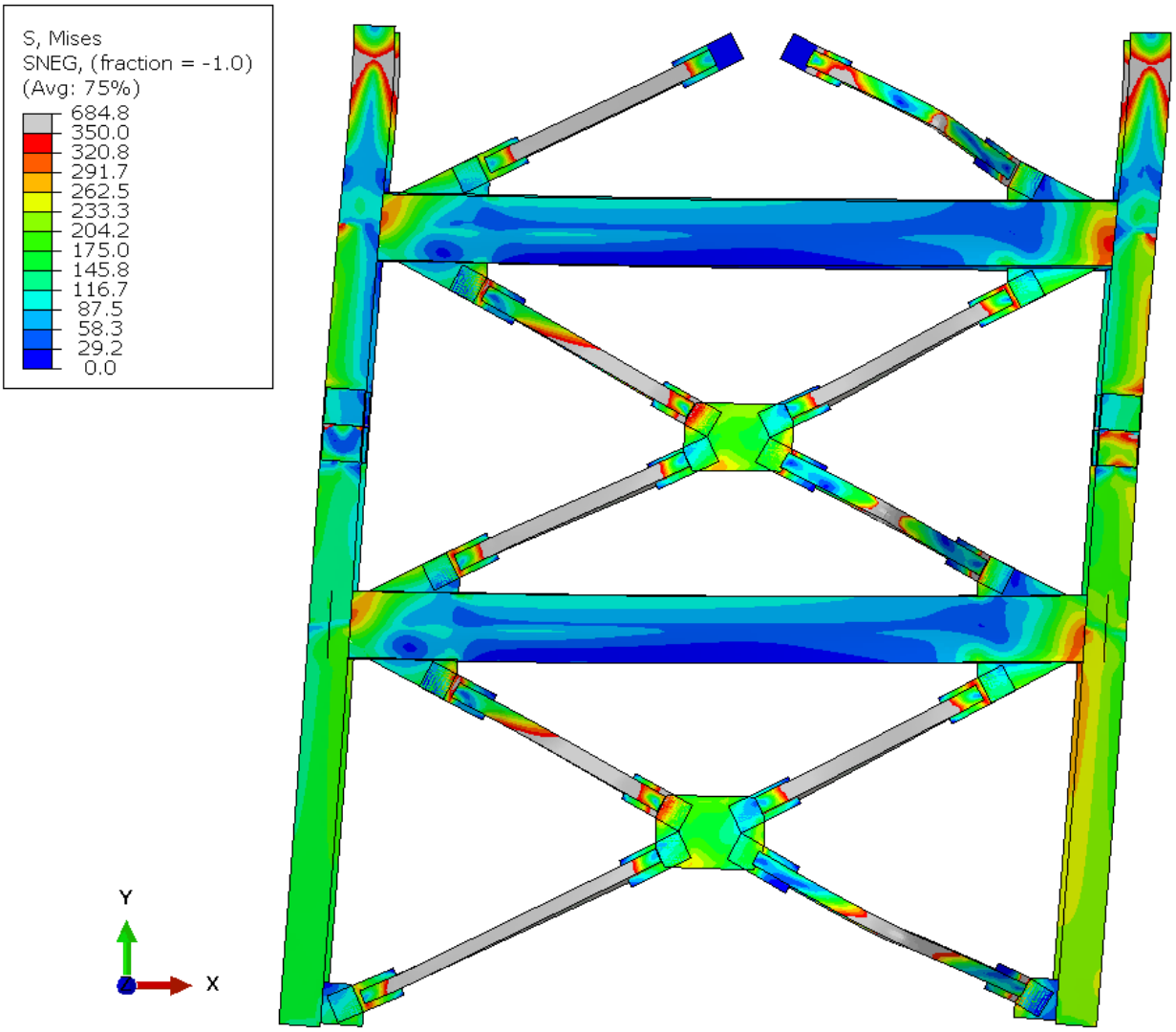

Figure 5.22: Deformed-shape and von-Mises stress (MPa) of the sub-assembly under displacement pattern corresponding to 1.5% of the storey height (deformation magnified x5)(elevation)

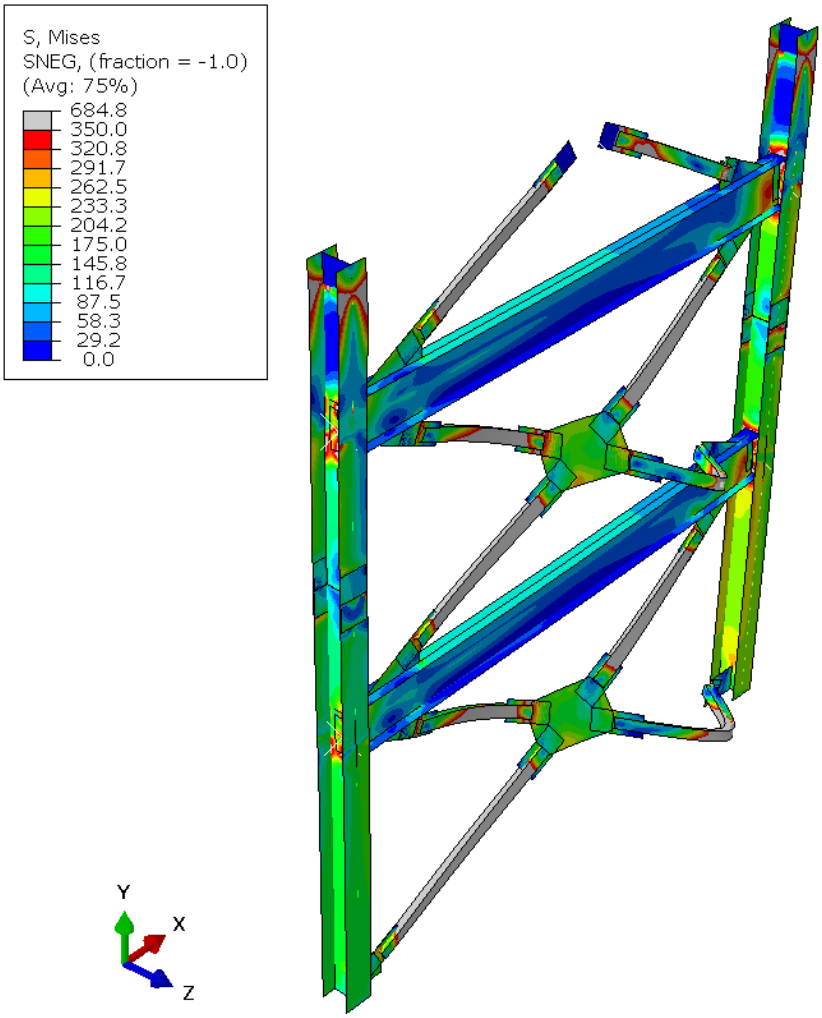

Figure 5.23: Deformed-shape and von-Mises stress (MPa) of the sub-assembly under displacement pattern corresponding to 1.5% of the storey height (deformation magnified x5)(3D)

Both loading cases studied forced the buckling of the braces, while other frame components, including beams, columns and connections remained elastic. Rectangular HSS braces selected in the design process of braced modules were oriented to buckle out-of-plane about their weak axis. As shown in Figure 5.24 for the first-storey module, out-of-plane buckling developed rotational hinges in the mid-length of the brace and at end connection plates within the designated 2*t* hinge

zone. The end plastic hinges were developed as expected, with no unsatisfactory limit states observed up to the expected lateral displacement. Braces that were under tensile forces yielded and elongated across their cross-sections. Second-storey braces showed similar behaviour to the braces on the first-storey module.

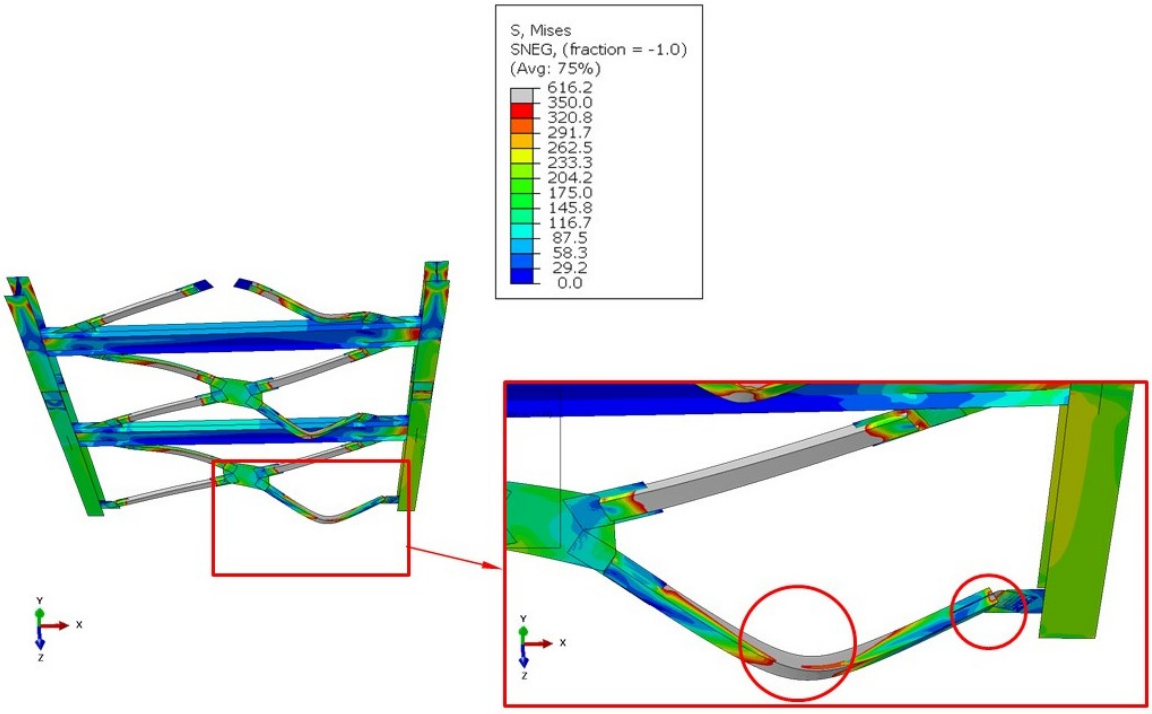

Figure 5.24: Buckling response of the first-storey module brace and the corresponding rotational hinges (deformation magnified x5)

The forces of the braces under both target displacement (obtained from MRSA and 1.5% of the storey height) are plotted in Figure 5.25 to examine if the drift value would disturb the brace buckling force. The response of braces in both storeys confirms that braces buckle in compression as expected. The plot of the first and second storey axial brace forces against the corresponding storey drift indicates good agreement in terms of buckling forces and plastic deformation between both target displacements. The results of the numerical model with target displacement equal to that obtained from MRSA are compared with the design forces calculated in accordance with CSA S16.

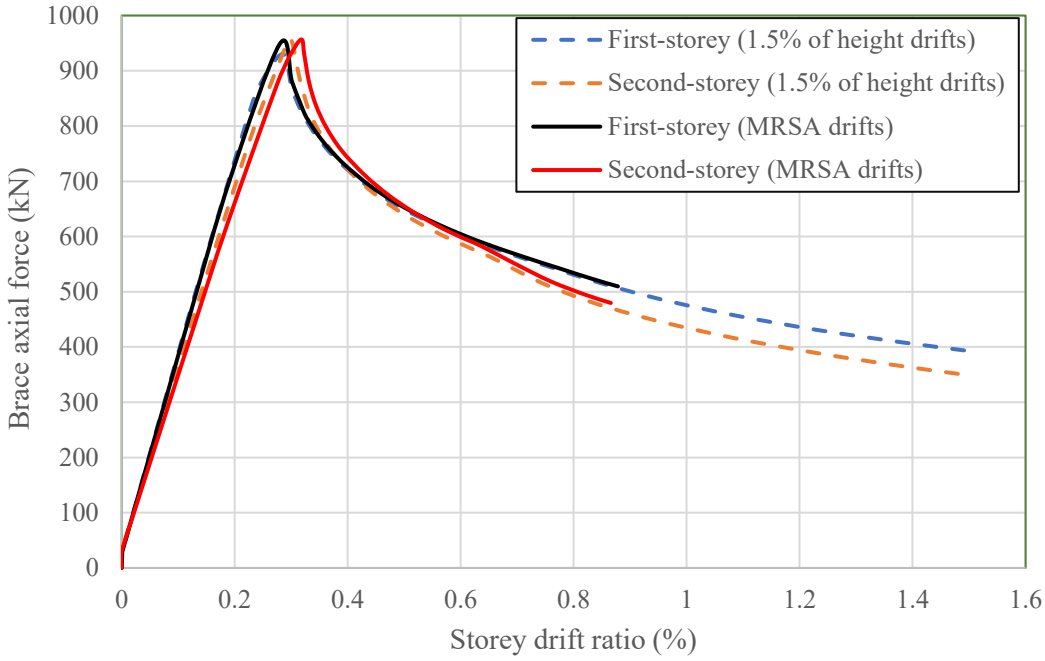

Figure 5.25: Brace axial compression forces under target disp. from MRSA and 1.5% of height

The member forces are examined here using the results obtained from the MRSA pattern only. Figure 5.26 shows brace axial forces for the first- and second-storey modules. The negative forces correspond to compression, whereas the positive forces represent tension in the braces. The horizontal lines on the graph represent the probable tension (T_u), and compression (C_u) forces calculated based on CSA S16. The first-storey braces reached yielding and buckling forces slightly before the second-storey braces. The forces of the third-floor braces were ignored due to the rigid body constraints applied at the mid-height of the storey. In general, the brace forces observed from the numerical model are in good agreement with the brace probable forces. It was also found that the discontinuity of braces at their mid-length where they meet the proposed middle connection of the modules did not significantly affect the behaviour of the brace when the sub-assembly is displaced laterally.

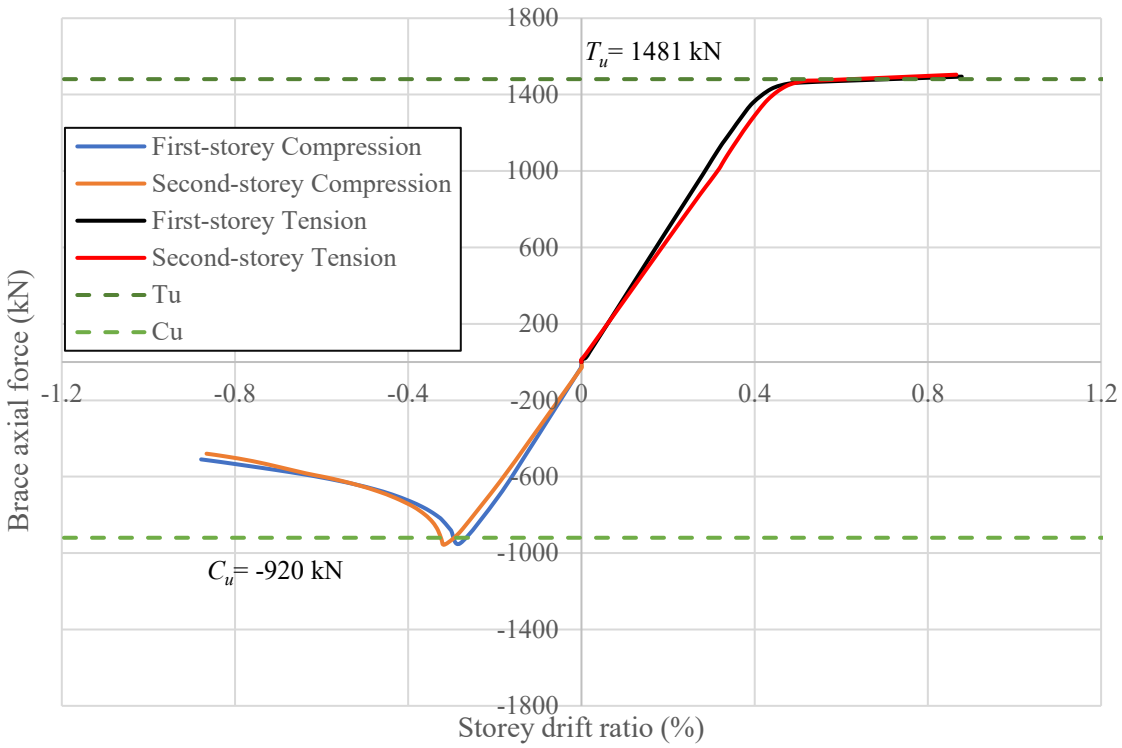

Figure 5.26: Braces axial forces for first and second storeys

The axial force of the first-storey brace under compression against the axial deformation of the brace is illustrated in Figure 5.27. The probable compression resistance (C_u) is represented using the horizontal line in the plot.

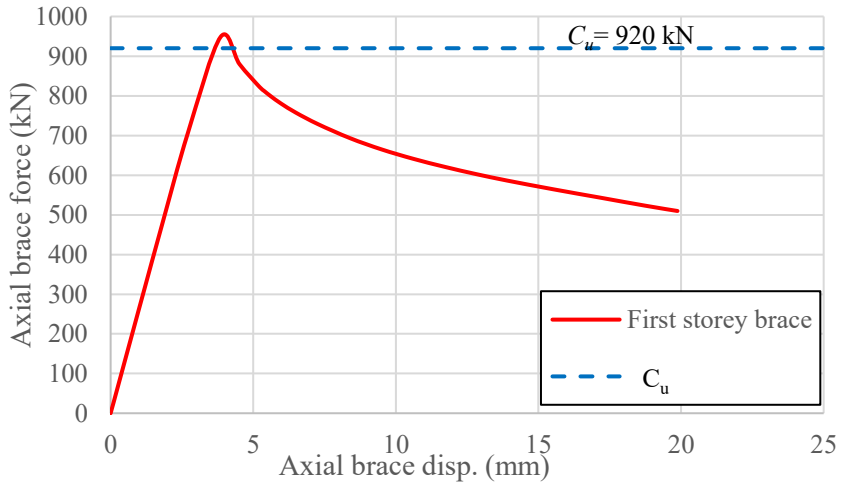

Figure 5.27: First-storey compressive brace force against the axial displacement of the brace

Strong axis moments recorded at the mid-span of the first and second storey beams are plotted against the applied storey drifts ratio in Figure 5.28. The first peak before the start of lateral displacement was due to the application of gravity loads. The beam moments are compared with the moment calculated at mid-span of a simply-supported beam with the same length $(WL^2/8)$ and illustrated using a red-dashed line in Figure 5.28. As shown, the module beam attracted less gravity moments than that calculated for a simply-supported beam, the reason being that the support provided by braces at the ends of the beam created rotational restraint. With the increase of the storey drift and when braces buckles, the beam strong axis moment increases gradually.

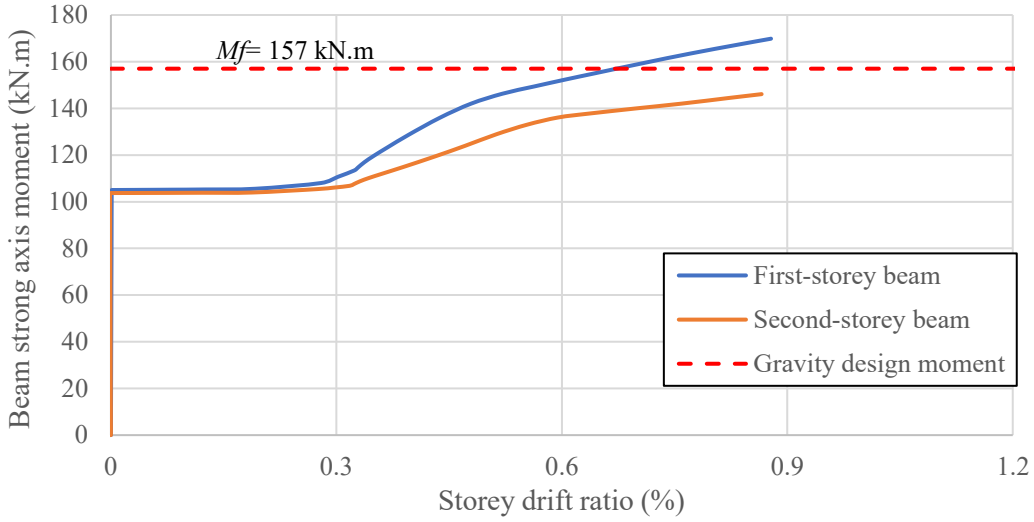

Figure 5.28: Strong axis bending moment of beams at the mid-span

The axial force at the mid-span of the beam is shown in Figure 5.29 under the gravity loads and lateral drift ratio. In this graph, positive represents axial compression forces. As shown, the axial forces obtained from the numerical model are lower than the design forces calculated under gravity loads plus brace axial resistances. This big difference between design forces and captured forces is due to the fact that design forces are calculated using the difference between post-buckling probable compressive resistance (C'_u) and probable tensile resistance (T_u). The braced module beams are designed under gravity moments and under post-buckling axial force. Therefore, even when the first-storey beam moment slightly exceeds the design moment, the section is still safe, as can be seen in the interaction diagram (Figure 5.30).

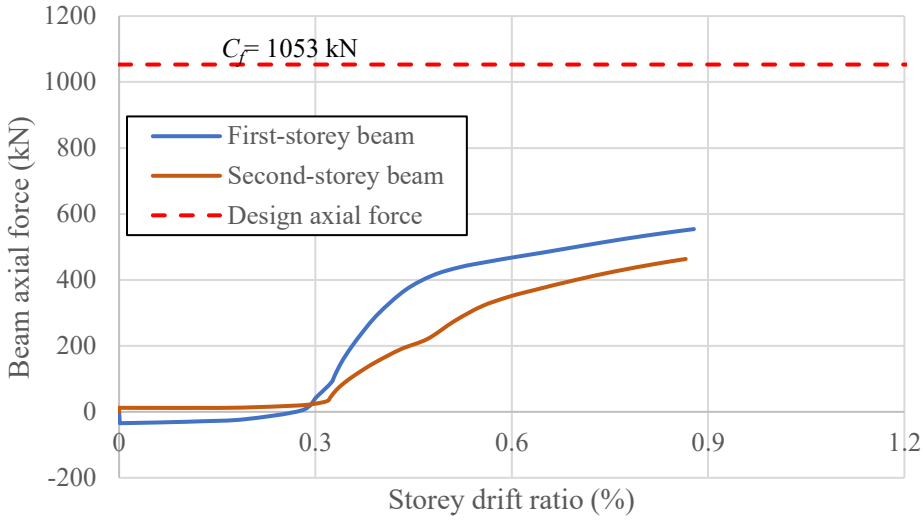

Figure 5.29: Axial force of beams at mid-span

The axial forces (C) and moments (M) of both modules' beams were normalized against (C_r=AF_y) and (M_{px} =Z_xF_y) and are represented in the axial force-bending moment interaction diagram for overall member strength limit state in Figure 5.30. As shown, both beams remain elastic under the combined effect of axial force and bending moment, as anticipated in the design. Note that the beam design was governed by shear, as described in Chapter 4.

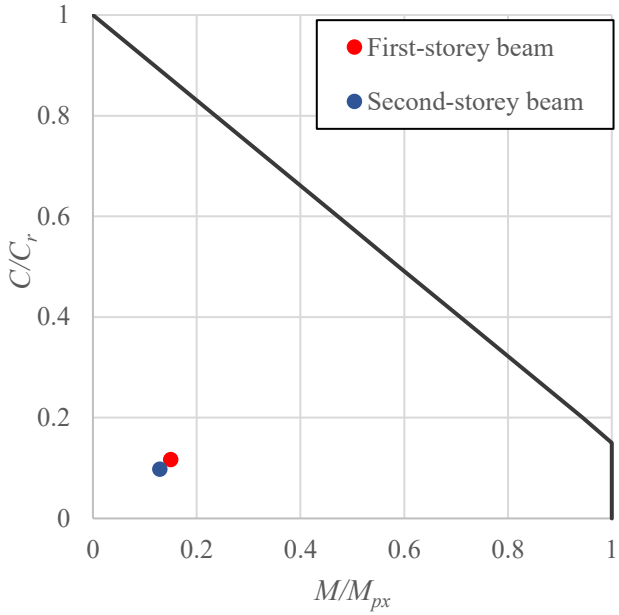

Figure 5.30: Axial force – bending moment interaction for beams

Shear forces on beams were captured at the beam-to-column connection end. The design shear forces on the first and second storeys' beams were identical since the braces used in both modules were the same sections. The shear force developed in the first-storey beam is plotted against the respective storey drift ratio in Figure 5.31. The developed shear force in the beam did not exceed the design shear force represented by the dashed red line. The second-storey beam showed an increase in the shear forces before decreasing because the end conditions applied to the second module upper brace changes the brace buckling force (C_u) affecting the beam. Therefore, the shear force developed at the target displacement is used for this study.

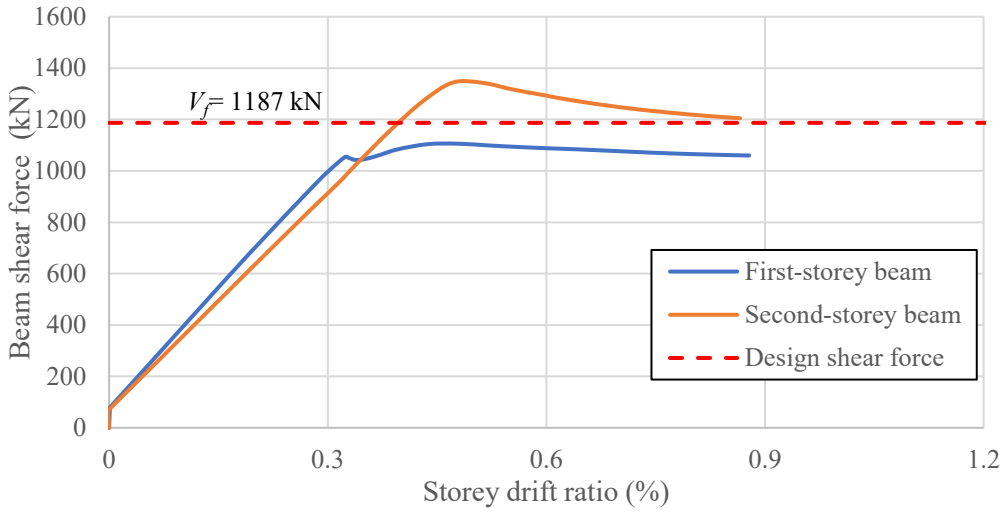

Figure 5.31: Shear forces at beam end vs. storey drift ratio

Column axial forces under gravity and seismic loads in both first and second storeys are plotted against the respective storey drift ratios in Figure 5.32. The column design force calculated is also shown using a horizontal line in the same plot for the comparison purpose. The positive and negative signs represent tensile and compressive forces, respectively, in the global Y-axis direction (see Figure 5.17). Good agreement was found when comparing the results from the numerical analysis and those predicted in design, which suggests that the S16 capacity design principle can predict the column demands well in the proposed modular system. It is worth noting that the slightly higher axial force compared to design values is associated with the material strain hardening in braces, which is neglected in the current S16 equation when calculating probable resistances.

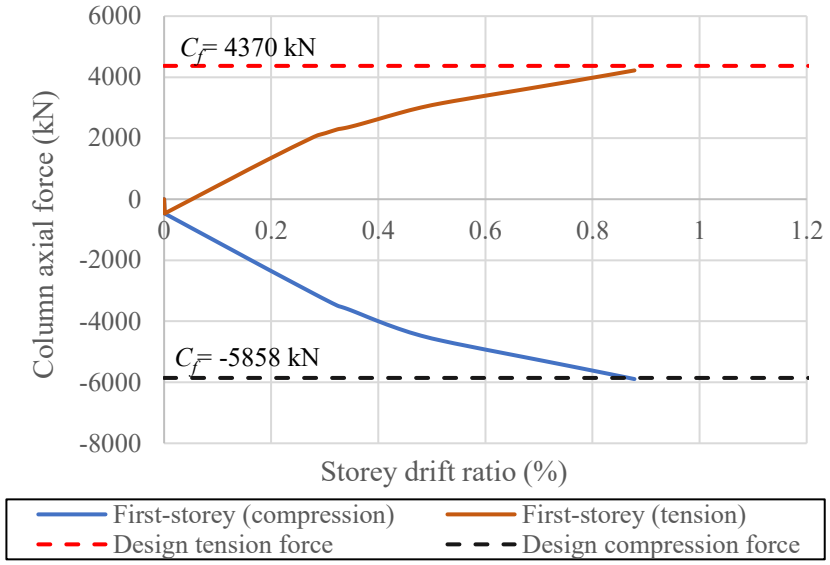

(a)

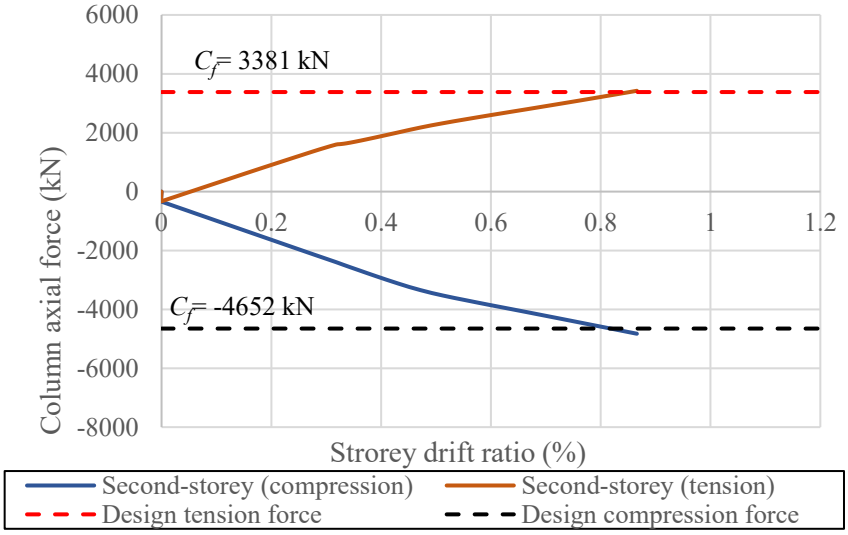

(b)

Figure 5.32: Columns axial force: (a) first-storey (b) second-storey

CSA S16 requires designing columns of CBFs for an in-plane moment equal to $0.2ZF_y$ of the selected column section in combination with the axial force. The column in-plane moment was recorded below the beam-to-column connection for each storey and plotted against the storey drift ratio in Figure 5.33. Columns of both modules have the same section; thus, the same design moment is given using a red dashed line. As shown, the in-plane moments induced in the columns

were significantly smaller than the design value, suggesting the code-specified moments are conservative for the studied modular system.

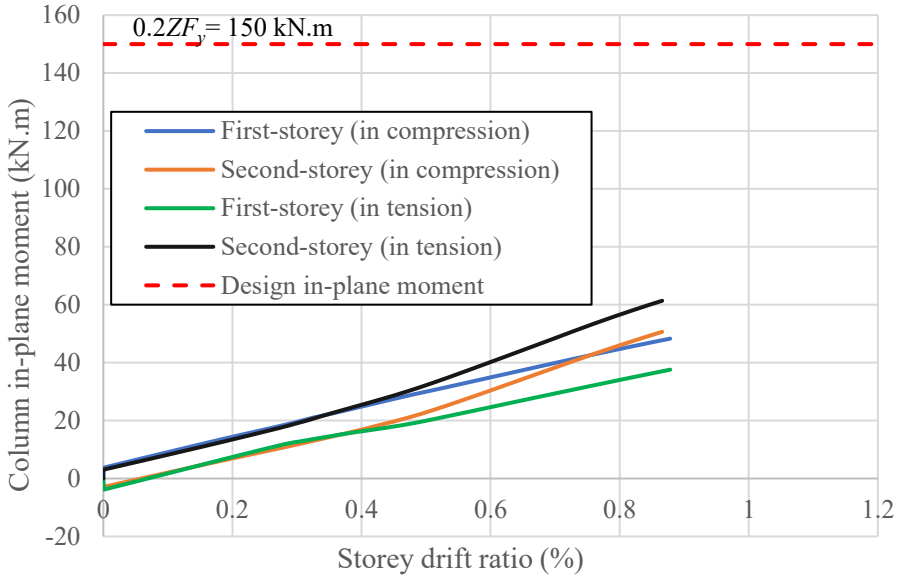

Figure 5.33: Column in-plane moments

Column out-of-plane moments are plotted against the storey drift in Figure 5.34. The out-of-plane moments were considered negligible and can be ignored in design, given the conservatism expected due to the in-plane moment demand. It should be noted that S16 does not require any moment in the out-of-plane direction, which is confirmed by this analysis.

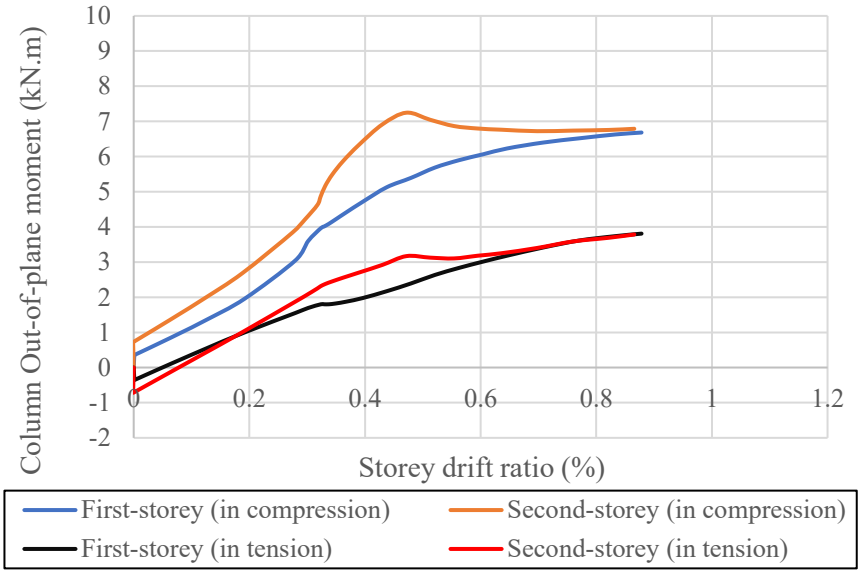

Figure 5.34: Columns out-plane moments

As shown in axial force – bending moment interaction for overall member strength limit state in Figure 5.35, both first- and second-storey columns remain stable under the applied loads, as expected in design.

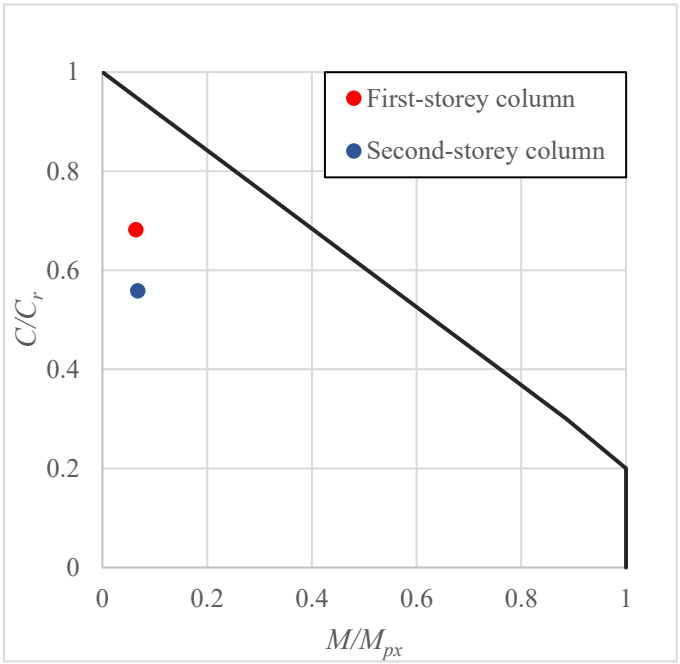

Figure 5.35: Axial force–bending moment interaction for columns

5.4 Summary of results

In summary, the results of the finite element analysis of the sub-assembly model under gravity and lateral loads showed a satisfactory seismic response. The forces induced in the force-controlled members of the subassembly did not exceed those predicted in design by CSA S16. Table 5.2 presents a comparison between the results obtained from the numerical analysis of the modular system and those predicted by CSA S16 for braces, beams, and columns. The percentages of the difference between the results of the modular system and the CSA S16 design forces are also presented in Table 5.2.

The brace axial forces developed after large axial deformations agreed with the brace probable resistances. The numerical model showed a marginally higher buckling load for the braces, which can be attributed to the contributions from the proposed end connections in the modules. This confirms that the CSA S16 seismic provisions can be used to design the proposed modular system.

Beam gravity moments showed an unremarkable difference between the modular sub-assembly model and the S16 predictions. Beam axial forces developed in beams of the sub-assembly model were significantly smaller than the design axial force required by S16. Shear forces developed at the model beam ends were slightly smaller than the required design shear force for the first-module beam. However, the second-module beam shows higher forces than predictions due to the end conditions applied to the brace.

The column forces developed in the model showed a good agreement with calculated design forces. The column in-plane moments recorded from the model were significantly lower than the design moments required by CSA S16. Out-of-plane moments developed in the columns were insignificant as expected. The nearly identical results verify the objective of this study to create a new modular system that can be designed with the currently available design standards.

Table 5.2: Summary of member forces obtained from the numerical analysis as compared to CSA S16 predictions

Parameter	**Proposed Modular system FEA results**		**CSA S16 design forces and moments**		**FEA to CSA S16 difference**	
Module	**First**	**Second**	**First**	**Second**	**First**	**Second**
Brace axial compression force (kN)	948.7	956.7	920.2	917.3	+3.1%	+4.3%
Brace axial tension force (kN)	1494	1504	1481.2	1481.2	+0.9%	+1.5%
Column axial compression force (kN)	5894.7	4827.9	5857.8	4652	+0.63%	+3.8%
Column axial tension force (kN)	4221.5	3422.9	4370.3	3380.9	-3.4%	+1.2%
Column in-plane moment (kN.m)	62.8	50.6	$0.2\ ZF_y$ = 150	$0.2\ ZF_y$ = 150	-58.1%	-66.3%
Beam moment (kN.m)	105	103	$(WL^2)/8$ =157	$(WL^2)/8$ =157	-33.1%	-34.4%
Beam axial force (kN)	554.1	463.5	1054	1054	-47.4%	-56%
Beam shear force (kN)	1059.7	1204.8	1187	1187	-10.7%	+1.5%

Chapter 6: Conclusions and recommendations for future study

6.1 Summary

The lack of background research on the construction efficiency and structural response of modular steel systems, which still have a small market share in the building industry in North America, motivated this research project. A new modular steel system for multi-storey buildings is proposed. Two types of modules, gravity and braced, were introduced to carry gravity and lateral loads, respectively. The members and connections were selected based on availability in the market, structural performance, and fabrication and erection benefits. A six-storey prototype building was selected to evaluate the construction efficiency and structural response of the proposed modular system under gravity and seismic loads. The building was designed as per the Canadian loading code (NBCC) and steel design standard (CSA S16). A braced frame sub-assembly consisting of the first- and second-storey modules was simulated using the Abaqus program. Nonlinear static (pushover) analyses were then performed to examine the lateral response of the sub-assembly focusing on the member forces and storey drift. The resulting member forces were compared to those predicted by CSA S16.

6.2 Conclusions

The key findings of this research can be summarized as follows:

- A new steel modular system was proposed in the framework of the Canadian steel design standard for multi-storey buildings to meet the constraints of the Canadian steel industry. The proposed system consists of two types of volumetric modules based on their load-carrying capability: gravity modules that resist vertical gravity loads and braced modules that are intended to carry gravity and lateral seismic loads.
- Both modules are proposed with only the structural members. Each module includes two bays in the long direction and one bay in the short direction, a flooring system that is surrounded by beams, and six columns that cover half of the storey height below the floor plus half of the storey height above the floor. The only exception pertains to the first-storey

module where the unit includes the total first-storey height and half of the second storey. Braced modules were designed as a Moderately-Ductile concentrically braced frame and included additional X-bracing in one of their bays in the long direction that is expected to be placed on the exterior wall of the building.

- The proposed modules measures 3.5 m in width (short direction), 14 m in length (long direction), and 3.6 m in height, except the first-storey module that is 5.4 m tall.
- Structural members used to produce the modules are steel wide-flange (W-shape) for beams and columns, and rectangular HSS for braces.
- The brace corner connection involves the connection to the storey beams without the need to connect to the adjacent columns. This connection was proposed such that it can reduce the assembly times while offering potential retrofitting advantages after a major seismic event.
- The results obtained from a preliminary cost evaluation showed that the proposed modular system, when compared to an equivalent system constructed conventionally, has the potential to reduce construction time duration without a dramatic increase in the cost. This estimation was solely based on steel tonnage and the number of connections.
- The finite element analysis of the braced frame subassembly consisting of the first- and second-storey modules showed that under a target displacement obtained from a modal response spectrum analysis. The braces of both adjacent modules and adjoining connections can provide sufficient lateral stiffness. This is while offering a large rotational capacity under lateral loads, which was obtained by tensile yielding and compressive buckling in out-of-plane. The other members, including beams and columns of the sub-assembly, were found to remain elastic under the applied loads.
- The force response of the sub-assembly members at a target displacement obtained from modal response spectrum analysis did not exceed the forces predicted in design in accordance with CSA S16. No significant yielding or instability was observed in beams and columns, which confirms that sufficient safety is implicit in the proposed modular system. Furthermore, the design provision specified can be used for the structural design of the proposed system.

6.3 Limitations

Although the proposed steel modular system appears to offer sufficient structural safety and construction advantages as compared to a system constructed using conventional methods, an examination of its limitations is critical.

- This study examined only one prototype building with one geometry and a unique number of storeys.
- The modules proposed in this study limited to main structural members including beams, columns, and diagonals. The flooring system, non-structural components such as exterior and interior (partitioning) walls, finishing, mechanical, electrical systems were not included.
- Cost estimation and comparison were performed, taking into account only the structural steel tonnage and the number of connections. Other influential parameters, including workforce hours, fabrication, storage, erection, transportation, and overhead costs, can fluctuate with time and location of the project that are not considered in this study.
- Vertical staking effects, settlements, out-of-plumpness of module columns, and other erection and construction imperfections were ignored when developing the proposed modular system.
- The finite element model developed in this study to examine the lateral response of the proposed braced modules only includes the first- and two-storey modules and neglects the effects of upper modules, floor system and adjacent gravity load-carrying system.

6.4 Recommendations and future work

The following research areas are recommended for future studies:

- The dimensions of the modules were selected to accommodate the transportation requirements of the province of Alberta. Future studies should investigate other dimensions based on specific constraints of the project.
- Refined global slenderness accounting for the brace length and the corner and middle gusset plates should be used in the design.

- Structural response of the proposed braced module when used in conjunction with other more common modular systems such as modular light-steel buildings or shipping containers.
- Flooring systems that can mimic the constraints and benefits of the proposed modular system should be developed so that the unit, including the structural members and flooring system, can be fabricated in the shop.
- A more detailed cost estimation taking into account all influential parameters when compared to the buildings constructed using conventional construction methods, should be performed.
- The influence of erection and construction imperfections such as stack effects, out-of-plumpness and settlement should be investigated, and sufficient tolerances and construction methods should be proposed.
- A similar study should be performed where the structural design of braced modules is governed by the wind load such as the building sites located in the province of Alberta.
- A full-scale experimental program is needed to study the interaction between modules and connection behaviour.
- A numerical parametric study using the nonlinear response history analysis method should be carried out to investigate the effects of various frame geometries, connection details and seismic loading. A more ductile system that can further improve the construction efficiency of the proposed braced module system in moderate-to-high seismic regions involves the application of a vertical link placed between the ends of brace halves between two adjacent modules, as shown in Figure 6.1. This will allow the braced module to act as an eccentrically braced frame (EBF) under seismic loads offering a higher ductility capacity while potentially reducing the construction time. Furthermore, the intermediate vertical link is expected to offer the benefit of replacement after a major seismic event.

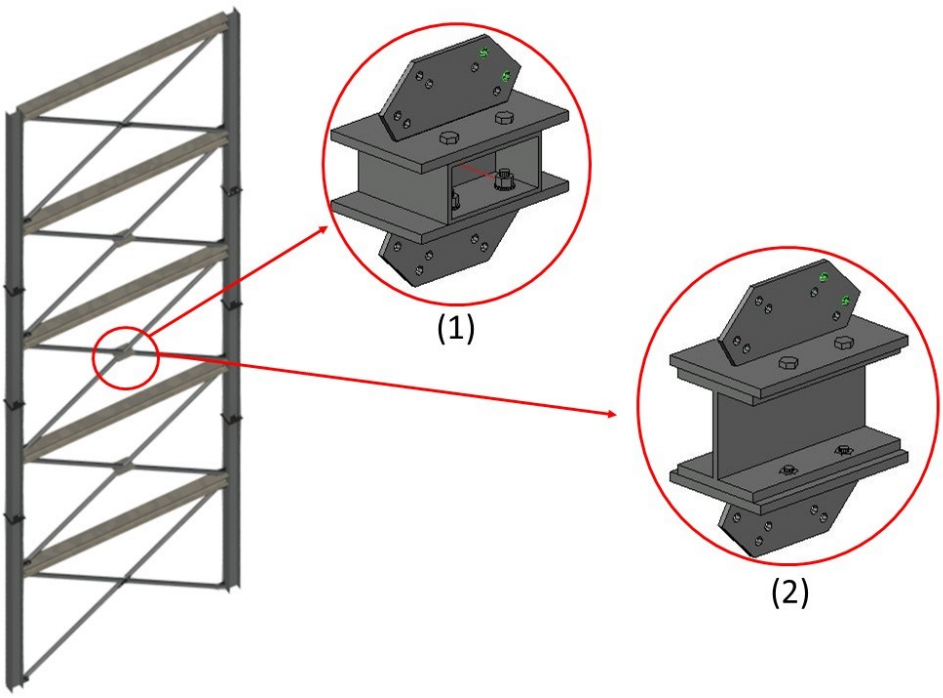

Figure 6.1: Proposed modular structural fuses

References

Adeeb, S. 2020. Introduction to Solid Mechanics & Finite Element Analysis. Available from https://sameradeeb-new.srv.ualberta.ca/

Annan, C., Youssef, M. and El Naggar, M.H. 2007. Seismic Performance of Modular Steel Braced Frames. Proceedings of Ninth Canadian Conference on Earthquake Engineering, Ottawa, Ontario, Canada

Annan, C.D., Youssef, M.A., and El Naggar, M.H. 2009. Experimental evaluation of the seismic performance of modular steel-braced frames. Engineering Structures, **31**(7): 1435-1446. Available from https://www.sciencedirect.com/science/article/pii/S0141029609000935. doi: https://doi.org/10.1016/j.engstruct.2009.02.024.

Canadian Institute of Steel Construction. 2016. Handbook of Steel Construction, Ontario, Canada.

Cano, P. and Imanpour, A. 2019. Evaluation of the Seismic Design Methods for Steel Multi-Tiered Concentrically Braced Frames, University of Alberta, Edmonton, AB, Canada.

Chen, L., Tremblay, R. and Tirca, L. 2012. Seismic performance of modular braced frames for multi-storey building applications. Proceedings of the 15th World Conference on Earthquake Engineering, Lisbon, Portugal.

Chen, Z., Li, H., Chen, A., Yu, Y., and Wang, H. 2017. Research on pretensioned modular frame test and simulations. Engineering Structures, **151**: 774-787. Available from

http://www.sciencedirect.com/science/article/pii/S0141029617310301. doi: https://doi.org/10.1016/j.engstruct.2017.08.019.

Chen, Z., Liu, J., and Yu, Y. 2017. Experimental study on interior connections in modular steel buildings. Engineering Structures, **147**: 625-638. Available from http://dx.doi.org/10.1016/j.engstruct.2017.06.002 [accessed Sep 15,]. doi: https://doi.org/10.1016/j.engstruct.2017.06.002.

CSA. 2019. CSA S16:19 Design of steel structures. Canadian Standards Association Group, Toronto, Ontario, Canada.

CSI Computers and Structures Inc 2009. SAP2000 Advanced, Version 14, Berkeley, CA

Dassault Systèmes 2019. Abaqus. Dassault Systèmes Simulia Corp, Providence, RI.

Davaran, A., Gélinas, A., and Tremblay, R. 2015. Inelastic Buckling Analysis of Steel X-Bracing with Bolted Single Shear Lap Connections. Journal of Structural Engineering, **141**(8): 4014204. Available from http://ascelibrary.org/doi/abs/10.1061/(ASCE)ST.1943-541X.0001141 [accessed Aug 1,]. doi: https://doi.org/10.1061/(ASCE)ST.1943-541X.0001141.

Etebarian, H. and Yang, T. 2018. Development and Assessment of Innovative Modular Damped H-Frame System. University of British Colombia, Vancouver, BC, Canada.

Fathieh, A., and Mercan, O. 2016. Seismic evaluation of modular steel buildings. Engineering Structures, **122**: 83-92. Available from http://dx.doi.org/10.1016/j.engstruct.2016.04.054 [accessed Sep 1,]. doi: https://doi.org/10.1016/j.engstruct.2016.04.054.

Government of Alberta 2018. Module 4: Weights and Dimensions. Available from https://www.alberta.ca/assets/documents/tr-module-4-weights-and-dimensions.pdf

Hong, S., Cho, B., Chung, K., and Moon, J. 2011. Behavior of framed modular building system with double skin steel panels. Journal of Constructional Steel Research, **67**(6): 936-946. Available from http://www.sciencedirect.com/science/article/pii/S0143974X11000411. doi: https://doi.org/10.1016/j.jcsr.2011.02.002.

Jiang, Y. 2013. Numerical and experimental seismic assessment and retrofit of steel tension-only double angle braced frames designed before the implementation of detailing provisions for ductile seismic response., Ecole Polytechnique, Montreal, QC, Canada.

Kamali, M., and Hewage, K. 2016. Life cycle performance of modular buildings: A critical review. Renewable and Sustainable Energy Reviews, 62: 1171-1183. Available from http://www.sciencedirect.com/science/article/pii/S1364032116301411 . doi: https://doi.org/10.1016/j.rser.2016.05.031 .

Lawson, M., Ogden, R. and Goodier, C. 2014. Design in Modular Construction. CRC Press LLC, Boca Raton, FL.

Lawson, R.M., and Richards, J. 2010. Modular design for high-rise buildings. Proceedings of the Institution of Civil Engineers - Structures and Buildings, **163**(3): 151-164 [accessed Jun]. doi: https://doi.org/10.1680/stbu.2010.163.3.151 .

Liu, X.C., Xu, A.X., Zhang, A.L., Ni, Z., Wang, H.X., and Wu, L. 2015. Static and seismic experiment for welded joints in modularized prefabricated steel structure. Journal of

Constructional Steel Research, **112**: 183-195. Available from http://dx.doi.org/10.1016/j.jcsr.2015.05.003 [accessed Sep]. doi: 10.1016/j.jcsr.2015.05.003.

Liu, X.C., Yang, Z.W., Wang, H.X., Zhang, A.L., Pu, S.H., Chai, S.T., and Wu, L. 2017. Seismic performance of H-section beam to HSS column connection in prefabricated structures. Journal of Constructional Steel Research, **138**: 1-16. Available from http://dx.doi.org/10.1016/j.jcsr.2017.06.029 [accessed Nov]. doi: 10.1016/j.jcsr.2017.06.029.

Liu, X.C., He, X.N., Wang, H.X., Yang, Z.W., Pu, S.H., and Ailin, Z. 2018. Bending-shear performance of column-to-column bolted-flange connections in prefabricated multi-high-rise steel structures. Journal of Constructional Steel Research, **145**: 28-48. Available from http://dx.doi.org/10.1016/j.jcsr.2018.02.017 [accessed Jun]. doi: 10.1016/j.jcsr.2018.02.017.

Liu, X.C., Zhan, X.X., Pu, S.H., Zhang, A.L., and Xu, L. 2018. Seismic performance study on slipping bolted truss-to-column connections in modularized prefabricated steel structures. Engineering Structures, **163**: 241-254. Available from http://dx.doi.org/10.1016/j.engstruct.2018.02.043 [accessed May 15,]. doi: 10.1016/j.engstruct.2018.02.043.

Liu, X., Zhang, A., Ma, J., Tan, Y., and Bai, Y. 2015. Design and Model Test of a Modularized Prefabricated Steel Frame Structure with Inclined Braces. Advances in Materials Science and Engineering, **2015**: 291481. Available from https://doi.org/10.1155/2015/291481. doi: 10.1155/2015/291481.

Liu, X., Zhou, X., Zhang, A., Tian, C., Zhang, X., and Tan, Y. 2018. Design and compilation of specifications for a modular-prefabricated high-rise steel frame structure with diagonal braces.

Part I: Integral structural design. The Structural Design of Tall and Special Buildings, **27**(2): e1415-n/a. Available from https://onlinelibrary.wiley.com/doi/abs/10.1002/tal.1415 [accessed Feb 10,]. doi: 10.1002/tal.1415.

Lopez, D., and Froese, T.M. 2016. Analysis of Costs and Benefits of Panelized and Modular Prefabricated Homes. Procedia Engineering, **145**: 1291-1297. Available from http://dx.doi.org/10.1016/j.proeng.2016.04.166. doi: 10.1016/j.proeng.2016.04.166.

Lu, N. 2007. Investigation of the designers' and general contractors' perceptions of offsite construction techniques in the United States construction industry, Clemson University.

Metten, A. and Driver, R. 2015. Structural Steel for Canadian Buildings| a designer's guide, Canada.

Modular building institute. 2019. 2019 Permanent Modular construction Report, Available from: https://www.modular.org/HtmlPage.aspx?name=pmc-2019-home.

National Research Council of Canada. 2015. National Building Code of Canada: 2015. National Research Council of Canada. Canadian Commission on Building and Fire Codes, Ontario, Canada.

Natural Resources Canada 2020. National Building Code of Canada seismic hazard values. Available from: https://earthquakescanada.nrcan.gc.ca/hazard-alea/interpolat/calc-en.php.

Packer, J., Sherman, D. and Lecce, M. 2010. Design Guide 24: Hollow Structural Section Connections. American Institute of Steel Construction, USA. Available from: https://www.aisc.org/Design-Guide-24-Hollow-Structural-Section-Connections.

Ramaji, I.,J. and Memari, A. 2013. Identification of structural issues in design and construction of multi-story modular buildings. Proceeding of the 1st Residential Building Design & Construction Conference, Bethlehem, PA.

Sabelli, R., Roeder, C., and Hajjar, J. 2013. Seismic Design of Steel Special Concentrically Braced Frame Systems| A Guide for Practicing Engineers. Available from: https://www.nist.gov/publications/nehrp-seismic-design-technical-brief-no-8-seismic-design-steel-special-concentrically.

Shen, J., Sabol, T., Akbas, B., Sutchiewcharn, N., and Cai, W. 2010. Seismic Demand on Column Splices in Steel Moment Frames. Proceeding of the 14th World Conference on Earthquake Engineering, Beijing, China.

Shi, G., Yin, H., and Hu, F. 2018. Experimental study on seismic behavior of full-scale fully prefabricated steel frame: Global response and composite action. Engineering Structures, **169**: 256-275. Available from http://dx.doi.org/10.1016/j.engstruct.2018.05.052.

Shi, G., Yin, H., Hu, F., and Cui, Y. 2018. Experimental study on seismic behavior of full-scale fully prefabricated steel frame: Members and joints. Engineering Structures, **169**: 162-178. Available from http://www.sciencedirect.com/science/article/pii/S0141029618302293. doi: https://doi.org/10.1016/j.engstruct.2018.04.087.

Sultana, P., and Youssef, M.A. 2018. Seismic Performance of Modular Steel-Braced Frames Utilizing Superelastic Shape Memory Alloy Bolts in the Vertical Module Connections. Journal of Earthquake Engineering: 1-25 [accessed Mar 22,]. doi: https://doi.org/10.1080/13632469.2018.1453394.

Suzuki, Y. and Lignos, D.G. 2015. Large scale collapse experiments of wide flange steel beam-columns. *In* 8th International Conference on Behavior of Steel Structures in Seismic Areas (STESSA), July 1-3, 2015, Shanghai, China.

Tremblay, R., Archambault, M.-., and Filiatrault, A. 2003. Seismic Response of Concentrically Braced Steel Frames Made with Rectangular Hollow Bracing Members. Journal of Structural Engineering, **129**(12): 1626-1636. Available from: http://ascelibrary.org/doi/abs/10.1061/(ASCE)0733-9445(2003)129:12(1626). doi: https://doi.org/10.1061/(ASCE)0733-9445(2003)129:12(1626).

WF Steel & Crane 2019. Discussions on modular structures design, connections, scheduling, and cost estimation. Nisku, AB, Canada.

Zhuo, S. 2018. Development of an innovative modular steel truss system, University of British Columbia. Vancouver, BC, Canada. Available from: https://open.library.ubc.ca/cIRcle/collections/ubctheses/24/items/1.0365961.